Thermal Design Studies

Final Report
Contract NAS8-5270

February 1967

Prepared for: George C. Marshall Space Flight Center
NASA
Huntsville, Alabama

Prepared by: Bureau of Engineering Research
University of Alabama
University, Alabama

N67-36017

FACILITY FORM 602

(ACCESSION NUMBER)	(THRU)
135 (PAGES)	1 (CODE)
CR 88135 (NASA CR OR TMX OR AD NUMBER)	14 (CATEGORY)

Thermal Design Studies

Final Report
Contract NAS8-5270

February 1967

Prepared for: George C. Marshall Space Flight Center
NASA
Huntsville, Alabama

Prepared by: Bureau of Engineering Research
University of Alabama
University, Alabama

CONTENTS

(BY PARTS)

PART I	SUMMARY
PART II	AN ELECTROMECHANICAL WEIGHTED-AREA INTEGRATING DEVICE
PART III	EXPERIMENTS IN DETERMINATION OF THE RADIATION CONFIGURATION FACTOR USING WAID
PART IV	A FEASIBILITY STUDY OF A DIRECT ACQUISITION DEVICE FOR DETERMINATION OF THE RADIATION CONFIGURATION FACTOR
PART V	A STUDY OF THE THERMAL SIMILARITY OF A SELECTED SET OF MODELS WITH SIGNIFICANT RADIATION AND CONDUCTION

PART I

SUMMARY

BACKGROUND. Over a period from April 1963 until September 1965 a parallel series of studies was conducted on the determination of the radiation view factor by an analog technique, and on thermal similitude and thermal scale modeling. These tests were summarized in a report dated September 1967 and the resulting data are not repeated here.

During an extension of the contract an electrical analog integrator was fabricated under the direction of Dr. R. E. Lueg. The statement summarizing the construction details and initial test of this device is included as Part II of this report, and is a self-contained section.

Having developed the Analog Integrator it was determined that this device should be used to acquire data on some unusual geometries as tests of the method. Part III describes two experiments that were conducted to determine data on the radiation configuration factor at discrete points on two models using the electronic integrator.

It had been suggested that the data for the radiation configuration factor might be acquired for a particular elemental area using a direct integrating device. The result of this study is included as Part IV.

A series of thermal models was designed which would have radiation and conduction exchanges of approximately the same order of magnitude. These models were not built, but were modeled to achieve a speed-up of time of 5 and 10. The results of these tests are presented in Part V.

WORK EFFORT. The work was handled as three autonomous projects. The electronic integrator absorbed about 35% of the total work effort, the direct acquisition method for determining the radiation view factor absorbed approximately 20% of the total work effort, and the thermal similitude studies together with the application of the electronic integrator (Part III) absorbed approximately 45% of the work effort.

Thermal Design Studies

Final Report
Contract NAS8-5270

PART II

AN ELECTROMECHANICAL WEIGHTED-AREA INTEGRATING DEVICE

by: Dr. R. E. Lueg
Mr. J. A. Chiang

February 1967

Prepared for: George C. Marshall Space Flight Center
NASA
Huntsville, Alabama

Prepared by: Bureau of Engineering Research
University of Alabama
University, Alabama

TABLE OF CONTENTS

Page

CHAPTER I INTRODUCTION..... 1

CHAPTER II BASIC BACKGROUND..... 6

A. VIEWFACTOR DEFINITION..... 6

B. PARABOLIC MIRROR PHOTOGRAPH..... 10

C. VIEWFACTOR DETERMINATION..... 13

CHAPTER III THE INTEGRATING DEVICE 22

A. OVERALL DESCRIPTION..... 22

B. PRACTICAL DESIGN CONSIDERATIONS..... 26

(a) Preparation of Tracing..... 26

(b) Turntable..... 28

(c) Readhead 29

(d) Operational Circuit..... 31

(i) Operational Amplifiers
(ii) Gain Selections -- Determination of $R_n R_a R_b$, and C

(e) Calibration Methods..... 38

(i) Zeroing of Operational Amplifier Offsets
(ii) Turntable Speed Balancing
(iii) Calibration of the Selector Ranges

(f) Switching Arrangement..... 43

(g) Power Supplies..... 45

(i) The Amplifier Power Supply
(ii) The Control Power Supply

C. ERROR ANALYSIS (THEORETICAL)..... 46

CHAPTER IV EXPERIMENTAL RESULST..... 55

CHAPTER V CONCLUSIONS..... 60

Table of Contents (Cont'd.)

Page

APPENDIX .....

A. CALIBRATION EQUATIONS FOR THE PARABOLIC MIRROR PHOTOGRAPH..... 62

B. OPERATIONAL AMPLIFIER CHARACTERISTICS..... 67

C. SAMPLE OF THE COUNTING GRID..... 69

BIBLIOGRAPHY..... 70

LIST OF ILLUSTRATIONS

Figure		Page
1.	Examples Showing the Viewfactor	1
2.	Block Diagram of the Integrating Device	4
3.	Element of the Geometry of Space for the Viewfactor	9
4.	Camera and Parabolic Mirror Location	11
5.	Increment of Viewfactor vs Constant Increment in r.	12
6.	A Parabolic Mirror Photograph Model Showing m Equally Divided Annular Bands	15
7.	Operational Amplifier Circuit	16
8.	An Integrating Circuit with Multiple Inputs	18
9.	Pictorial Diagram of the Integrating Device	20
10.	Input-Output Waveforms Showing the n-th Input	21
11.	A sample of the Tracing	27
12.	Physical Construction of the Readhead	30
13.	Simplified Circuit Diagram of the WAID	33
14.	Circuits for Setting R_n and R_b	37
15.	Amplifier Balancing Circuit	39
16.	Selector Arrangement	41
17.	Control Sequence Diagram	44
18.	Control Power Supply Diagram	48
19.	Example Showing Error Due to Wiper Shape	49
20.	Examples Showing Errors Due to Area Shape and Wiper Position	49
21.	Equivalent Actual Operational Circuit	51
22.	Curves Showing Errors Due to Operational Amplifier	54

CHAPTER I

INTRODUCTION

The primary purpose of this thesis is to present the design, fabrication and test procedures used in the development of an electromechanical Weighted-Area Integrating Device (hereafter called WAID) which will automatically perform in integration over a complex planar surface. This complex surface represents a radiation "viewfactor"[1] between surfaces of arbitrary configuration.

In the study of radiation heat transfer, the viewfactor between a pair of black bodies with surfaces of A_1 and A_2 may be interpreted as the "fraction" of the radiation energy leaving A_1 that strikes A_2. For example take two parallel plates of surfaces A_1 and A_2 as shown in Figure 1(a).

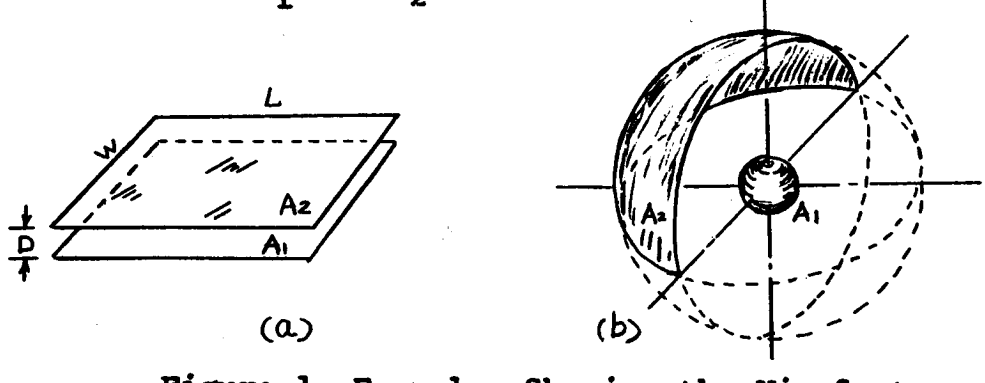

Figure 1 Examples Showing the Viewfactor

---

[1] Viewfactor is also called "configuration factor, shape factor, or geometry factor. See more detail in Chapter II, Section A.

Assume D is very small compared to W and L and neglect the fringing effect. The fraction of the energy radiating from A_1 which is intercepted by A_2 is almost unity (100%), i.e. the viewfactor $F_{12} \approx 1$. When one surface A_1 is completely enclosed by a second surface A_2, the shape factor F_{12} is unity. Another example showing a viewfactor smaller than unity is as depicted in Figure 1 (b). Assume a small spheric black body of surface A_1 radiating its energy uniformly in all directions. The fraction of the radiation which is received by the black surface of quadrasphere A_2 is 1/4, i.e. $F_{12} = 0.25$. If the second surface is a hemisphere, then $F_{12} = 0.5$. If A_2 is a spheric surface completely enclosing A_1, the shape factor becomes maximum (unity).

Thus the radiation viewfactor is important in the study of radiation heat transfer. Methods for the evaluation of the viewfactor have been rigorously studied recently. There are many available techniques whereby the viewfactor can be determined such as: (1) the four experimental methods described by Hamilton and Morgan[2] in 1952: (2) the parabolic morror photographic technique by Hickman[3] in 1962; and (3) other alternative feasible techniques. These alternative methods include: (a) the use of a pulse-light beam: (b) a photoreader

---

[2] NACA 2836. Dec. 1952

[3] R.S. Hickman, "The Measurement of Radiation Configuration Factors with Parabolic Mirrors. Proceedings of the 1962 Heat Transfer and Fluid Mechanics Institute. Stanford University Press.

coupled with parabolic mirror technique; and (c) a photosensitive meter technique, all of which were suggested by Matheny and Carden [4] in 1965. Among all of the available methods the parabolic mirror photographic technique yields excellent results which are well within the accuracy needed in design calculations[5]. In addition, this method yields more accurate results than can be obtained by other known methods.

In the parabolic mirror technique each of the "local" viewfactors (f) is first obtained by integrating over the corresponding exposed area of the parabolic mirror photographic images. Then the "overall" viewfactor (F_{12}) is calculated by numerical approximate integration approaches; e.g., by using the Trapezoidal rule or Simpson's rule. The WAID is used to determine the "local viewfactor".

Since the local viewfactor "density" on the parabolic mirror photographic image is of nonuniform distribution along its radial direction, commercially available areaintegrators such as the planimeter cannot be used to obtain the viewfactor. Grid counting by a human operator is possible but it is time consuming, costly, and subject to human error. The use of the "WAID" is considered as the most desirable and suitable method

---

4.5 J.E. Matheny, A. E. Carden, "Thermal Design Studies Final Report," September 1965. Contract NAS8-5270. Bureau of Engineering Research, University of Alabama.

for integrating over this particular "weighted area" surface for the following reasons: (1) Quick and automatic data acquisition is possible (by simply pushing the "compute" button, the answer will automatically appear on the readout 3.6 sec. later); (2) Because the operation is so simple and no actual enlarged photograph is needed, the cost is low; (3) Since less human error is involved good accuracy is obtainable.

As shown in Figure 2, the WAID is composed of the following: (1) A turntable which is driven by a motor which turns at a synchronous speed; (2) A readhead which contains a series of 64 electric contacts which are evenly mounted on a 3.5" radial arm over the turntable; (3) Two operational amplifiers connected in cascade as a summer and an integrator; and (4) A readout unit which is essentially a digital voltmeter. A silver

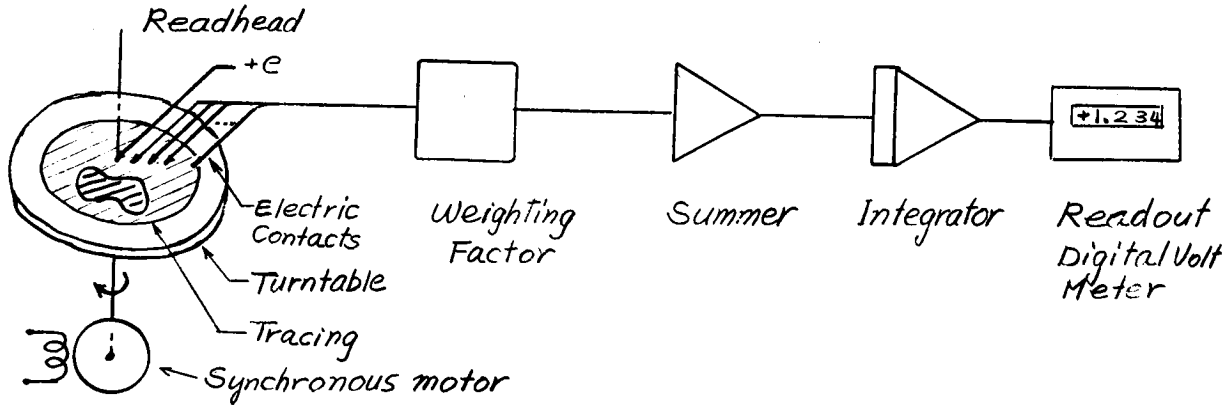

Figure 2. Block Diagram of the Integrating Device

painted tracing, which has been prepared before running the machine, is placed on the turntable. The painted area on the tracing represents the image of the parabolic mirror photograph from which the viewfactor can be determined. When the readhead scans one revolution over the tracing, the painted area of the image is read by the electric contacts and is properly "weighted" with the parallel input impedances (which are denoted as the "weighting factors" in Figure 2) to the summing amplifier. The weighted area is integrated by the integrator. The voltage output of the integrator, i.e., the desired viewfactor, is readout from the digital voltmeter.

Thus the WAID can be used to integrate over the "weighted area" of the parabolic mirror photographic image. The characteristics of the photographic image and the method of obtaining the photograph are discussed in Chapter II. Included in Chapter II are the equations which must be integrated. These are: (1) the equation which defines the viewfactor; (2) the calibration equation of the parabolic mirror image (the weighting factor is determined from this equation); and (3)the difference integral equation from which the WAID is designed.

Detailed descriptions of the WAID and its practical design considerations are presented in Chapter III. The experimental results and conclusions are given in Chapters IV and V, respectively.

CHAPTER II

BASIC BACKGROUND

A. VIEWFACTOR DEFINITION

In the study of radiant heat transfer, the relation for the energy emitted by surface A_1 and intercepted by surface A_2 can be expressed as

$$E_{12} = A_1 F_{12} \sigma T_1^4 \qquad (2\text{-}1)$$

where T_1 is the absolute temperature on A_1 (assume A_1 is an isothermal surface), σ is the Stefan-Boltzmann's constant ($=0.1713 \times 10^{-8}$ Btu/ft^2-hr-$^\circ$R^4) and F_{12} is the radiation viewfactor of A_1 with respect to A_2. A similar expression for the energy originating at surface A_2 and arriving at surface A_1 is $E_{21} = A_2 \times F_{21} \sigma T_2^4$ where F_{21} and F_{12} are generally not equal, but the reciprocal relation $A_1 F_{12} = A_2 F_{21}$ does exist. The net interchange of radiant energy between the two blackbody (a black surface is defined as one which absorbs all oncoming radiation) surfaces

A_1 and A_2 is

$$q_{1\to 2} = E_{12} - E_{21} = A_1 F_{12} \sigma (T_1^4 - T_2^4) \qquad (2\text{-}2)$$

Thus F_{12} may be interpreted as the fraction of the radiation leaving a black surface A_1 which is intercepted by surface A_2. In general, the radiation viewfactor between a body of finite surface A_1 and a second body A_2 is defined [1] by the equation:

$$F_{12} = \frac{1}{A_1} \int_{A_1} \int_{A_2} \frac{\cos\theta_1 \cos\theta_2}{\pi R^2} \, dA_2 \, dA_1 \qquad (2\text{-}3)$$

The double integral may be evaluated for configuration of surfaces and is a purely geometric property of the two surfaces (see Figure 3).

The double integral of Eq. 2-3 can be written as

$$F_{12} = \frac{1}{A_1} \int_{A_1} f_{ij} \, dA_1 \qquad (2\text{-}4)$$

The integral F_{12} is defined as the "overall" viewfactor. Integrand f_{ij} is defined, in contrast, as the "local" viewfactor "viewed" from a plane point (i,j) with infinitesimal area dA_1 on A_1 to the second surface A_2. The subscripts i,j denote the location of the plane point on A_1. From Eqs. 2-3 and 2-4 f_{ij} may be defined as

$$f_{ij} = \int_{A_2} \frac{\cos\theta_1 \cos\theta_2}{\pi R^2} \, dA_2 \qquad (2\text{-}5)$$

By referring to Figure 3, the local viewfactor is simply the ratio of the conic-plane projection of A_2 to the area of the base plane of the unit hemisphere, i.e., $f = A_2''/\pi$ (subscripts are ommitted for simplicity).

---

[1] Nusselt's geometric interpretation.

In Figure 3, dA_2' denotes the conic projection of the increment of area dA_2 onto unit hemisphere and A_2'' is the plane projection of dA_2' on-to the base-plane. For surfaces of arbitrary configuration, the conic-plane projection A_2'' can not be easily obtained. The parabolic mirror photographic technique is considered to be the best way to record the modified projection of A_2'' . The modified projection is the parabolic mirror image. By integrating over the image area the local viewfactor "viewed" from the particular location of dA_1 is determined. The WAID is used to determine by electronic means the local viewfactor. By properly dividing the surface A_1 into a finite number of incremental areas, the photographs for each location of the incremental areas on A_1 are taken. After the corresponding local viewfactors are obtained with the WAID, numerical approximate integration is applicable for solving Eq. 2-4 to yield the overall viewfactor. (The methods for solving for the overall viewfactor are not included in this thesis).

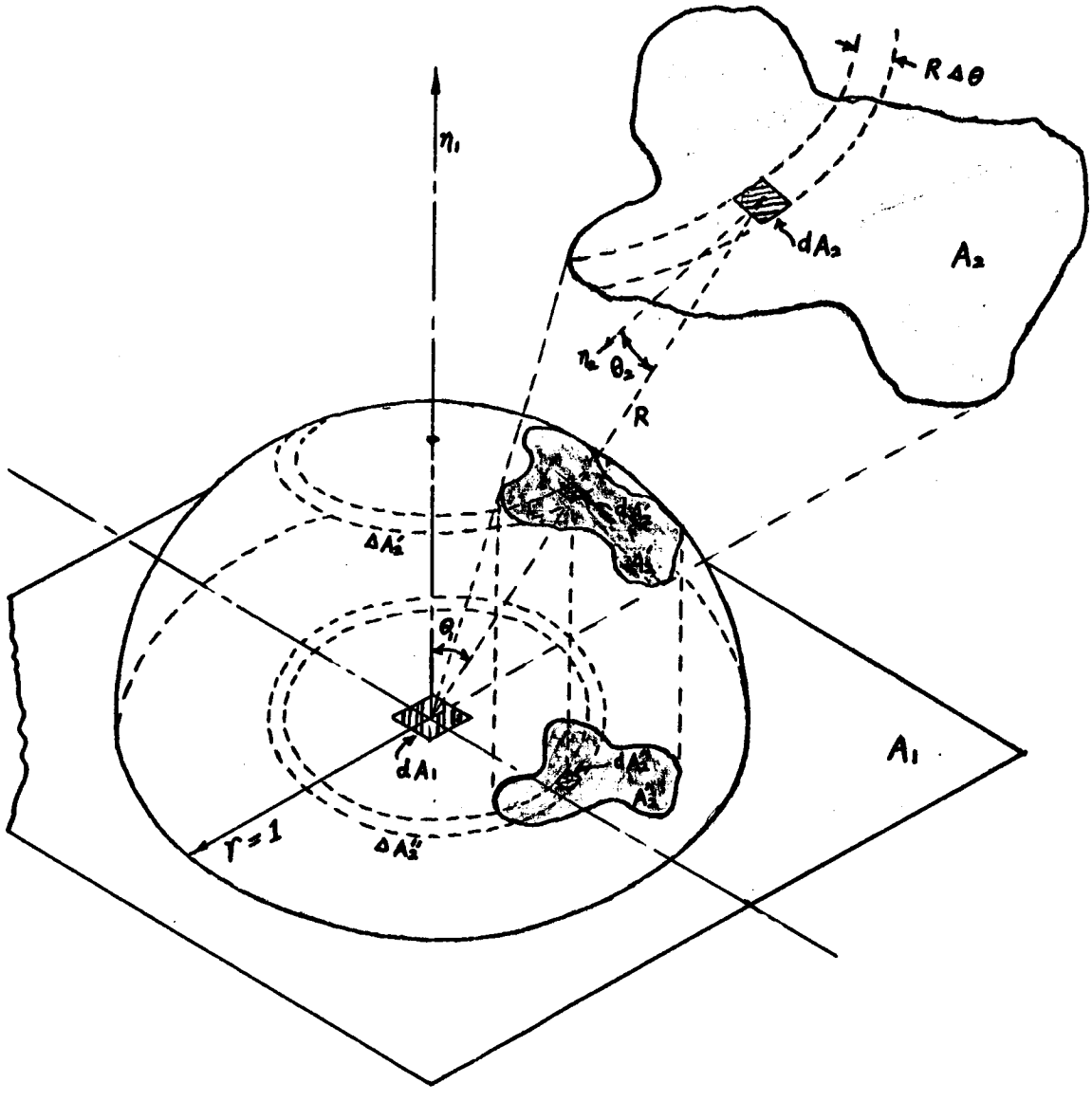

$$F_{12} = \frac{1}{A_1} \int_{A_1} \int_{A_2} \frac{\cos\theta_1 \cdot \cos\theta_2}{\pi R^2} \cdot dA_2\, dA_1$$

$$f = \int_{A_2} \frac{\cos\theta_1 \cdot \cos\theta_2}{\pi R^2} dA_2 = \frac{A_2''}{\pi}$$

Figure 3. Element of the Geometry of Space for the Configuration Factor.

B. PARABOLIC MIRROR PHOTOGRAPH

A parabolic mirror has the property of "seeing" all objects in the hemisphere above its base. In addition it can focus light rays from these objects into parallel rays which can be directed toward a recording device. The photograph taken by a telephotolens camera coupled with a parabolic mirror (as shown in Figure 4) is called the parabolic mirror photograph.

It is evident that the image of the surface A_2 recorded on the photograph is not exactly the same in shape and size as the conic-plane projection of A_2. It has been modified by the parabolic mirror. That is, the weighting factor in the photographic image is not uniform in the radial direction. Thus the viewfactor is not directly proportional to the exposed area of the photograph.

The weighting factor variation of the photograph is as shown in Figure 5. This characteristic curve shows the increment of viewfactor for constant increment in radius. The curve is plotted from the data which is calculated with the aid of a digital computer from the calibration equation

$$\Delta f_n \triangleq f_{(n-1)\to n} = \frac{4r_n^2(1+r_{n-1}^2)^2 - 4r_{n-1}^2(1+r_n^2)^2}{(1+r_n^2)^2(1+r_{n-1}^2)^2} \qquad (2\text{-}6)$$

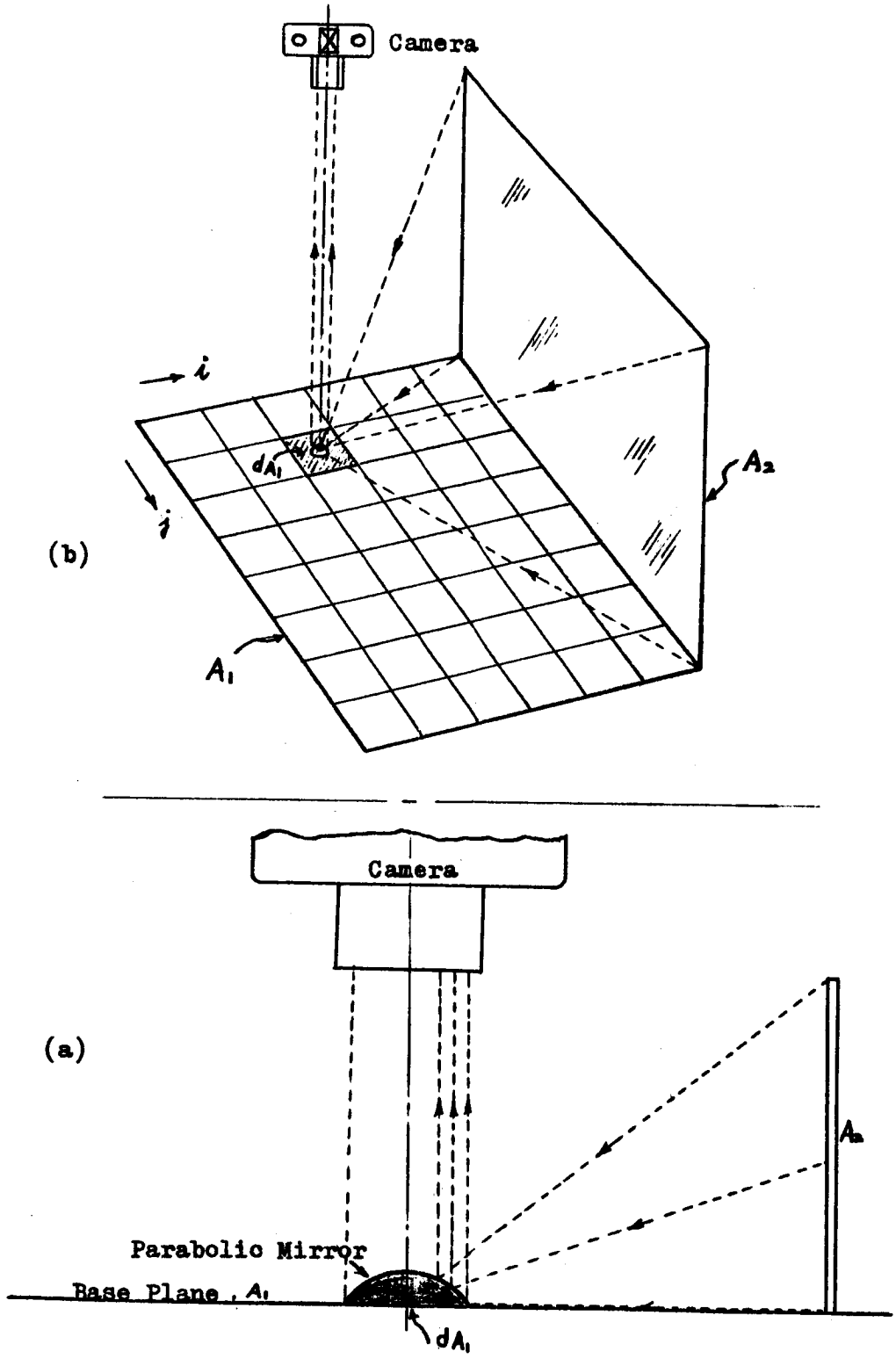

Figure 4. Camera and Parabolic Mirror Location.

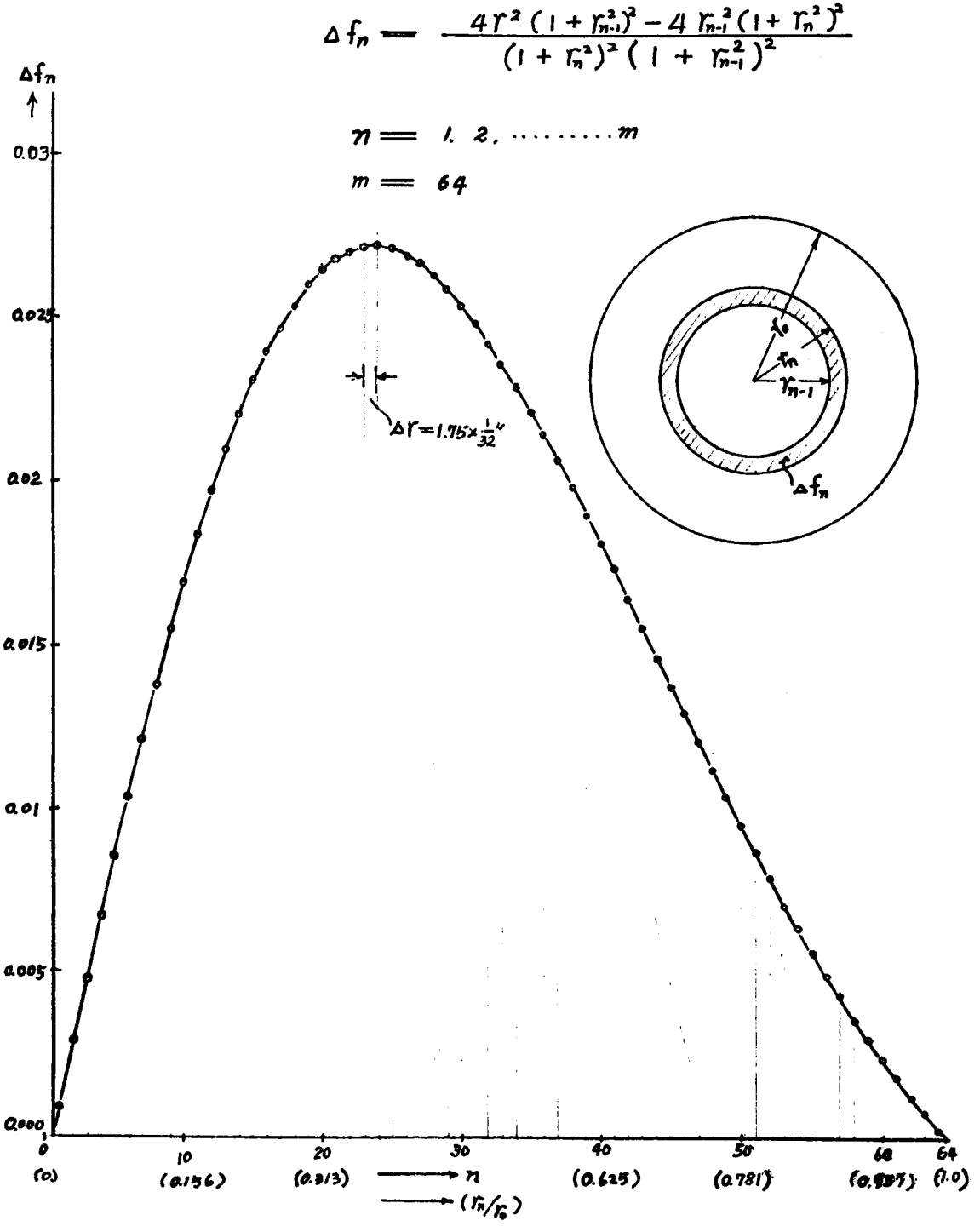

Figure 5. Increment of Viewfactor vs Constant Increment in r

where Δf_n is the increment of viewfactor represented by the circular band having radii of r_{n-1} and r_n (see Appendix A for its detailed derivations and data calculated for m = 64).

C. VIEWFACTOR DETERMINATION

To determine the viewfactor from a given parabolic mirror photograph, two feasible ways can be considered: (1) Equal increment in radius, Δr, and variable increment in viewfactor Δf_n; and (2) Equal increment in viewfactor, Δf, and variable increment in radius, Δr_n. For grid counting by human operators the second method may be more suitable. This method is adopted by Matheny and Carden. In this method a 7" ϕ photograph had been divided into 20 equal Δf annular bands and each of the bands was further divided into 50 equal grids. But for analogous simulation, the first method is easier because it enables one to make uniform distribution of the readhead elements, i.e., the electric contacts (see detail in Chapter III).

In this thesis the first method using equal increments of radius was developed and employed in the problem solution. Consider the normalized unit circle of a photograph as shown in Figure 6. The photograph has been divided into m concentric circles

of equal increment in radius, $\Delta r = \frac{1}{m}$. The increment of viewfactor Δf_n contributed by the annular area between r_{n-1} and r_n can be determined from Eq. 2-6. Then the increment of viewfactor for a portion of the same annular area can be represented as

$$(\Delta f)_n = \frac{\theta_{n2} - \theta_{n1}}{2\pi} \Delta f_n, \quad n = 1, 2, \ldots, m \qquad (2\text{-}7)$$

where m is the number of annular bands into which the unit circular area is divided. The total viewfactor represented by the exposed area of the photograph is

$$f = \lim_{m\to\infty} \sum_{n=1}^{m} (\Delta f)_n = \lim_{m\to\infty} \sum_{n=1}^{m} \frac{\theta_{n2} - \theta_{n1}}{2\pi} \Delta f_n \qquad (2\text{-}8)$$

Assume the area has a normally smooth shape and m is large then

$$f \approx \sum_{n=1}^{m} \frac{\theta_{n2} - \theta_{n1}}{2\pi} \Delta f_n, \quad m \gg 1 \qquad (2\text{-}9)$$

Since $(\theta_{n2} - \theta_{n1})/2\pi$ is a dimensionless ratio, it can be replaced by $(t_{n2} - t_{n1})/T$, where t_{n2}, t_{n1}, and T are in seconds corresponding to θ_{n2}, θ_{n1}, and 2π in radians. Eq. 2-9 then can be expressed as a function of time

$$f \approx \sum_{n=1}^{m} \frac{t_{n2} - t_{n1}}{T} \Delta f_n = \frac{1}{T} \sum_{n=1}^{m} \int_{t_{n1}}^{t_{n2}} \Delta f_n \, dt \qquad (2\text{-}10)$$

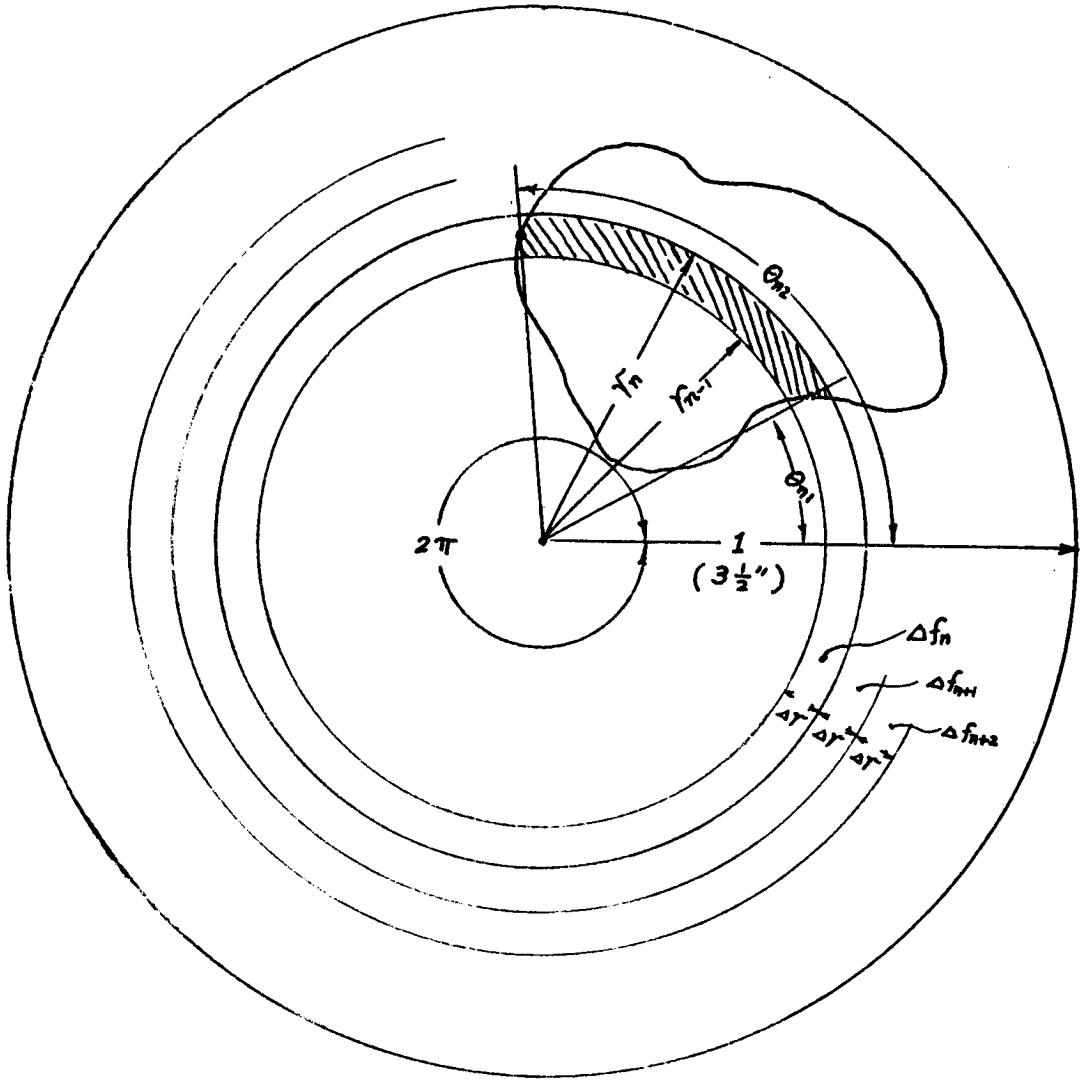

$$f \approx \sum_{n=1}^{m} \frac{\theta_{n2} - \theta_{n1}}{2\pi} \cdot \Delta f_n = \sum_{n=1}^{m} \frac{t_{n2} - t_{n1}}{T} \cdot \Delta f_n$$

$$f \approx \frac{1}{T} \sum_{n=1}^{m} \int_{t_{n1}}^{t_{n2}} \Delta f_n \cdot dt \qquad n = 1, 2, \ldots m \qquad m \gg 1$$

Figure 6. A Parabolic Mirror Photograph Model Showing m Equally Divided Annular Bands

which is the equation that must be integrated by the WAID. Eq. 2-10 shows that the viewfactor can be obtained by performing integration, summation, and multiplication by the correct weighting factor over the properly enlarged parabolic mirror photograph. The accuracy of this approximate equation depends upon the value of m being chosen. (The larger the m chosen the higher the accuracy is).

Operational amplifiers are used in the analogous simulation of Eq. 2-10 because of their simplicity, reliability, good performance, and miniature size.

Consider an operational amplifier circuit as shown in Figure 7. To simplify the quantitative expression for the relationship between E_o and E_1, the following assumptions regarding the amplifier are made: (1) the amplifier is assumed to have infinite input impedance; (2) the amplifier has nearly infinite gain and bandwidth; (3) the output impedance of the amplifier is zero.

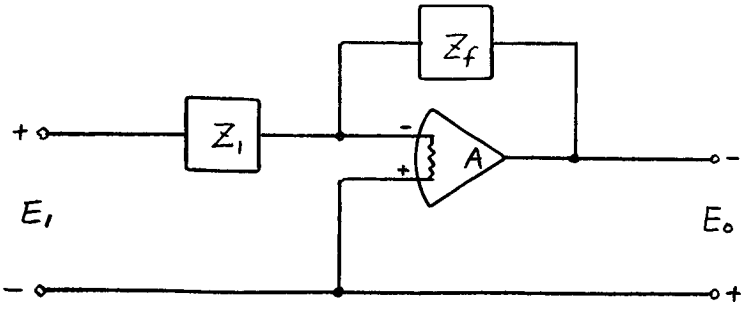

Figure 7 Operational Amplifier Circuit

Then the output relating to the input voltage can be expressed as

$$E_o(s) = - E_i(s)\frac{Z_f(s)}{Z_i(s)} \qquad (2\text{-}11)$$

Thus the output E_o is simply the input E_1 times the ratio of the feedback impedance and the input impedance. (Here each parameter in Eq. 2-11 is expressed in Laplace transforms.) This conclusion is valid in most actual cases since most of the solidstate operational amplifiers have open loop gains A in the range from 10^4 to 10^9; very high input impedances from 100 kilohms to several megohms; and very small output impedance from 10 to 500 ohms.

For circuit with multiple inputs Eq. 2-10 becomes

$$E_o(s) = - \sum_{n=1}^{m} \frac{E_n(s)\cdot Z_f(s)}{Z_n(s)} \;, \quad n = 1, 2, \cdots m \qquad (2\text{-}12)$$

When Z_n and Z_f are represented by resistors R_n and R_f, respectively, the circuit which can be expressed by Eq. 2-12 becomes a summer. If Z_f is replaced by a capacitor C and Z_1 by R_1, the circuit shown in Figure 7 becomes an integrator. For a circuit having multiple input resistors R_n and a feedback capacitor C as shown in Figure 8.

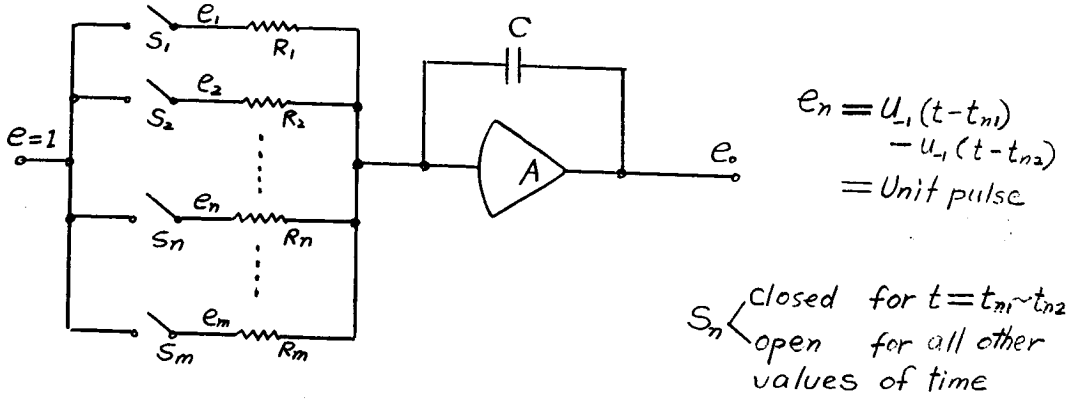

Figure 8. An Integrating Circuit with Multiple Inputs

where S_n stands for a switch which is assumed to be closed for $t = t_{n1} \sim t_{n2}$ and open for all other values of time. The input becomes a unit pulse and the output can be expressed in time domain as

$$e_o \approx -\sum_{n=1}^{m} \frac{1}{R_n C} \int_{t_{n1}}^{t_{n2}} e_n \, dt = -\sum_{n=1}^{m} \frac{t_{n2}-t_{n1}}{R_n C} \qquad (2\text{-}13)$$

It is shown by Eq. 2-13 that the operational circuit of Figure 8 can be used to perform summation, multiplication and integration at one time. Thus the circuit configuration can be used for the evaluation of Eq. 2-10.

In the WAID , two operational amplifiers (one for a summer and the other for an integrator) are used for easy gain selection arrangements of the operational circuit. For the minimization of the output

error due to drift and noise the number of inputs and the gain of an integrator should be kept as small as possible. In the WAID, the maximum gain of 100 is chosen for the integrator. The maximum overall gain of 67 is used when viewfactor is small; e.g., 0.01-0.001.

The pictorial diagram of the WAID is as shown in Figure 9. From the diagram the output voltage which is the viewfactor, can be expressed by the equation,

$$e_o = \sum_{n=1}^{m} \frac{R_a}{R_n} \cdot \frac{t_{n2} - t_{n1}}{R_b C} \qquad (2\text{-}14)$$

Comparing Eq. 2-14 with Eq. 2-10 the gain of the summer can be adjusted to match the weighting factor by

$$\sum_{n=1}^{m} \frac{R_a}{R_n} = \sum_{n=1}^{m} \Delta f_n = 1 \quad or \quad \Delta f_n = \frac{R_a}{R_n} \qquad (2\text{-}15)$$

and the gain of the integrator can be determined by:

$$\frac{1}{T} = \frac{1}{R_b C} \qquad (2\text{-}16)$$

where the "computing" time T is determined from the constant r.p.m. of the turntable i.e. T = 60/rpm(sec.). Electrical wipers are used to form the readhead because it is simpler and more reliable than others such as

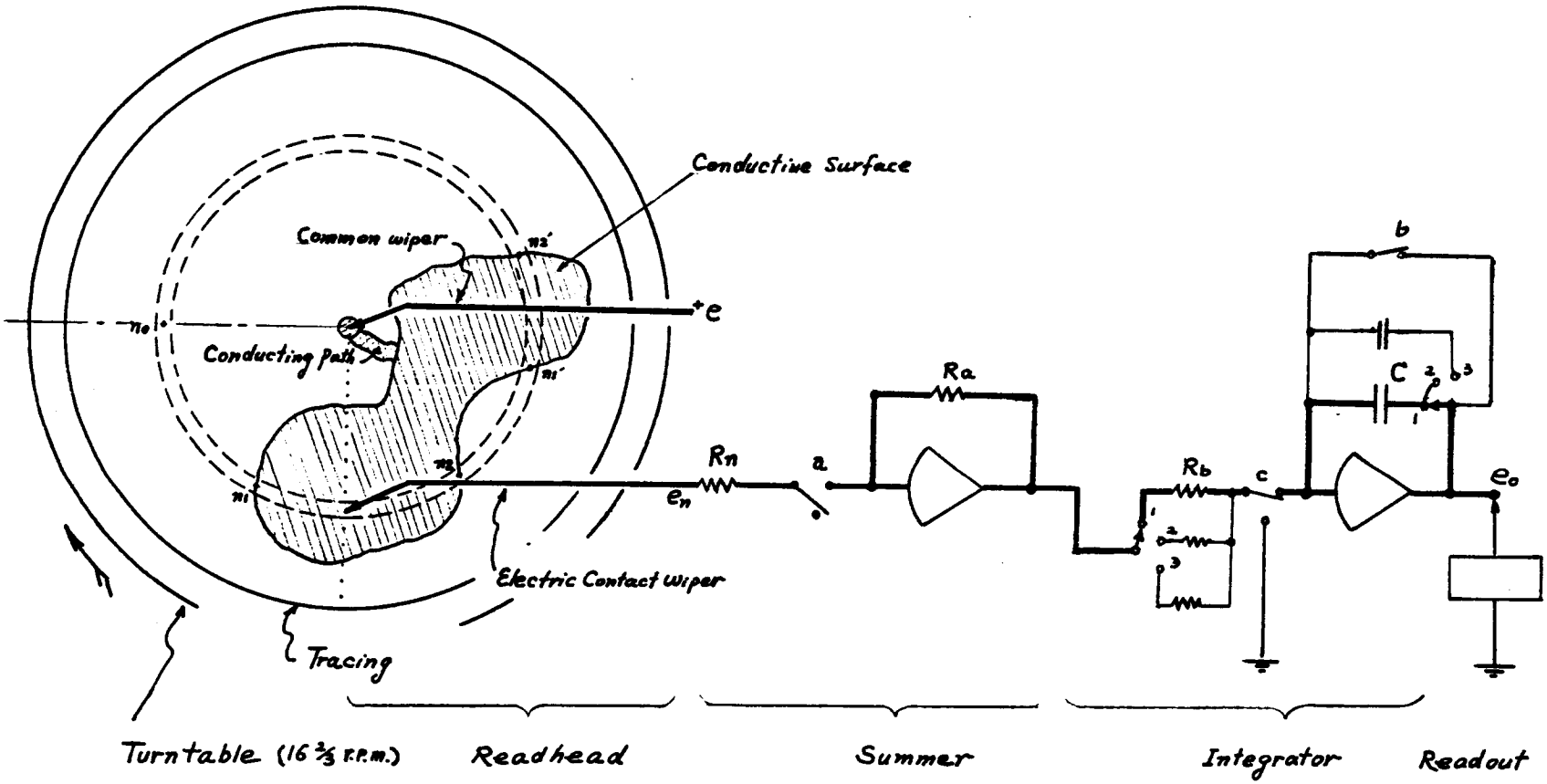

Figure 9. Pictorial Diagram of the Integrating Device.

photosensor. The electrical wiper is equivalent to the switch S_n in Fig. 8. The input to the summer will be "on" or "off" depending upon whether or not the wiper is touching the conductive surface. To clarify the performance of the operational circuit, only the n-th wiper is considered and the input, output waveforms are as shown in Figure 10. The total performance is simply the superimposed value of each of the individual results.

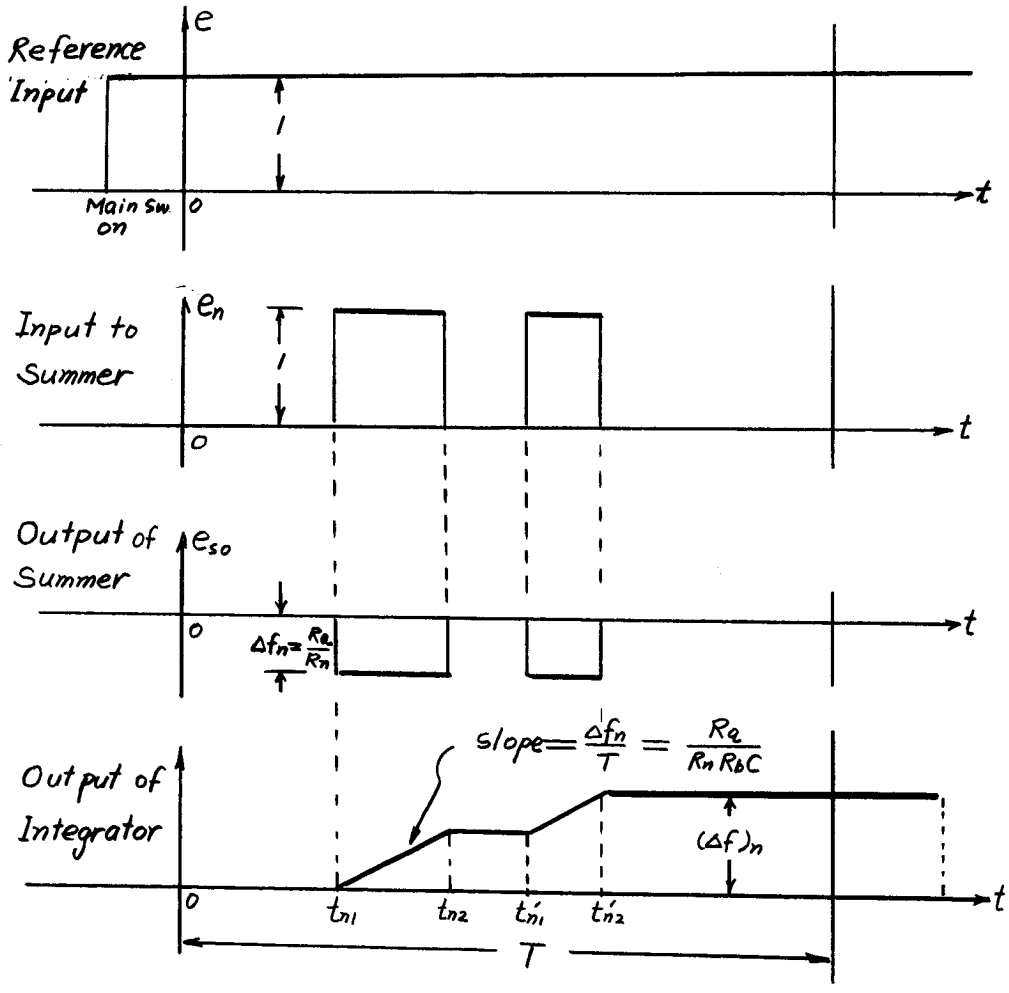

Figure 10 Input Output Waveforms Showing the n-th Input

CHAPTER III

THE INTEGRATING DEVICE

A. OVERALL DESCRIPTION

As described in the Introduction, the Weighted-Area Integrating Device (WAID), is used to determine the viewfactor by integrating over the exposed area of a parabolic mirror photographic image. The WAID is composed of: a constant speed turntable; an electric contact type readhead; a summer; an integrator; and a digital voltmeter readout. With a 3.5" effective length of readhead, the maximum area which can be integrated by the WAID is confined to a 7" diameter circle. The photographic image on which the surface to be integrated is situated is enlarged to exactly 7" diameter and traced onto a piece of tracing paper. The exposed area on the tracing is filled in with a metallic paint, such as General Cement's silver print. A conducting path is provided between the conductive area and the center. (This is explained in more

detail in Section B(a)).

To perform integration, the tracing is placed on the turntable and securely affixed to the turntable surface with adhesive tapes. The tracing is so placed that its center coincides with that of the turntable. After the tracing is seated properly on the turntable, the readhead arm is situated over the turntable. Then individual contacts which are evenly distributed over the readhead arm are spring loaded to ride on the surface of the tracing. When the main switch is closed, a reference voltage is continuously applied to the common contact located at the center of the tracing. Through the conducting path the reference voltage appears on the whole conductive surface. As the turntable turns, some of the contacts pass over the conductive surface. As long as one of the contacts is touching the surface, the reference voltage input is applied to its corresponding input circuit of the summer amplifier. When the turntable reaches the desired constant speed (16 2/3 rpm) a "compute" switch is thrown. At this instant, the relay contact "a" is closed. (See Fig. 9). The output of the summer is fed into the input circuit of the integrator. A short instant after the switch is thrown (0-3.6 sec. depending on

the position of the turntable trigger when the switch is thrown), the turntable trips an "integrate" relay (to open "b" contact). At this instant, integration starts. Exactly one revolution (T = 3.6 sec.) later, the turntable trips a "hold" relay (to open "c" contact). Integration is stopped and the output of the integrator is "held" and appears on a digital readout which is connected to the output of the integrator. The digital output is the desired viewfactor. A "reset" switch can be thrown at any time to "reset" the WAID.

One range selector is provided for viewfactor range selection. Three ranges available are: (1) 1.0-0.1; (2) 0.1-0.01; (3) 0.01-0.001. The gains of the WAID are so calibrated that if proper range selection is made, the output reading will always be in the range from 10v to 1v. The equivalent viewfactors corresponding to output reading for each range selection are as shown in Table I.

TABLE I

Selector Range	Output Reading (V)	Equivalent Viewfactor (f)
1.0 - 0.1	10.00 1.000	1.0 0.1
0.1 - 0.01	10.00 1.000	0.1 0.01
0.01 - 0.001	10.00 1.000 0.100	0.01 0.001 0.0001

The range should always be properly selected so that the output will be in the optimum range of 10v - 1v. Whenever the output exceeds 10v it is overloaded, since the maximum rated output is 10v. The operator may have to select judiciously a proper range before running the machine. If the output is higher than 10 volts, the next higher range should be used and another computation made. On the other hand, if the output is much lower than 1 volt the next lower range should be used.

Two calibrations are suggested before using the WAID. One is for offset balancing of the two operational amplifiers. Another one is for the turntable speed calibration. In an ideal case, the output should be zero when the input is zero. Actually this is not always the case because of minor variations in temperature, power supply, etc. Two offset balancing circuits are provided for each amplifier. Each balancing circuit consists of two trimming potentiometers for voltage-offset (E_{os}) zeroing and current-offset (I_{os}) zeroing. The turntable speed is calibrated by adjusting a fine speed knob which is attached to the turntable panel. Detailed descriptions regarding the calibration methods and control sequence are included as a part of the following section on Practical Design Considerations.

B. PRACTICAL DESIGN CONSIDERATIONS

(a) Preparation of Tracing

High quality tracing paper is used for the tracing. This paper has negligible shrinkage due to moisture or temperature changes. For convenience the size of the paper should be 8 1/2 inches in diameter. Two concentric circles with diameters of 7" and 3/16", respectively, are printed on the paper. A pair of perpendicular center-lines are also printed on the paper for coinciding the center of the paper with the center of the turntable. To prepare a tracing, a photographic image is projected onto the tracing paper. By adjusting the focus of the projector, the image is enlarged exactly to 7" in diameter and situated so that it coincides with the 7" diameter circle on the paper. With a pencil, the outline of the exposed area of the image is carefully drawn. The whole area and the small circle at the center are then filled in with a metallic paint such as silver print or copper print. The same print is used to provide a conduction path of around 3/8" width from the center to the exposed area. (The shortest path is preferable). After the paint has dried, the conductive path must be painted with an overlay of insulating lacquer. The lacquer can also be used to "erase"

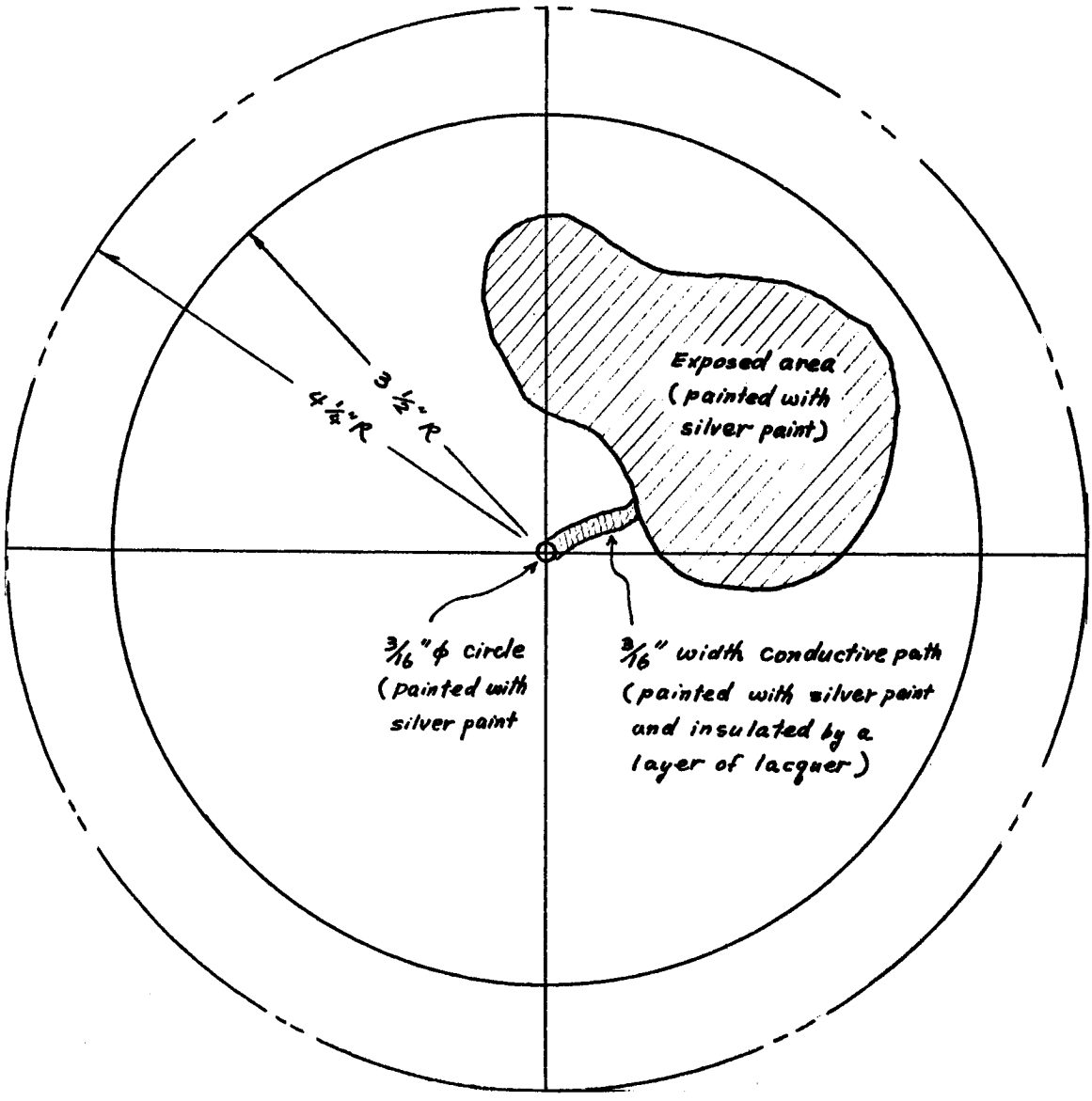

Figure 11. A Sample of the Tracing
(not in scale)

any mispainted area. A sample of the actual tracing is as shown in Figure 11.

(b) Turntable

Since the integrating time of the WAID is directly coupled to the speed of the turntable, a dynamically balanced turntable with absolutely constant rotating speed is the most desirable. The turntable chosen for the WAID is a conventional broadcast type phonograph turntable (Thorens Model TD-124). A flat aluminum disc of 12" diameter and 1/2" thickness is mounted on the turntable, providing a smooth surface for the tracing. On the surface of the disc, a pair of perpendicular center-lines are marked for center fixing of the tracing. The lowest available speed of 16 2/3 r.p.m. was chosen as the turntable operating speed. For lower speeds, the contact resistances between the electric contacts and the painted surface on the tracing are smaller and more stable. The lowest speed provides ample time (T = 3.6 sec) for a satisfactory operation of the digital voltmeter and the relays which are used in the control circuit. Also, this lowest speed makes possible a reasonable input impedance (R_b = T/C) to the integrator. An auxiliary dc motor (27V, 0.05A) is used to com-

pensate the rotating torque of the turntable motor. A built-in stroboscope enables one to maintain the rated speed to the highest accuracy of 0.1% by adjusting a fine-speed knob which is attached on the turntable panel and has adjustable limits of ± 3%.

(c) Readhead

It is evident that a better accuracy of the WAID is obtainable by increasing the number of the electrical wipers, m. In the practical design there is a limit on value of m. The input impedances to the summer will be increased by increasing m. From Eq.2-15, the relation $\sum \frac{1}{R_n} = \frac{1}{R_a}$ exists. Thus for a constant feedback, R_a, the input resistance R_n will be increased by increasing m. In addition m is limited by the realizable physical spacing between contacts for a limited length of the readhead arm (3.5").

In the grid counting method[1], m = 20 was used in the division of a 7" diameter photograph and an average accuracy of ± 1% was obtained [2]. By considering the above two limitations and also the accuracy requirement, m = 64 was chosen as the best compromise value. The physical construction of the readhead is as shown in Figure 12. The electric wipers

---

[1]See Footnote (1) in Chapter II, Section C.

[2]Matheny and Carden, "Thermal Design Studies", Final Report Contract NAS8-5270 Sept., 1965, pp 110.

are made of conductive wires which have proper stiffness to provide springloading on the tracing. The load pressure is adjustable at the end of the readhead arm.

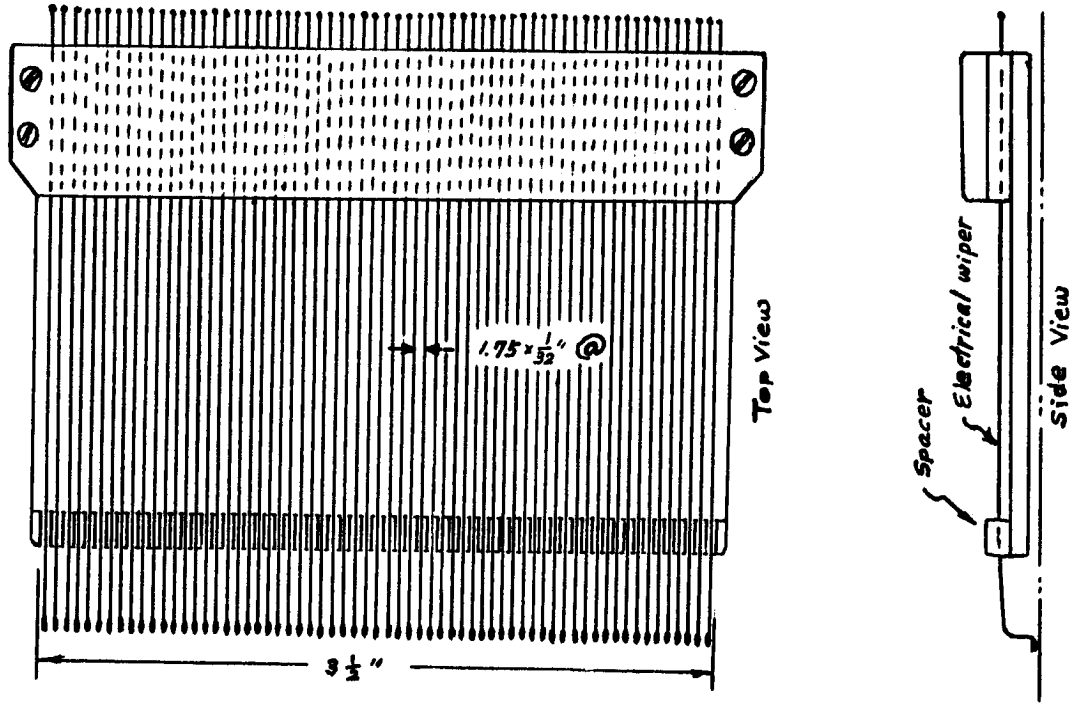

Figure 12 Physical Construction of the Readhead.

(d) Operational Circuit

(i) Operational Amplifiers. The operational amplifier used in the WAID is the heart of the integrating device. Two NEXUS CLA-3 all-silicon solid-state amplifiers are used in the operational circuit because of their: (1) good electrical stability over a wide range of temperature (-24°C to + 85°C); (2) low input offset current characteristics ($\pm$ 1.5 nano A, max.); (3) high gain (60,000); (4) high input impedance (Z_d = 1 meg ohm); (5) high degree of protection (against electrical overload); and (6) minature size (2 x 1.1 x 0.6"). Some important characteristic data regarding this type of operational amplifier are shown in Appendix B.

(ii) Gain Selections and the Determination of R_n, R_a, R_b, and C. The overall gain of the operational circuits must be adjusted to meet the possible range variation in viewfactor from 1.0 to 0.001 so that the output can always be kept in the optimum range of 10V - IV. (If the output is lower than IV it will degrade the accuracy. For example: If 4-digit readout unit is used and f = 0.001234, then e_o=0.012 for gain of 1; e_o= 0.123 for gain of 10; and e_o=1.234 for gain of 100.) For easy conversion of

the output (voltage) into viewfactor, the circuitry is so calibrated that when the output is 10V the equivalent viewfactor will be 1, 0.1 or 0.01, depending on the overall gain chosen. With a reference input voltage being chosen as +15 volts D.C., the gain distribution is as shown in Table II. (The reference input voltage was so chosen because it is the maximum allowable rated input of the amplifier and is also the only available highly regulated constant voltage source in the WAID).

TABLE II

Selector Range (f)	Summer Gain	Integrator Gain	Overall Gain	Output Voltage	Equivalent View factor (V)
1-0.1	2/3	1	0.6667	10 1	1.0 0.1
0.1-0.01	2/3	10	6.667	10 1	0.1 0.01
0.01-0.001	2/3	100	66.67	10 1	0.01 0.001

To determine each parameter in the operational circuit, consider the simplified circuit diagram of the WAID as shown in Figure 13. The bold line portion in the figure represents a circuit for unity viewfactor (f=1).

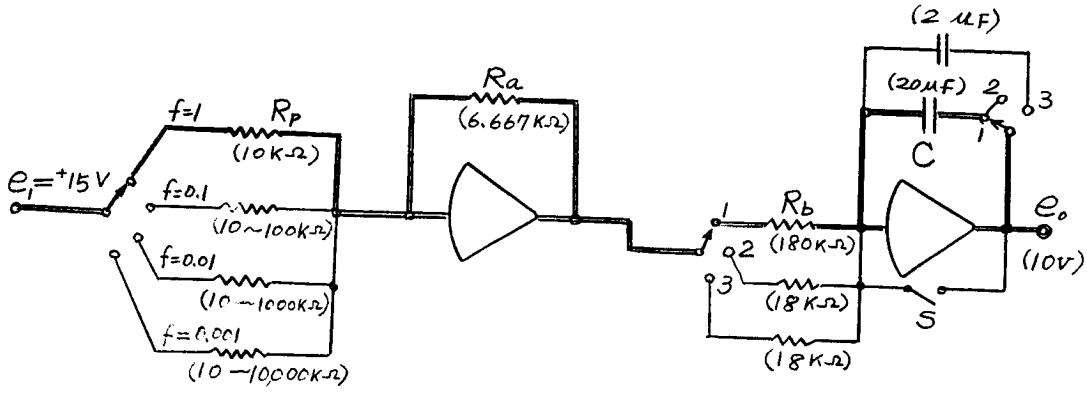

Figure 13 Simplified Circuit Diagram of the WAID.

where $R_P = \sum_{n=1}^{m} \frac{1}{R_n}$ is the equivalent parallel input resistance when f = 1.

Then the output e_o can be written as

$$e_o = e_1 \frac{R_a}{R_p} \cdot \frac{t}{R_b C} \qquad (3\text{-}1)$$

Now for $f \rightarrow 1$; i.e. $t \rightarrow T = 3.6$ sec.; $e_o \rightarrow 10V.$;

$$\frac{1}{R_P} \rightarrow \sum_{n=1}^{m} \frac{1}{R_n}$$

and $e_1 = 15$, Eq. 3-1 becomes

$$f = \frac{e_o}{10} = \left[\frac{e_1}{10} \sum_{n=1}^{m} \frac{R_a}{R_n}\right]\left[\frac{T}{R_b C}\right] \qquad (3\text{-}2)$$

or

$$f = 1 = \left[\sum_{n=1}^{m} \frac{1.5\, R_a}{R_n}\right]\left[\frac{T}{R_b C}\right]$$

and Eq. 2-10 yields

$$f = \sum_{n=1}^{m} \Delta f_n \frac{t_{n2} - t_{n1}}{T} = \sum_{n=1}^{m} \Delta f_n \cdot (1) = 1 \qquad (3\text{-}3)$$

Comparing the above two equations, the circuit parameters, R_n, R_a, R_b and C, can be determined by the following two equations:

$$R_n = \frac{1.5\, R_a}{\Delta f_n} \quad , \quad n = 1, 2, 3 \cdots\cdots m \qquad (3\text{-}4)$$

$$R_b C = T \qquad (3\text{-}5)$$

The capacitor C is a critical component in the integrating circuit. The stringent requirements are for large capacity, small size and very good tolerance stability. A larger capacity is desirable to maintain steady output when the operational circuit is switched to "hold" position for reading out the output. Two metalized mylar capacitors of 20 μf and 2 μf (by Texas Capacitor Co.) were selected because of their good performances (0.03% change in capacity per ^{o}C over the temperature range from 0^{o}C to 40^{o}C). With C = 20 μf and T = 3.6 the input resistance to the integrator is R_b = 180 KΩ.

The input resistances R_n are limited to a few megohms for all practical purposes. This follows,

because as a rule of thumb, the summing impedance should not be much greater than the amplifier's open loop input impedance Z_{in} which for most solid state operational amplifiers is in the range from 0.1 to 1 megohm (NEXUS Type CLA-3 has 1 MΩ). As the summing impedance becomes much greater than Z_{in}, voltage drift and noise become degraded.

By choosing R_a = 100/15 kilohms, the values for R_n vary from 368 kilohm to 40.33 megohm. The data as shown in Table III is calculated from Eq. 2-6 with the aid of a digital computer. (See Appendix A for the calculation of Δf_n for each value of n).

TABLE III ($Ra = \frac{100}{15}$ kΩ, $m = 64$)

n	Δf_n	$1/\Delta f_n$	$R_n = \frac{1.5 Ra}{\Delta f_n}$ (MΩ)
1	0.000976086	1024.50000	10.245000
2	0.002922545	342.16749	3.421675
3	0.004851934	206.10339	2.061034
4	0.006753074	148.08071	1.480807
5	0.008615107	116.07518	1.160752
6	0.010427575	95.89957	0.958996
7	0.012180580	82.09790	0.820979
8	0.013864823	72.12497	0.721250
9	0.015471728	64.63402	0.646340
10	0.016993539	58.84589	0.588459
11	0.018423311	54.27906	0.542781
12	0.019755001	50.62009	0.506201
13	0.020983584	47.65630	0.476563
14	0.022104859	45.23892	0.452389
15	0.023115714	43.26062	0.432606
16	0.024013818	41.64269	0.416427
17	0.024789081	40.32570	0.403257
18	0.025467870	39.26516	0.392652
19	0.025023994	38.42608	0.384261
20	0.026467429	37.78229	0.377823
21	0.026800561	37.31265	0.373127
22	0.027025760	37.00174	0.370017
23	0.027146883	36.83664	0.368366
24	0.027167426	36.80879	0.368088

25	0.027092037	36.91122	0.369112
26	0.026925516	37.13949	0.371395
27	0.026673102	37.59095	0.374910
28	0.026339903	37.96521	0.379652
29	0.025932095	38.56225	0.385623
30	0.025454871	39.28521	0.392852
31	0.024914609	40.13709	0.401371
32	0.024316589	41.12419	0.411242
33	0.023667144	42.25267	0.422527
34	0.022971580	43.53205	0.435321
35	0.022236009	44.97210	0.449721
36	0.021465364	46.58668	0.465867
37	0.020665316	48.39026	0.483903
38	0.019840510	50.40193	0.504019
39	0.018996239	52.64200	0.526420
40	0.018136631	55.13703	0.551370
41	0.017266223	57.91655	0.579166
42	0.016388956	61.01670	0.610167
43	0.015508760	64.47969	0.644797
44	0.014628618	68.35916	0.683592
45	0.013752380	72.71469	0.727147
46	0.012882373	77.62545	0.776255
47	0.012021667	83.18314	0.831831
48	0.011172263	89.50738	0.895074
49	0.010336621	96.74341	0.967434
50	0.009516315	105.08269	1.050827
51	0.008713433	114.76532	1.147653
52	0.007929027	126.11887	1.261189
53	0.007164578	139.57557	1.395756
54	0.006420776	155.74442	1.557444
55	0.005698975	175.47015	1.754702
56	0.004999477	200.02092	2.000209
57	0.004322870	231.32781	2.313278
58	0.003669699	272.50194	2.725019
59	0.003040202	328.92550	3.289255
60	0.002434303	410.79517	4.107952
61	0.001852369	539.84936	5.398494
62	0.001294038	772.77501	7.727750
63	0.000759400	1316.82840	13.168284
64	0.000247928	4033.43510	40.334351

Each of the input and feedback resistors (R_n, R_a, R_b) is composed of a fixed and a variable resistor connected in series. The correct value of each of these resistors is of little importance since we are interested only in the correct ratios of the feedback impedance to each input resistance, i.e. R_a/R_n, $1/R_bC$. One of the best and easiest ways to set these resistors is to make use of the actual operational circuitry. This method is illustrated as shown in Figure 14.

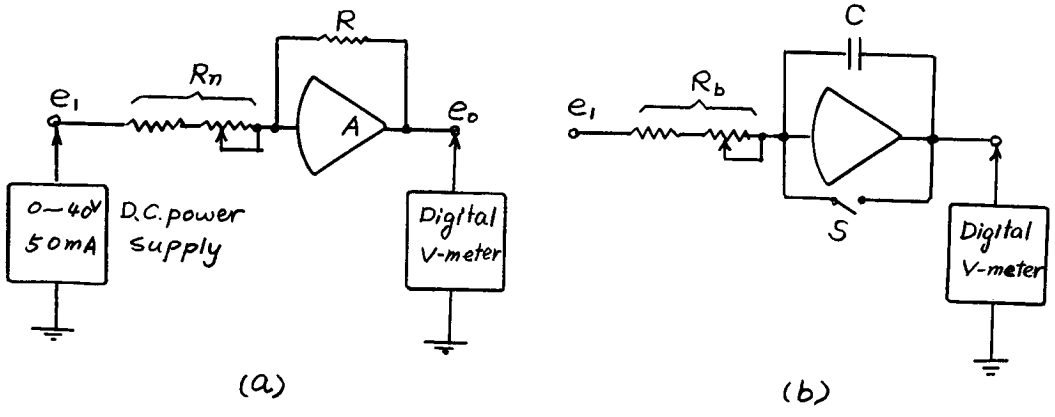

Figure 14 Circuits for Setting R_n and R_b

To set R_n, circuit (a) is used. For a fixed resistor R and a known input, e_1, R_n can be adjusted so that the output reading from a digital voltmeter, e_o, satisfies the equation:

$$e_o = - e_i \frac{R}{R_n} = - e_i \Delta f_n$$

where Δf_n is given in Table III. All other R_n values can be adjusted in the same way.

To set R_b circuit (b) is used. By fixing C and e_1, R_b can be adjusted such that $e_o = -e_1 \frac{t}{R_b C}$, where switch S is open for t = 3.6 sec. (The actual switching circuit is used to control the by-pass switch S)

Using the above method, any weighting factor can be easily adjusted to meet any different weighting function.

(e) Calibration Methods

One should balance the operational amplifiers and check the turntable speed before using the WAID.

(i) Zeroing of Operational Amplifiers. A built-in balancing circuit is provided in the WAID for the zeroing of voltage offset and currect offset of each amplifier. The schematic diagram of the balancing circuit is as shown in Figure 15 (only one of the operational amplifiers is shown). This balancing circuit was obtained from the NEXUS manufacturers. The offset voltage can be balanced to zero by adjusting trimpot E_{os}. With a closed loop gain of 100 in the E_{os} zeroing circuit, every $\pm$ 10 μV of offset voltage is visible on the digital voltmeter (4-digit). After the offset voltage has been balanced, zeroing

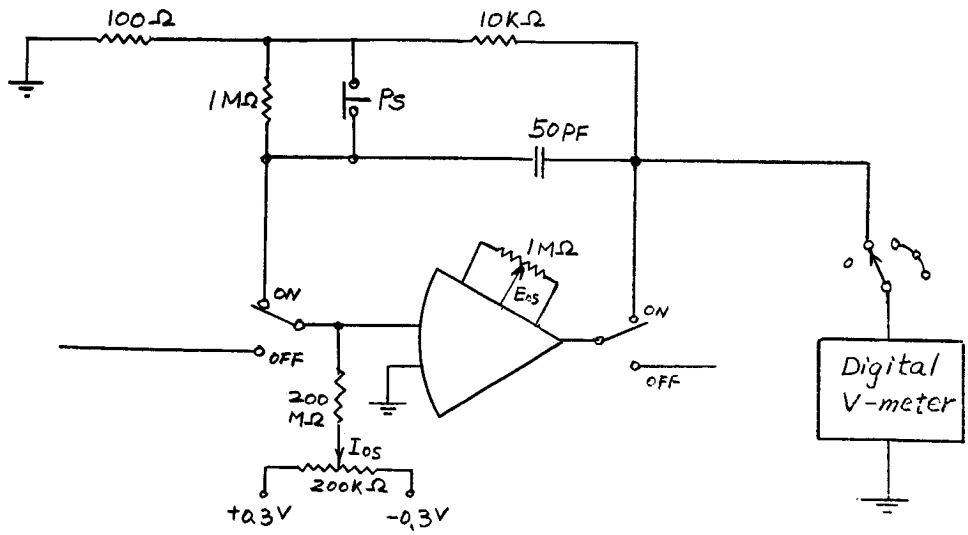

Figure 15 Amplifier Balancing Circuit

of the current offset can be made by pushing and holding switch ps and adjusting trim-pot I_{os}. Using this circuit, as little as 10^{-2} nanoampere of offset current can be detected by the digital voltmeter. The amplifiers should be balanced only after reaching thermal equilibrium (a few minutes after the unit is turned on).

(ii) Turntable Speed Balancing -- Integrating Time Calibration. It may be seen from Eq. (3-1) that the output of the WAID is determined by the input-feedback impedances of the integrating circuit and the integrating time (T) which is proportional

to the turntable speed. Since the output for each selector range has been precalibrated (according to Table II) at the rated speed of 16 2/3 r.p.m., a speed check is as important as the zeroing of the operational amplifiers. The integrating time (the turntable speed) should be checked every time when the load conditions are appreciably changed, e.g., when the readhead spring tension has been adjusted or much change is made in the painted area of the tracing. The following procedures are suggested for checking both the speed and the overall performance of the WAID:

(1) Check reference input (Adjust R_a). Set selector 1 (see Figure 16) at Cal. 2 and selector 2 at f = 0.1. Turn on the motor. Push "compute" switch and then read the output of the summer from the digital meter. The correct reading should be 1.000 ± 0.002. If not, adjust R_a.

(2) Check integrating time (Adjust turntable speed). Set selector 1 at the first range (1.0-0.1) and selector 2 at f = 0.1. Place the readhead on any tracing which must be integrated and compute. If the integrating time is correct (also assume R_b is correct), the output should be 1.000 ± 0.002. If not, adjust the fine speed knob 1 and rerun it until the

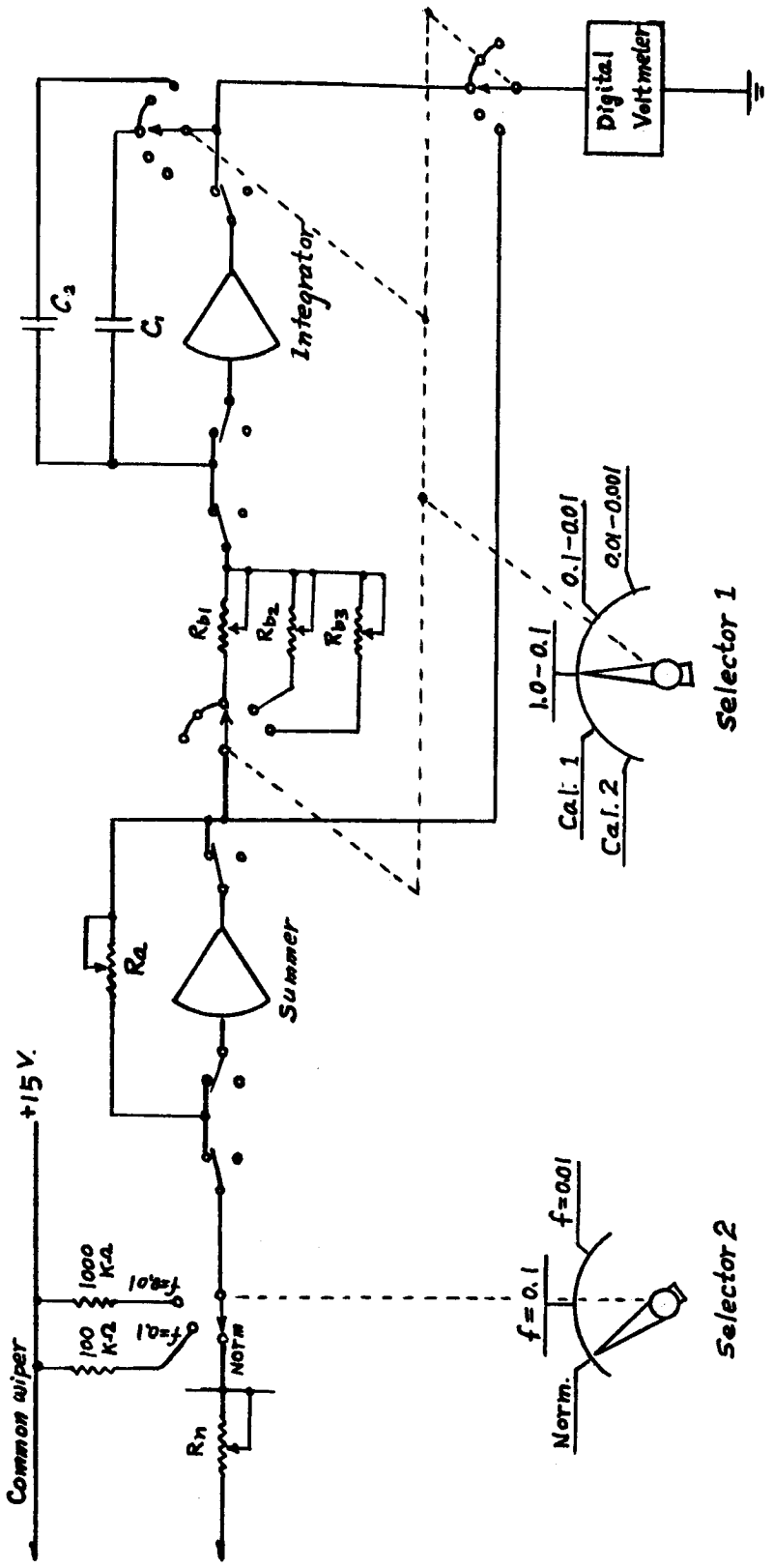

Figure 16 Selector Arrangement.

correct reading is obtained. In case the speed knob 1 is out of its adjustable limit (± 3% of speed or ± 0.006 V of the digital meter), reset the knob at the middle position and adjust the auxiliary motor knob 2. to the rated speed of 16 2/3 r.p.m. by watching the stroboscope.

(3) Overall check (Adjust readhead spring and R_a). Use an actual tracing of unity viewfactor and repeat the procedures in step (1) except set selector 2 at the Normal position. If each of the contact conditions of the readhead is normal and the input resistances R_n are correct, the output of the summer should be 10.00 ± 0.02. If the reading is too far out of range, the readhead wiring should be checked first and then if necessary, each R_n should be calibrated according to the method described in Section B-(d), Chapter III.

(iii) Calibration of the Selector Ranges-Adjust R_b. The range calibrations should be made at rated speed (16 2/3 r.p.m.) and for the correct summer output which is 1.000 or 0.100 depending on whether the position of selector 2 is at f = 0.1 or f = 0.01. Rb1 and Rb2 are calibrated for the first and second range, respectively, by setting selector 2 at f = 0.1. Rb3 is then calibrated for the third range by setting selector 2 at f = 0.01.

(f) Switching Arrangement

A properly arranged switching circuit as shown in Figure 17, enables one to control automatically and accurately the integrating time of the WAID. To start the computation, push the "compute" switch (a normally open push-button switch). Relay Y_1 is energized and selfholds (through y_{11} and the reset switch). Also y_{12}, y_{13} and y_{14} are subsequently closed. When the turntable trigger activates micro switch M_{s1}, relay Y_2 is energized (through "Reset", y_{12}, y'_{31}, and M_{s1}), closing y_{21}, y_{23} and opening y'_{22}. At the instant y'_{22} is opened, the integration starts. The turntable trigger then trips M_{s2} which energizes Y_3 (through y_{23} and M_{s2}). As soon as Y_3 is energized, it selfholds (through y_{32}) and closes y_{31}. Exactly one revolution (3.6 sec) later, the turntable trigger trips M_{s1} again. At this instant, relay Y_4 is energized (through y_{14}, y_{31} and M_{s1}),opening y'_{42}. The integration stops at the same instant. The output is kept in "hold"position until the "reset" switch is pushed down. The "reset" switch can be thrown at any time to "reset" the whole control circuit as well as the operational circuit. Thus the integrating time is controlled by the turntable trigger which trips M_{s1} and indirectly trips y'_{22} and y'_{42}. Since

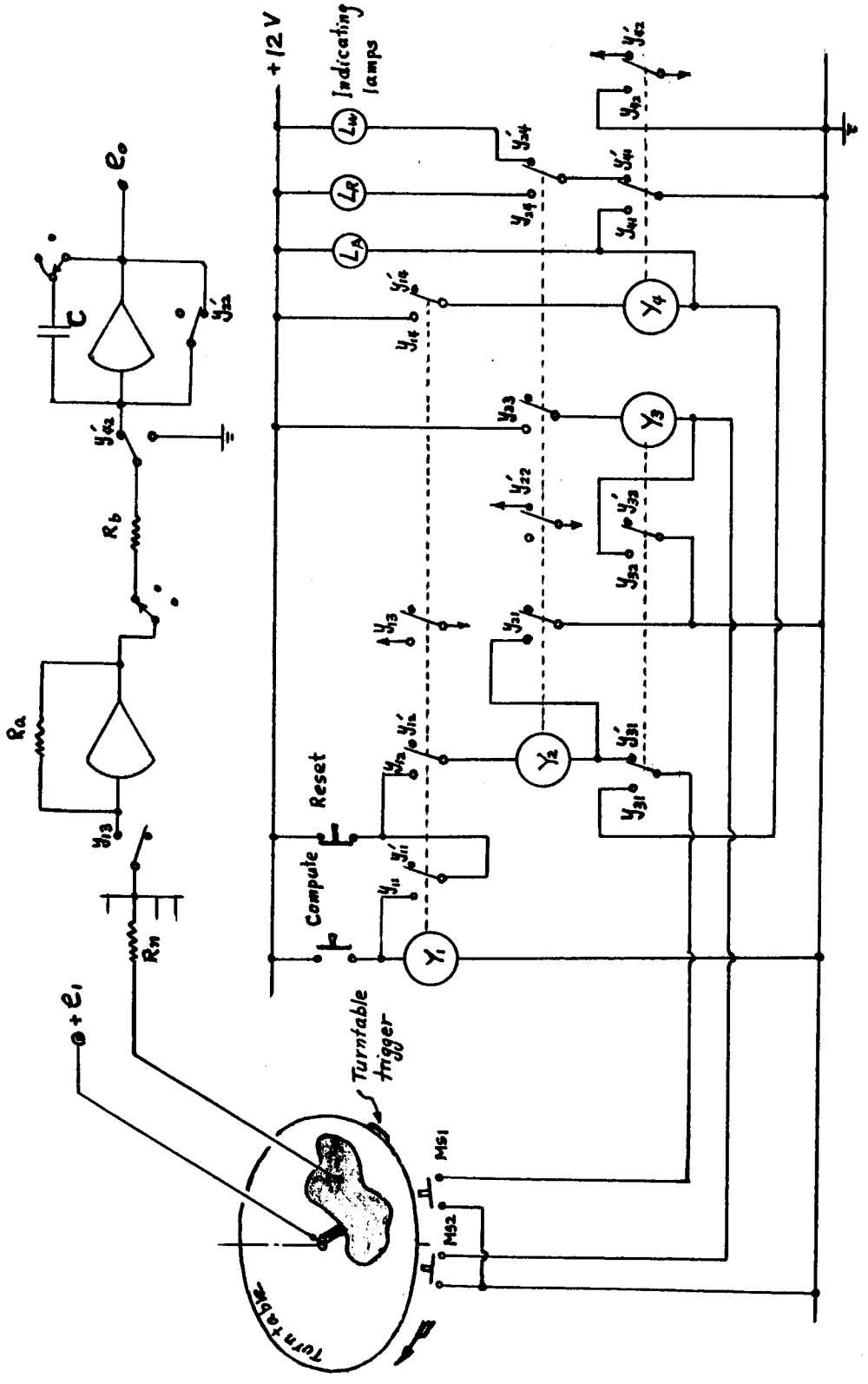

Figure 17. Control Sequence Diagram

two relays of the same type (Dry Reed relay, Magnacraft, Type 103 PC DPDT) are used, the error due to different release time of the two relays (average release time = 0.5 millisecond) is negligible. Consequently, the time error due to the switching circuit is negligibly small.

(g) Power Supplies

In the WAID, two different ratings of power supply are needed:

(i) The Amplifier Power Supply. (± 15 V.D.C., 30 mA/115 V.A.C. 1ø 50-60 cps.) This DC power supply is used for the two NEXUS CLA-3 operational amplifiers. A highly regulated constant output voltage is of absolute necessity. One NEXUS (Type SNP-2) all-silicon dual regulated power supply is used because of its good voltage regulation (less that 0.01V, typically 0.001V, over rated load of 150 ma and line variation from 105V to 130 VAC/50-400 cps).

(ii) The Control Power Supply. (+12 V.D.C. 0.2 -1.0 A/115 V.A.C. 1ø 50-60 cps.) This is used for energizing the relays and the indicating lamps. The voltage regulations of the relay control source is not as stringent as that of the previous one. Normally ± 10 percent voltage fluctuation is tolerable

for relay operation. However, because of the appreciable variation in load current (from 0.2 A at "reset" condition to 1A at "hold" condition), care was taken in the circuit design. A transistorized feedback regulator circuit is used as shown in Figure 18. Using this circuitry the regulation is better than 2 percent.

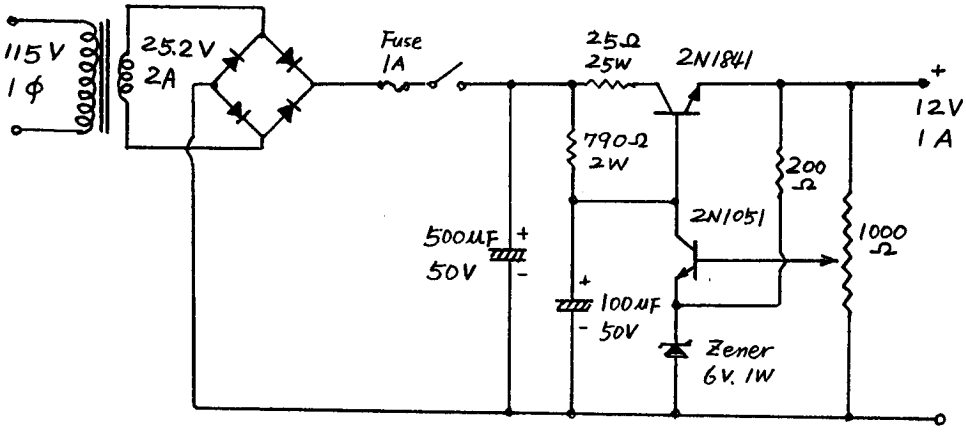

Figure 18 Control Power Supply Diagram

C. ERROR ANALYSIS

Like most electromechanical devices, the WAID is susceptable to error from a number of sources. The possible errors which might affect the WAID are those from: (a) the tracing; (b) the digital voltmeter; (c) the turntable; (d) the control relays; (e) the readhead; (f) the operational amplifiers; and (g) others such as reference input voltage fluctuation, input-feedback impedance variations, etc.

(a) Tracing error

As can be seen from Section B the area to be integrated is enlarged from an original small photographic image of around 1 inch diameter to a 7 inch diameter image on tracing paper. Any incorrect enlargement, incorrect painting and/or any shrinkage of the tracing will all contribute to errors. Aside from these factors, any improper location of the tracing on the turntable will also cause an error. All of these errors can be minimized by the careful attention of a skilled operator.

(b) Digital voltmeter

Depending on the model, 4 or 5 digits may be provided with an accuracy of 0.01% of the maximum applied voltage. If a 4-digit voltmeter is used, an accuracy of 0.1% of reading $\pm$ 1digit is obtainable. Using a 4-digit voltmeter, any viewfactor between 1 and 0.001 can be displayed in a four-digit number; e.g., if f = 0.003859 and if range 3 is selected, the reading will be 3.859 volt.

(c) Turntable speed

The most stringent requirement for the turntable is its absolutely "constant" or "steady" rotating speed. No speed fluctuation at any instant

is desirable. By adjusting a fine speed knob on the turntable, the highest accuracy of 0.1% can be maintained. The mechanically balanced heavy rotating disc (about 20 lbs) helps to eliminate speed fluctuation. Therefore errors due to the turntable speed variation are very small.

(d) Control relays

In order to avoid overlap integration over the tracing, the integrating time must be exactly "one period" of the turntable rotation. As described in Section B -(f), two normally closed relay contacts are used to control the integrating time, and both the two contacts are controlled, in turn, by a microswitch (M_{s1}). Assuming that M_{s1} gives no error and that the release-time difference between the two contacts is less than 0.36 m sec (average release time is 0.5 m sec.), then the maximum error is less than

$$\frac{0.36 \times 10^{-3}}{3.6} = 0.0001 \text{ unit.}$$

(e) Readhead

The number of the electric wipers and the shape of both the wiper tips and the weighted area will all affect the accuracy of the WAID. Ideally, the wiper tips should be a point contact. Figure 19 shows errors which will be picked up by a rectangular shaped wiper tip (WxL). Actually this error is negligibly small because of the small integrating band area (width = 1.7f x 1/32").

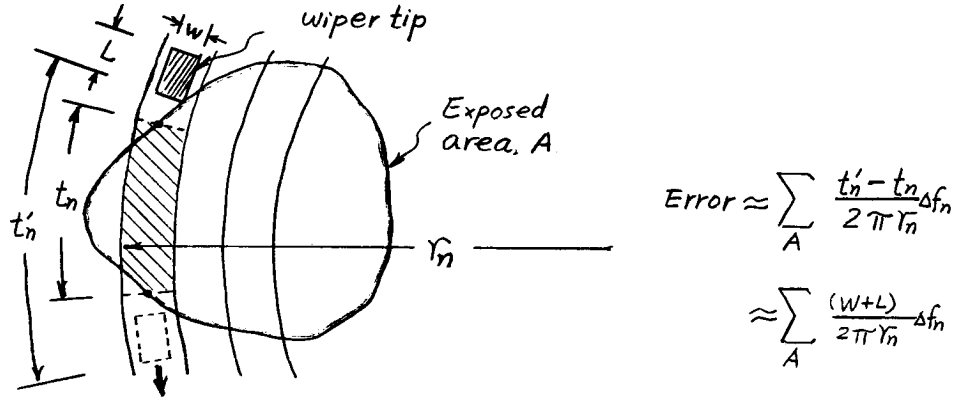

Figure 19 Example Showing Error Due to Wiper Shape

For an extremely irregular shape of the weighted area such as an area which is composed of a number of small annular bands, the accuracy will be largely degraded (See Figure 20a). Fortunately, most areas in the practical cases are of fairly smooth shape. For area shape as shown in Figure 20b, the maximum possible error will be around $\pm$ 0.013 unit. But this case will hardly occur in most practical configurations.

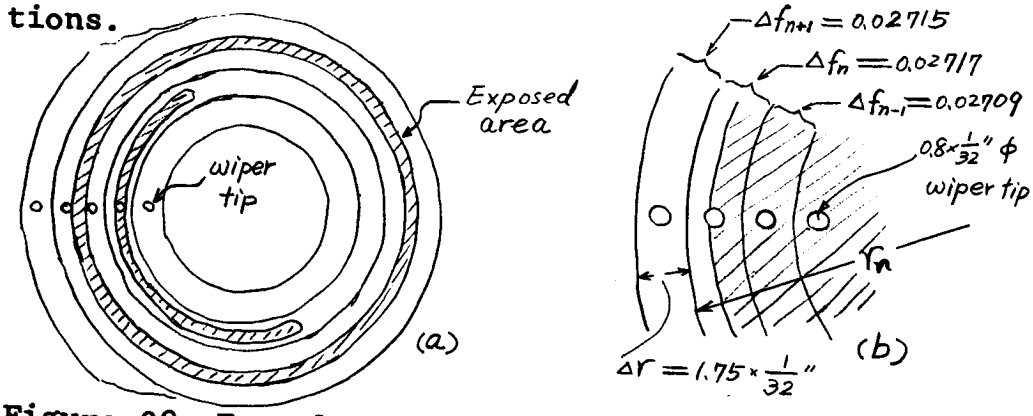

Figure 20 Examples Showing Errors Due to Area Shape and Wiper Position

(f) Operational amplifiers

An ideal operational amplifier would have infinite open loop gain and bandwidth and zero input noise, offset and drift. Although, of course, no amplifier has these ideal qualities, the performance of modern solid state amplifiers closely approaches these limits. As it can be seen from an experimental result (Figure 22), errors due to operational amplifiers are not significant in the WAID.

The errors due to the non-ideal characteristic of operational amplifiers can be classified as: (1) static errors due to finite gain; (2) dynamic errors due to bandwidth limitations; (3) errors due to initial voltage and current offsets; (4) voltage and current drift caused by temperature change, time stability and supply voltage fluctuation; (5) errors due to noise; and (6) errors due to finite input and output impedances. To analyze quantitatively the errors from the operational amplifiers, an equivalent actual operational circuit as shown in Figure 21 is considered (to simplify the notations, all quantities expressed in capital letters stand for Laplace transforms).

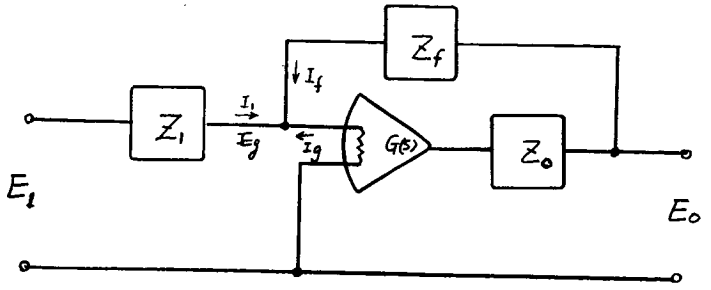

Figure 21 Equivalent Actual Operational Circuit

From the equivalent circuit, the output can be expressed as

$$E_o = -\left[\frac{E_i Z_f}{Z_1} + I_g Z_f + \frac{I_o Z_o}{G}\left(1+\frac{Z_f}{Z_1}\right) + E_d\left(1+\frac{Z_f}{Z_1}\right)\right] \times \left[\frac{G}{G+\left(1+\frac{Z_f}{Z_1}\right)}\right] \qquad (3\text{-}6)$$

Each term on the right side of Eq. 3-6, except the first one, which is the ideal value, is an error term which is respectively due to: grid or base current I_g; finite output impedance Z_o; drift and noise voltage E_d; and amplifier gain A, where $G(s) = \frac{A}{Ts + 1}$ (assuming that the amplifier has a flat frequency response characteristic from zero cps to the cutoff frequency $f_1 = \frac{1}{T}$ and the attenuation beyond f_1 is 6 db/oct). From the given characteristic data of the CLA-3 operational amplifier the total output voltage is calculated for the worst case when the operational amplifier is used as an

integrator with the highest closed loop gain of 100. From the calculation result e_o = 10.00107 volt, the error is 0.00107 volt. Figure 22 shows an experimental result which was obtained for zero viewfactor; i.e. $R_n = \infty$ (open circuit). The result reveals that the overall error due to the two operational amplifiers is increased with increase in time as well as gain. For example, when the integrator gain is increased from 1 to 100 the error increases by a factor of 40~50. Though the total error becomes appreciable when the range selector is set at 3, this error (at t = 3.6, e_o = 0.010V) can be completely eliminated by integrating twice, once for the actual integration and the other for zero viewfactor integration ($R_n = \infty$), and taking the difference value as the correct answer. When the first and the second ranges are used, the error due to the operational amplifiers is negligible provided that the amplifier zeroing has been done before using the WAID.

(g) Errors Due to Changes in Reference Input, R_n, R_a, R_b and C

The voltage regulation of the power supply (NEXUS NPS-2) is less than 10 millivolt over rated

load (150 ma) and line variations (105-130 V). Assuming 1 millivolt change (since this is a typical value and realizing that the actual load of the two operational amplifiers used in the WAID is less than 10% of the rated) the maximum error due to the voltage change is $0.001 \times \frac{10}{15} = 0.000667$ volt. Errors due to changes in impedances are caused primarily by a change in ambient temperature. Assuming that the capacitance change is 0.02%/°C, e_o= 10V, C = 20 μf, and a plus 10°C temperature variation the new value of the capacitance C is 20.04 μf and the new output voltage e_o is 9.98004 volts. The error voltage is therefore 10-9.98004 or 0.01996 volts. The same type of evaluation can be made for changes in resistance.

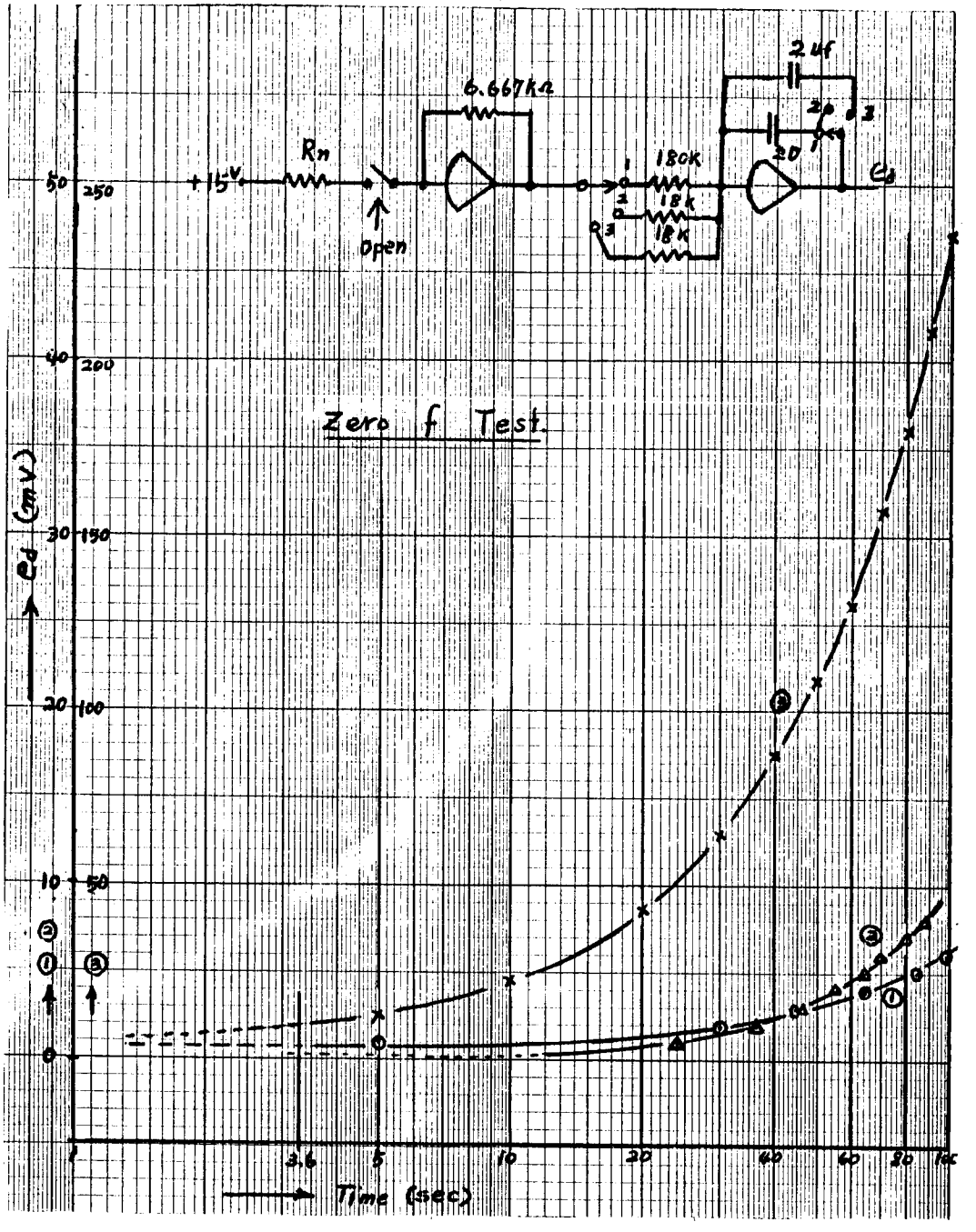

Figure 22. Errors Due to Operational Amplifiers.

CHAPTER IV

EXPERIMENTAL RESULTS

The experimental results are composed of: (A) zero viewfactor test; (B) range calibration test; and (C) actual sample integrations.

A. ZERO VIEWFACTOR TEST

The purpose of this test is to observe the drift and noise of the WAID for zero viewfactor integration. This test is made by lifting up the readhead and recording the average output for the integrating time of 3.6 sec. As shown in Table IV the drift output is negligibly small for the first and the second range but it is about +0.025 for the third range even when the two operational amplifiers are balanced. Therefore in the actual integration the drift error should be substracted from the digital reading in order to give the correct answer.

TABLE IV Inherent Output of the WAID Due to Drift and Noise

Summer		Integrator		Output		
E_{os}	I_{os}	I_{os}	E_{os}	Range 1	Range 2	Range 3
0	0	0	0	0.000	+0.002	+0.025
0	0	+0.100	+0.100	-0.001	-0.010	-0.080
0	0	-0.100	-0.100	+0.001	+0.013	+0.160
+0.100	+0.100	0	0	+0.001	+0.013	+0.160
-0.100	-0.100	0	0	-0.001	-0.010	-0.060
+0.100	+0.100	+0.100	+0.100	+0.000	+0.001	+0.030
-0.100	-0.100	+0.100	+0.100	-0.004	-0.020	-0.180
+0.100	+0.100	-0.100	-0.100	+0.001	+0.022	+0.245

B. RANGE CALIBRATION TEST

According to the calibration methods described in the previous chapter, the WAID is so calibrated that the summer output (i.e. the input to the integrator) is +1.000 to +1.002 volts, corresponding to f = 0.1 (equivalent input resistor of 100 KΩ), and that the integrator outputs are +1.000 to 1.003 volts and +10.02 to +10.04 volts for ranges 1 and 2, respectively. The integrator output for range 3 is calibrated so as to be equal to +10.25 V corresponding to a viewfactor f = 0.01. Table V shows the calibration results. The fractional value for each

range of the integrator outputs is considered to be the corresponding drift voltage. Ten readings for each range were taken to show the repetition consistency.

TABLE V

f= 0.1 (Equivalent R_n=100KΩ , f = 0.01 (Equivalent R_n=1000 KΩ)

Range 1	Range 2	Range 3	Range 1	Range 2	Range 3
+1.002	+10.04	+13.27	+0.098	+1.004	+10.20
1.003	10.05	-	0.098	1.005	10.24
1.002	10.04	-	0.097	1.004	10.24
1.003	10.05	-	0.098	1.005	10.23
1.003	10.05	Saturated	0.098	1.004	10.26
1.002	10.04	-	0.098	1.004	10.24
1.002	10.04	-	0.098	1.004	10.24
1.002	10.04	-	0.097	1.004	10.24
1.002	10.05	-	0.098	1.004	10.24
1.002	10.04	13.27	0.098	1.004	10.23

C. ACTUAL SAMPLE INTEGRATIONS

Twelve samples with a viewfactor range from 1.00 to 0.005 were prepared for the test of the actual performance of the WAID. By properly adjusting the spring loading of the readhead, the output readings for each sample were quite stable and repetitive. Experimental results show that the readhead spring need not be adjusted for each integration of different samples but the turntable speed should best be adjusted every time before integrating a new tracing. TABLE VI shows the average values of the experimental results. The observed value for each sample was estimated by the grid counting method (see Appendix C). The results reveal that the overall deviation will not exceed $\pm$ 0.003 unit provided that the turntable speed can be accurately controlled.

In the actual application, ranges 1 and 2 will provide very good results which are well within the accuracy needed in design calculation since the second range is able to give the fractional value as low as 0.00001 unit and its effective value is 0.0001 unit. Theoretically, range 3 could give one more digit lower than range 2 but because the drift voltage and the decay of the output reading are both around ten times that of the second range, the actual reliable digital reading is about the same. The calculated deviation as shown in TABLE VI is based on the assumption that the observed deviation is zero.

TABLE VI Actual Sample Test Results

Sample Number	Observed Viewfactor Value (Unit)	Range 1			Range 2			Range 3		
		WAID Output (Volt)	Output (Unit)	Deviation (Unit)	WAID Output (Volt)	Output (Unit)	Deviation (Unit)	WAID Output (Volt)	Output (Unit)	Deviation (Unit)
1	1.000	9.975	0.9975	-0.0025	13.27			13.27		
2-a	0.750	7.508	0.7508	+0.0008	13.27			13.27		
2-b	0.750	7.499	0.7499	-0.0001	13.27			13.27		
3-a	0.500	5.028	0.5028	+0.0028	13.27			13.27		
3-b	0.500	5.006	0.5006	+0.0006	13.27			13.27		
4	0.250	2.518	0.2518	+0.0018	13.27			13.27		
5	0.100	1.032	0.1032	+0.0032	10.37	1.037	+0.0037	13.27		
6	0.075	0.779	0.0779	+0.0029	7.761	0.07761	+0.00261	13.27		
7	0.050	0.516	0.0516	+0.0016	5.164	0.05164	+0.00164	13.27		
8	0.025	0.256	0.0256	+0.0006	2.595	0.02595	+0.00095	13.27		
9	0.010	0.115	0.0115	+0.0015	1.138	0.01138	+0.00138	11.81	0.01181	+0.00181
10	0.005	0.049	0.0049	-0.0001	0.510	0.00510	+0.0001	5.180	0.00518	+0.00018

CHAPTER V

CONCLUSIONS

The WAID is used to determine the local viewfactor from a given parabolic mirror photographic image by integrating over the area of the image which is enlarged onto a 7" diameter tracing. From a list of the local viewfactors obtained with the WAID, the overall viewfactor between surfaces of arbitrary configuration can then be calculated by numerical integration (which is not included in the thesis). Experimental results show that the problem solution obtained with the WAID is faster, easier, lower cost and probably the same or better accuracy than the other possible ways such as the grid counting method. By careful operation of the machine including correct preparation of the tracing and calibration of the turntable speed, the effective digital reading of the solution may be as small as 0.0001 unit (with 4-digit voltmeter) which is well within the accuracy needed in design calculation. Three selector ranges are provided in the WAID to meet the wide range of variation in viewfactor from 1.000 to 0.001000. The first and the second range will give satisfactory performance

but the third range is not as useful as it could be because of its unstable output which is caused by noise error due to using a higher gain (100) of the operational amplifier. The two most critical parts which affect the overall accuracy are the readhead and the turntable motor. Ideally, ball shape point contacts would be more suitable for the electric contacts of the readhead. The motor should have a proper torque which is strong enough to maintain the absolutely constant rated speed for the load change due to the friction between the electric contacts and the tracing. By changing the input resistances to the summer the integrating device can be used to integrate other types of weighted areas. As a special case the integrating device acts as a planimeter to integrate over geometrical areas which have uniform weighting factors. This is possible by using equal input resistances to the summer and changing the circular integration to a linear integration.

APPENDIX A

Calibration Equations for Parabolic Mirror Photograph.

The shape of a parabolic mirror is a paraboloid of revolution. Let the outside radius of the base of the parabolic mirror be r_o and the radius vector of variable which describes this parabolic surface be r_p (See Figure A-1). Then the relationship between r_o and r_p can be written as

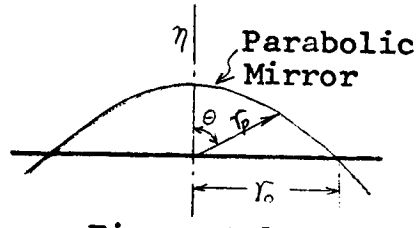

Figure A-1

$$r_p = \frac{r_o}{1+\cos\theta} \tag{A-1}$$

where θ is the angle between r_p and the center line normal to the mirror base.

For a general interpretation, the radiation viewfactor between areas A_1 and A_2 (See Figure A-2) is defined as

$$F_{12} = \frac{1}{A_1}\int_{A_1}\int_{A_2} \frac{\cos\theta_1 \cos\theta_2}{\pi R^2}\, dA_2\, dA_1 \tag{A-2}$$

When the element of area dA_1 is considered as the area A_1, Equation (A-2) becomes

$$f = \int_{A_2} \frac{\cos\theta_1 \cos\theta_2}{\pi R^2}\, dA_2 \tag{A-3}$$

The solid angle subtended by the element of area A_2 is

$$d\omega_2 = \frac{dA_2 \cos\theta_2}{R^2} \tag{A-4}$$

and $$d\omega_2 = \frac{dA_s}{r_o^2} \qquad \text{(A-5)}$$

therefore $$\frac{dA_2 \cos\theta_2}{R^2} = \frac{dA_s}{r_o^2} \qquad \text{(A-6)}$$

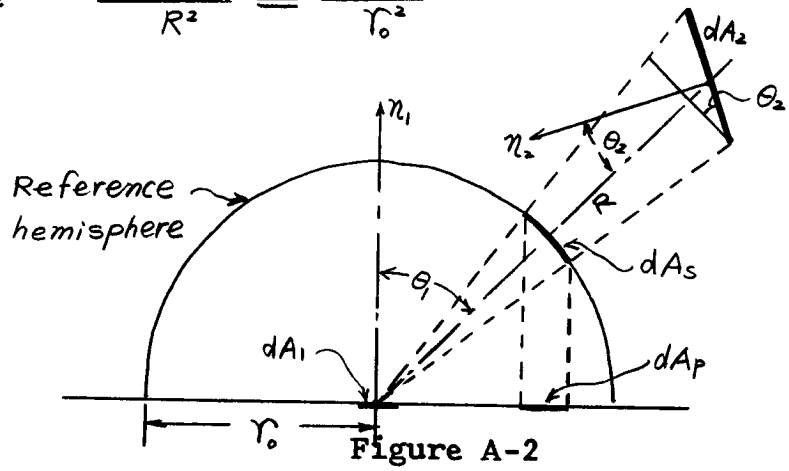

Figure A-2

Substituting Equation (A-6) into Equation (A-3) yields

$$f = \int_{A_2} \frac{\cos\theta_1}{\pi r_o^2}\, dA_s = \frac{1}{\pi r_o^2} \int_{A_2} dA_p \qquad \text{(A-7)}$$

Now consider the case of a circular object located with center on the line perpendicular to the area dA_1, as shown in Figure A-3.

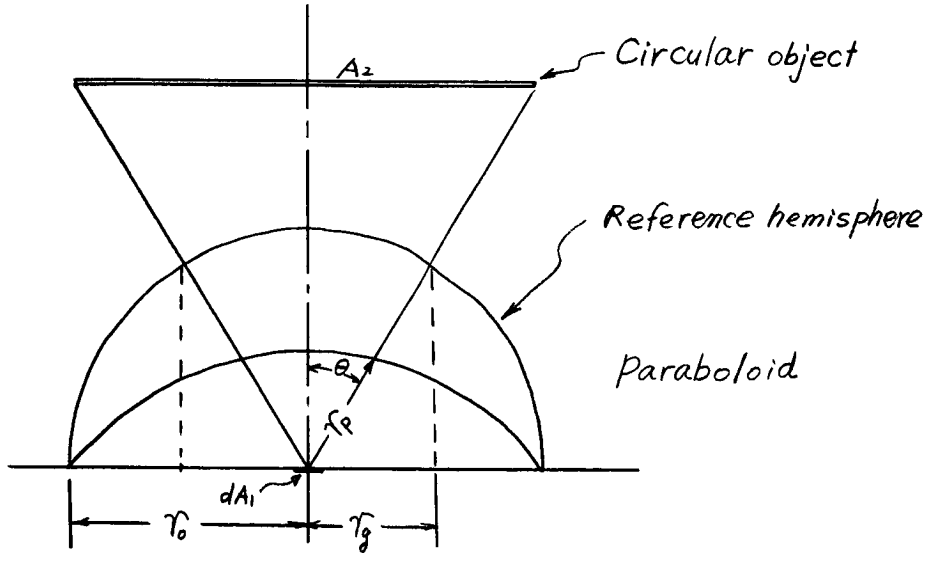

Figure A-3

From Figure A-3 $$\int_{A_2} dA_P = \pi r_g^2 \tag{A-8}$$

and $$r_g = \frac{r_o r_n}{r_p} \tag{A-9}$$

Substituting Equation (A-8) into Equation (A-7)

$$f = \frac{r_g^2}{r_o^2}$$

or $$r_g = r_o \sqrt{f} \tag{A-10}$$

From Equations (A-9), (A-10) and (A-1), one obtains

$$r_n = r_p \sqrt{f} = \frac{r_o \sqrt{f}}{1 + \cos\theta} \tag{A-11}$$

From Figure A-3 and Equation (A-10)

$$\sin\theta = \frac{r_g}{r_o} = \sqrt{f}$$

or $$\cos\theta = \sqrt{1 - \sin^2\theta} = \sqrt{1-f} \tag{A-12}$$

Putting Equation (A-12) into Equation (A-11) yields

$$r_n = \frac{r_o \sqrt{f}}{1 + \sqrt{1-f}} \tag{A-13}$$

Let $r_o = 1$, $f = f_n$, then Eq. (A-13) can be written as

$$f_n = \left(\frac{2 r_n}{1 + r_n^2} \right) \tag{A-14}$$

and $$\Delta f_n \triangleq \Delta f_{(n-1)\to n} = \frac{4 r_n^2 (1 + r_{n-1}^2)^2 - 4 r_{n-1}^2 (1 + r_n^2)^2}{(1 + r_n^2)^2 (1 + r_{n-1}^2)^2} \tag{A-15}$$

where Δf_n represents the increment of viewfactor contributed by the circular band having radii of r_{n-1} and r_n.

From Equation A-15 Δf_n are calculated for each value of n. with the aid of a digital computer. For example for n = 1, $\gamma_{n-1} = \gamma_0 = 0$, $\gamma_n = \gamma_1 = \Delta\gamma = \frac{1}{64} \therefore \Delta f_1 = 0.00097608590$; for n = 2, $\gamma_{n-1} = \gamma_1 = \frac{1}{64}$, $\gamma_n = \gamma_2 = \frac{2}{64} \therefore \Delta f_2 = 0.0029225453$ and so on

n	γ_n	Δf_n	$1/\Delta f_n$
1	0.0156250	0.000976086	1024.50000
2	0.0312500	0.002922545	342.16749
3	0.046875	0.004851934	206.10339
4	0.062500	0.006753074	148.08071
5	0.078125	0.008615107	116.07518
6	0.093750	0.010427575	95.899574
7	0.109375	0.012180580	82.097897
8	0.125000	0.013864823	72.124974
9	0.140625	0.015471728	64.634021
10	0.156250	0.016993539	58.845894
11	0.171875	0.018423311	54.279060
12	0.187500	0.019755001	50.620094
13	0.203125	0.020983584	47.656301
14	0.218750	0.022104859	45.238922
15	0.234375	0.023115714	43.260615
16	0.250000	0.024013818	41.642691
17	0.265625	0.024798081	40.325701
18	0.281250	0.026023994	39.265160
19	0.296875	0.026467429	38.426077
20	0.312500	0.026800561	37.782287
21	0.328125	0.027025760	37.312652
22	0.343750	0.027146883	37.001735
23	0.359375	0.027167426	36.836642
24	0.375000	0.027092037	36.808787
25	0.390625	0.026925516	36.911215
26	0.406250	0.026925516	37.139493
27	0.421875	0.026673102	37.490952
28	0.437500	0.026339903	37.965212
29	0.453125	0.025932096	38.562251
30	0.468750	0.025454871	39.285212
31	0.484375	0.024914609	40.137094
32	0.500000	0.024316589	41.124189
33	0.515625	0.023667144	42.252669
34	0.531250	0.022971580	43.532051
35	0.546875	0.022236009	44.972099
36	0.562500	0.021465364	46.586678
37	0.578125	0.020665316	48.390259
38	0.593750	0.019840510	50.401930
39	0.609375	0.018996239	52.641999
40	0.625000	0.018136631	55.137032

41	0.640625	0.017266223	57.916546
42	0.656250	0.016388956	61.016698
43	0.671875	0.015508760	64.479688
44	0.687500	0.014628618	68.359157
45	0.703125	0.013752380	72.714686
46	0.718750	0.012882373	77.625450
47	0.734375	0.012021667	83.183139
48	0.750000	0.011172263	89.507381
49	0.765625	0.010336621	96.743414
50	0.781250	0.009516315	105.08269
51	0.796850	0.008713433	114.76532
52	0.812500	0.007929027	126.11887
53	0.828125	0.007164578	139.57557
54	0.843750	0.006420776	155.74442
55	0.859375	0.005698975	175.47015
56	0.875000	0.004999477	200.02092
57	0.890625	0.004322870	231.32781
58	0.906250	0.003669699	272.50194
59	0.921875	0.003040202	328.92550
60	0.937500	0.002434303	410.79517
61	0.953125	0.001852369	539.84936
62	0.968750	0.001294038	772.77501
63	0.984375	0.000759400	1316.8284
64	1.000000	0.000247928	4033.4351

APPENDIX B

Operational Amplifiers

The NEXUS CLA-3 all silicon solid state miniature encapsulated operational amplifier is a premium grade analog module, featuring a high degree of protection against input overdrive signals, as well as the high electrical stability, and low input offset current. Carefully selected silicon planar transistors are used throughout to insure long term stability. A high thermal conductivity encapsulant provides an isothermal environment as well as mechanical protection for components. Each amplifier is stabilized by prolonged baking at elevated temperatures before encapsulation and is individually tested for electrical performance over the range -25°C to +85°C.

The input circuitry of type CLA-3 is fully protected against the possibility of permanent damage due to accidental connection of the input terminals across the power supply. The output circuitry is also protected against short circuits to grounds, and will withstand temporary (not to exceed one minute) connection to either power supply terminal.

Absolute Maximum Ratings

Storage Temperature	-65°C to +125°C
Operating Temperature	-25°C to +85°C
Supply Voltage	+16 V DC
Common Mode Input Voltage	±11 V DC
Differential Input Voltage	±15 V DC
Input Overdrive Current	±15 mA
Output Overdrive Current	±10 mA

Characteristics(@ 25°C Unless noted)

Supply Voltage (3-wire DC)	Vcc = ± 15V DC
Supply Current (Full Output)	Icc = ± 9 mA DC
Output Voltage Range, Full Load R_L = 3.3KΩ	E_o = ± V p-p
Output Current Range	I_o = ± 3 mA p-p
Voltage Offset Stability @ Const. Temp. (30 Days)	E_{os} = ± 100 μV
Offset Voltage Temperature -25°C to + 85°C	$\Delta E_{os}/T$ = ± 5~15 μV/°C
Offset Voltage/Supply Voltage Stability Coeff.	$\Delta E_{os}/V_{cc}$ = 200 μV/°C
Input Offset Current	I_{os} = ± 0.5~1.5 nA
Offset Current Temperature Coeff -25°C to +85°C	I_{os}/T = 0.02 0.2 A/°C
Open Loop Gain @ DC R_L = 10KΩ	A_o = 60,000 (Typical)
Unity Gain Crossover Freq.	f_t = 0.5 Mc
Freq. Limit for Full Output (Unity Gain Inverter)	f_p = 2.0 Kc
Differential Input Impedance @ DC	Z = 1.0 MΩ
External Offset Voltage Zero Trim Potentiometer	R_{os} = 1.0 MΩ

APPENDIX C

Sample of the Counting Grid

This counting grid is used in the so-called "grid counting method" to determine the viewfactor. The 7" diameter circular area is divided into 1000 blocks and each block has an equal increment of viewfactor (Δf) of 0.001.

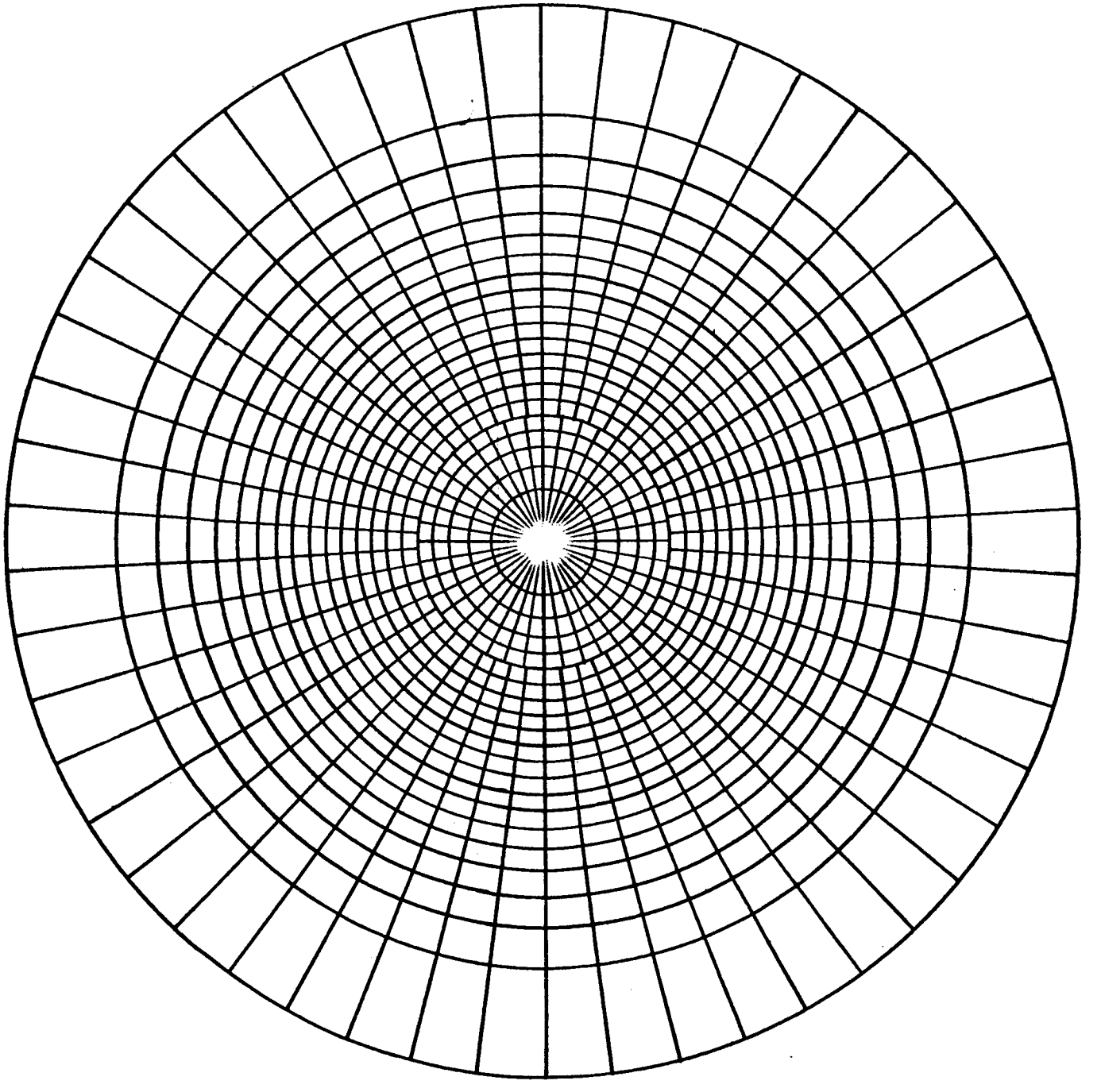

BIBLIOGRAPHY

1. Jackson, Albert S.: "Analog Computation," McGraw-Hill Book Company, Inc. 1960.

2. Stata , Ray: "Operational Amplifiers," Electromechanical Design, Sept. and Nov., 1965.

3. Fifer, Stanley: "Analogue Computation," Vol. I, II, and III, McGraw-Hill Book Company, Inc., 1961.

4. Keister, Ritchie and Washburn: "The Design of Switching Circuits," D. Van Nostrand Company, Inc., 1951.

5. Siskind, Charles S.: "Electrical Control Systems in Industry," McGraw-Hill Book Company, Inc., 1963.

6. Texas Instruments Incorporated: "Transistor Circuit Design," McGraw-Hill Book Company, Inc., 1963.

7. Matheny, J.D. and Carden, A.E.: "Thermal Design Studies," Final Report Contract NAS8-5270, Sept., 1965.

8. Chapman, Alan J.: "Heat Transfer," The MacMillan Company, 1960.

9. Rohsenow and Choi: "Heat, Mass and Momentum Transfer," Prentice Hall, Inc., 1961.

Thermal Design Studies

Final Report
Contract NAS8-5270

PART III

EXPERIMENTS IN DETERMINATION OF THE RADIATION CONFIGURATION FACTOR USING WAID

February 1967

Prepared for: George C. Marshall Space Flight Center
NASA
Huntsville, Alabama

Prepared by: Bureau of Engineering Research
University of Alabama
University, Alabama

PART III

A. Introduction. The Weighted-Area Integrating Device was completed by Dr. R. E. Lueg with sufficient time remaining before the termination of the contract to allow its use in the study of some real configurations. Two such geometric configurations were suggested by Mr. James Watkins of NASA.

In each case a model was built and a sequence of photographs taken using the parabolic mirror technique reported in detail in September 1965.

The two configurations studied were as shown in Figure 1 (a circular disk which was allowed to 'set' below the horizon) and in Figure 2 (the disk-stem-disk geometry studied in the first series of similarity studies). Figure 3 shows a photograph of the model.

B. Description of Tests. The photographs of the models were obtained using a 35 m.m., single lens reflex camera with a 135 m.m. telephoto lens. The film was developed via usual commercial channels and printed. The prints were used to select the best photograph from a series of three taken of each position. These were taken at f stops as indicated by a light meter, and at 1/2 greater and lesser f stops. Since set-up time is the major time factor, snapping the extra photographs was cheap insurance.

The WAID requires that the 'enlargement' of the parabolic mirror be to exactly seven inches. A seven inch target circle was printed on 100%

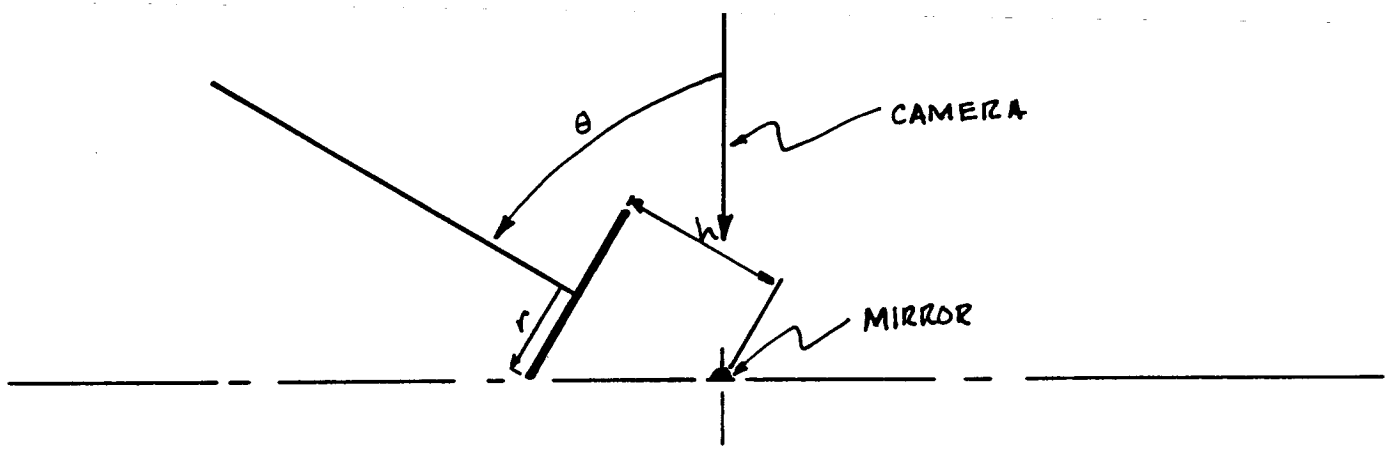

r/h RATIO	15	30	45	60	75	90	105	120	135	150	θ, DEGREES
5	5-15	5-30	5-45	5-60	5-75	5-90	5-105	5-120	5-135	5-150	
4	4-15	4-30	4-45	4-60	4-75	4-90	4-105	4-120	4-135	4-150	
2	2-15	2-30	2-45	2-60	2-75	2-90	2-105	2-120	2-135	2-150	
1	1-15	1-30	1-45	1-60	1-75	1-90	1-105	1-120	1-135	1-150	

GUIDE TO PICTURES TAKEN FOR PROJECT NAS8-5270, AUGUST, 1966.

RMH.

Figure 1. Geometry of First Configuration Factor Study

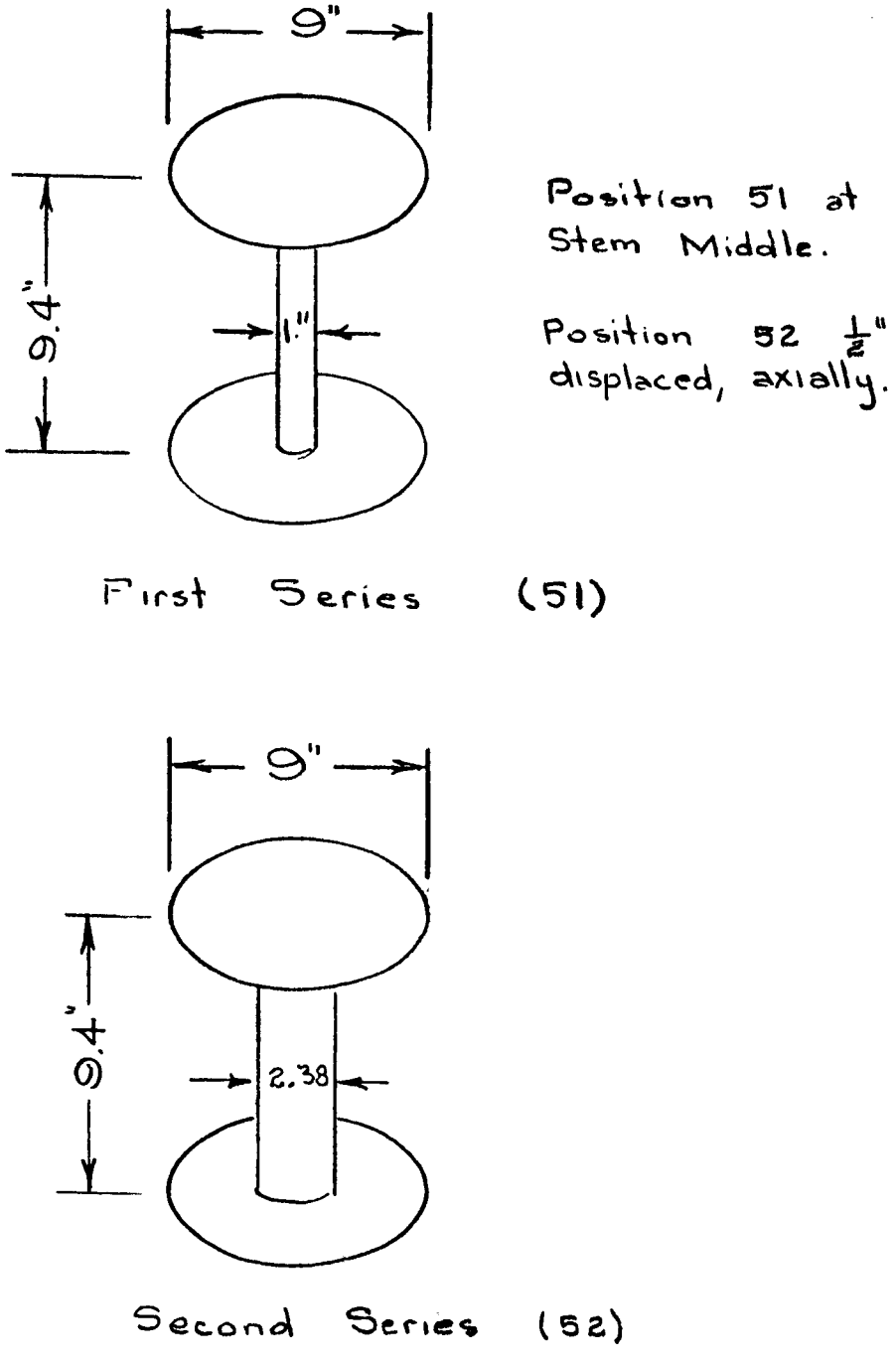

Figure 2. Geometry for Second Configuration Factor Study

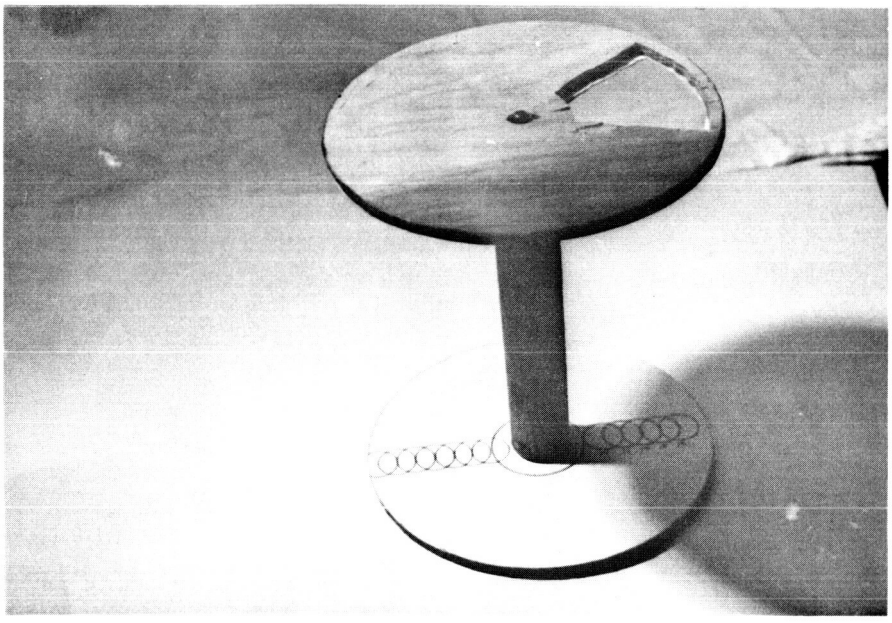

Figure 3. Disk-Stem-Disk Model for Photographic Study Showing Mirror Locations

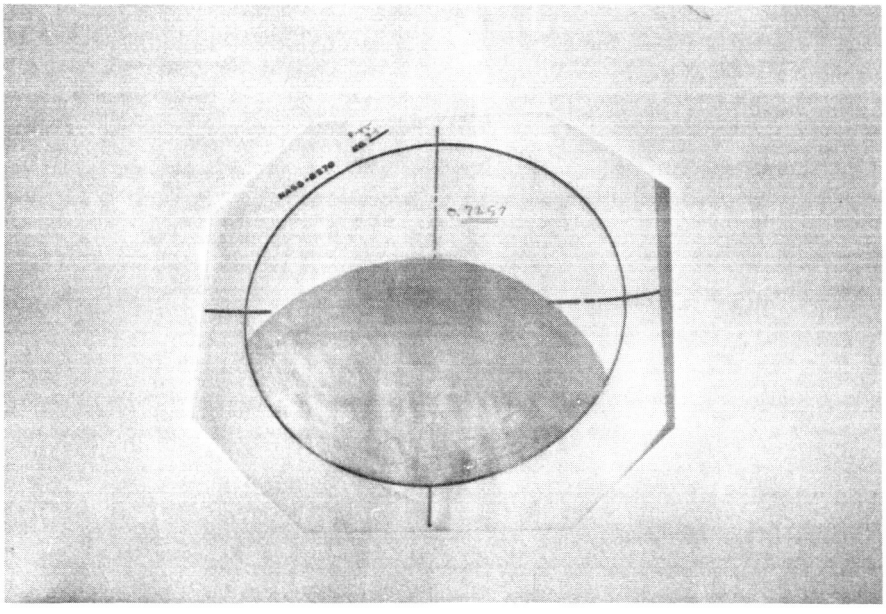

Figure 4. Photograph prepared for integration on WAID

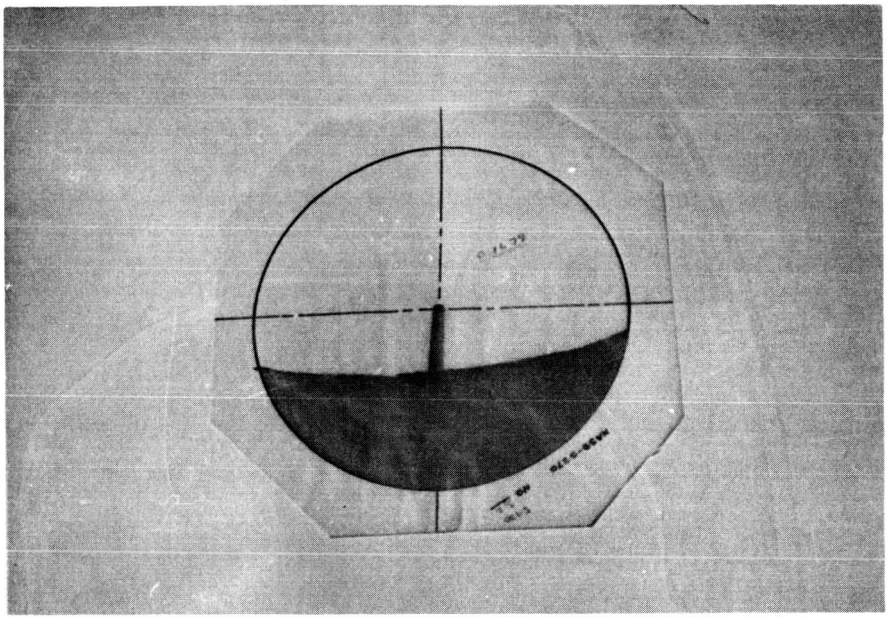

Figure 5. Photograph whose area does not include the potential source

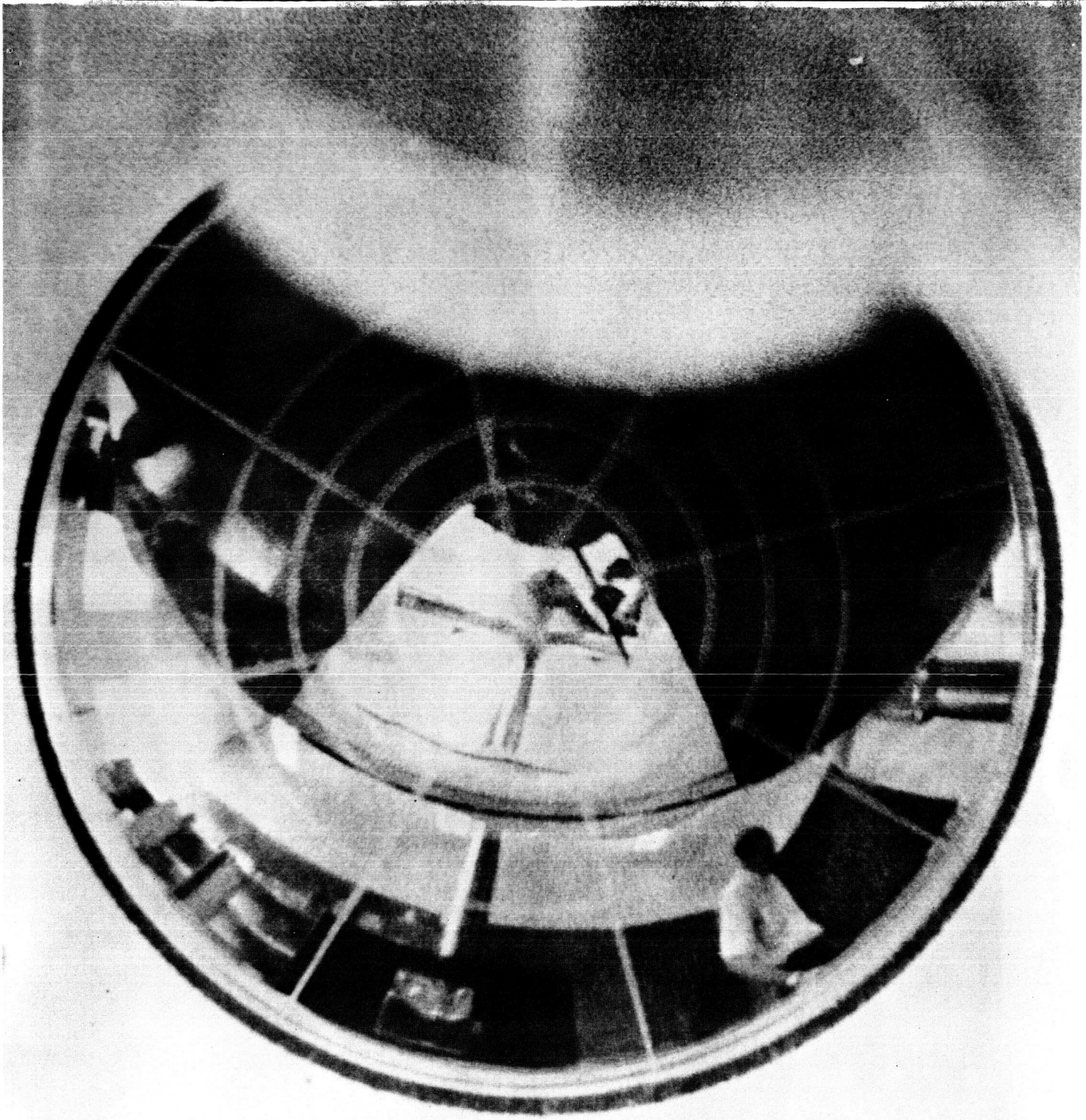

Figure 6. Photograph showing dark area (disk), photographer (Mr. Hamner) and bystander (Dr. Matheny).

rag tracing paper, and a large number of these run-off using off-set printing. This circle served as a target. A 50 m.m. enlarging lens was mounted in a standard photo enlarger together with a 35 m.m. film transport. The enlarger was adjusted so that the parabolic mirror exactly filled the target circle. The single area of interest was located in the field and traced by hand on the paper field. This process was repeated until all the areas of interest had been traced.

It should be noted that when the mirror was located on the stem (see Figure 3) there resulted two areas of interest; namely the upper and lower disks. Since the configuration factor from the stem to each of the disks was desired separately, it was necessary to identify each of the areas and prepare separate tracings of each on different pieces of rag paper.

The tracings, once obtained, were painted over using silver print. Figure 4 and Figure 5 show two separate situations which occurred.

The WAID has an arm with about 65 contacts. The centermost of these is a source of potential which is applied to the silver print. The area to be integrated as shown in Figure 4 is of such a shape that the potential source touches the area painted with silver print. Because the electrical current through the silver print is extremely small, it is essentially at a constant electrical potential and the other 64 pick-ups 'read' either this potential or zero as the turntable rotates.

Figure 5 shows a specimen ready for integration where the silver print did not pass beneath the center contact which supplies potential to

the painted area. To avoid this difficulty a conducting path has been added to the photo and after this was dry, the undesired area was coated with clear nail lacquer.

After the areas were painted the excess paper was removed as can be seen in Figure 4 and Figure 5.

The instructions in detail for operating WAID are included in Appendix I as a procedure for a non-skiller operator.

The results of the first study are shown in Appendix II. Figure 1 shows the location of the data points. A number of readings were taken for the local configuration factor, and these were averaged.

The missing points in the collection of data of Appendix II are points for which the geometry precluded a meaning to the configuration factor (the disk had set) or for which the disk could not be brought close enough to the parabolic mirror for physical reasons.

In the second test two stem diameters were used (see Figure 2). The 51 series tests used the one inch diameter stem, while the 52 series tests used a 2.380 in. diameter stem. The data are for equally spaced points along the stem from below the center-line of the figure to either of the disks. The words large and small identify the configuration factor from the element of area at the center of the bottom of the parabolic mirror to the near and far disks respectively. The locations are at increments of one half inch.

The data which form the results of this test are included as Appendix III.

APPENDIX I

Calibration & Operation of the WAID

A. Calibration

1. a) On WAID Control Unit

i) Turn "AC Power" Switch to ON

ii) Turn "DC Relays" Switch to ON (Leave On)

b) On HP 3430, a Digital Voltmeter

Turn AC "Line" Switch to ON

Allow 15 minutes for Equip. Warm Up

2. a) On HP 3430

i) Zero HP 3430 Using Zero Potentiometer

ii) This Setting should be Checked Frequently to Avoid Erroneous Readings due to Drift.

iii) Set HP 3430 Range SW to 10V

b) On WAID Control Unit

i) Turn "Selector 1" to CAL 1

ii) Turn "INT" SW Up. Adjust Potentiometer "E" (above INT SW) until HP3430 Reads 0.00

iii) Depress Red "I" Button. Adjust Potentiometer "I" (above INT SW) Until HP 3430 Reads 0.00

iv) Return "INT" SW to Down Position.

v) Turn "SUM" SW to Up Position. Adjust Pot. "E" (above "SUM" SW) until HP 3430 reads 0.00.

vi) Depress Red "I" Button. (Same Button as Step C) Adjust Pot "I" (above "SUM" SW) Until HP 3430 Reads 0.00

vii) Return "SUM" SW to Down Position

3. a) Reference Voltage Calibration on Turntable Unit
Turn "Selector 2" to f:0.1

b) On WAID Control Unit turn "Selector 1" to CAL 2

c) Turn on the turntable Motor.

d) Depress 'Reset' button

e) Depress Black "Compute" Button. Output on HP 3430 should read 1.00 ± 0.002.

f) If not, Adjust Pot. "REF" and Repeat Process Until HP3430 reads $1.00 \pm .002$

B. Operation

a) On HP 3430 turn Range SW to 10V

b) On WAID Control Unit:

i) Check that the "INT" and "SUM" Switches are in Down Position

ii) Check that "DC Relays" SW is On

iii) Turn "Selector 1" to the Range that F is Presumed to lie in. (1.0-0.1; 0.1-0.01; 0.01-0.00.)

iv) Depress Red "Reset" Button and Notice that White "Reset" Light is Lighted.

c) On Turntable Unit

i) Turn "Selector 2" to NORM

ii) Place Object to be Integrated on Turntable. Use Great Care to Assure that Object is Centered.

iii) Place Readhead on the Surface.

iv) Lock Readhead in Place

v) Turn Turntable "Power" SW to On
(Allow a Few Revolutions for the Turntable to gain Stability)

vi) Look at Rotating Dots through the Small Window on the Surface of the Turntable Base.

vii) Adjust Turntable "Speed" Pot Until the Outer Row of Dots Appears to be Motionless. On the Waid Control Unit at 16 2/3 rpm.

viii) Depress the Black "Compute" Button and Notice the Red "Compute" Light is Lighted.

ix) After 3.6 Seconds the Red "Compute" Light should go Out and the Amber "Hold" Light Should Light. When the "Hold" Light Lights, read the Output on the HP3430.

x) Depress the "Reset" Button.

xi) WAID is now Ready to Integrate Again (Steps 6 - 10)

Notes:

1. Readhead contacts should be Cleaned Frequently to Insure Accurate Readings. (Contact Cleaners such as Carbon Tetrachloride should be used.)

2. The Objects to be Integrated Should be Painted with a Conductive Paint. (Silver Print No. 21-2 G. C. Electronics, Rockford, Ill.)

3. It is suggested that one circular area be left on the table for locating later areas.

APPENDIX II

DATA FROM DISK AND ELEMENTAL AREA

DESIGNATION*	DATA TAKEN	AVERAGE
1-15		
1-30	0.434	0.434
	0.435	
	0.434	
1-45		
1-60	0.261	0.262
	0.261	
	0.262	
	0.262	
	0.263	
	0.262	
	0.262	
1-75	0.110	0.108
	0.111	
	0.113	
	0.110	
	0.108	
	0.107	
	0.112	
	0.111	
	0.108	
1-90	0.0930	0.0932
	0.0933	
	0.0934	
	0.0931	
	0.0932	
	0.0932	
	0.0933	
	0.0931	
	0.0932	
	0.0933	

*See Fig. 1.

DESIGNATION	DATA TAKEN	AVERAGE
1-90 (cont)	0.0930	
	0.0931	
	0.0934	
	0.0930	
	0.0932	
1-105	0.0413	0.0412
	0.0413	
	0.0413	
	0.0413	
	0.0411	
	0.0413	
	0.0413	
	0.0412	
	0.0411	
	0.0410	
	0.0410	
	0.0413	
	0.0412	
	0.0412	
	0.0412	
	0.0411	
1-120	0.0784	0.080
	0.0784	
	0.0784	
	0.080	
	0.080	
	0.081	
1-135	0.0028	0.0031
	0.0028	
	0.0029	
	0.0030	
	0.0029	
	0.0031	
	0.0030	
	0.0031	
	0.0031	
	0.0031	
	0.0031	
	0.0031	

DESIGNATION	DATA TAKEN	AVERAGE
1-135 (cont)	0.0031	
	0.0032	
	0.0031	
1-150		
2-15		
2-30	0.7000	0.7033
	0.7016	
	0.7026	
	0.7028	
	0.7044	
	0.7047	
	0.7036	
	0.7040	
	0.7041	
	0.7041	
	0.7026	
	0.7047	
2-45	0.6210	0.6209
	0.6203	
	0.6210	
	0.6207	
	0.6210	
	0.6212	
	0.6210	
2-60	0.420	0.422
	0.420	
	0.421	
	0.422	
	0.422	
	0.422	
	0.422	
	0.422	
	0.422	

DESIGNATION	DATA TAKEN	AVERAGE
2-75		
2-90	0.2358	0.2362
	0.2357	
	0.2358	
	0.2361	
	0.2365	
	0.2365	
	0.2363	
	0.2363	
	0.2363	
	0.2361	
	0.2365	
	0.2365	
	0.2361	
	0.2362	
	0.2360	
2-105	0.1447	0.1541
	0.1474	
	0.1544	
	0.1542	
	0.1542	
	0.1539	
	0.1539	
	0.1541	
	0.1540	
	0.1539	
	0.1539	
	0.1539	
	0.1542	
	0.1545	
	0.1543	
2-120	0.0604	0.0598
	0.0590	
	0.0597	
	0.0599	
	0.0601	

DESIGNATION	DATA TAKEN	AVERAGE
2-135	0.0206	0.0209
	0.0207	
	0.0208	
	0.0209	
	0.0209	
	0.0202	
	0.0208	
	0.0209	
	0.0210	
	0.0210	
	0.0211	
	0.0210	
	0.0210	
	0.0210	
	0.0210	
2-150	0.0049	0.0050
	0.0050	
	0.0050	
	0.0050	
	0.0050	
	0.0050	
	0.0050	
	0.0050	
	0.0050	
	0.0050	
	0.0050	
	0.0050	
	0.0050	
	0.0050	
	0.0050	
4-15		
4-30	0.8150	0.8172
	0.8156	
	0.8170	
	0.8175	
	0.8180	
	0.8169	
	0.8185	
	0.8181	

DESIGNATION	DATA TAKEN	AVERAGE
4-30 (cont)	0.8181	
	0.8170	
	0.8181	
4-45	0.7257	0.7257
	0.7260	
	0.7256	
	0.7255	
4-60	0.5815	0.5872
	0.5854	
	0.5862	
	0.5875	
	0.5883	
	0.5884	
	0.5886	
	0.5889	
	0.5890	
	0.5879	
4-75	NOT TAKEN	
4-90	NOT TAKEN	
4-105	NOT TAKEN	
4-120	NOT TAKEN	
4-135	NOT TAKEN	
4-150	NOT TAKEN	
5-30	0.8553	0.8569
	0.8548	
	0.8551	
	0.8555	

DESIGNATION	DATA TAKEN	AVERAGE
5-30 (cont)	0.8558	
	0.8570	
	0.8572	
	0.8569	
	0.8569	
	0.8572	
	0.8569	
	0.8559	
	0.8569	
	0.8568	
	0.8568	
5-15	NOT TAKEN	
5-45	0.7303	0.7330
	0.7313	
	0.7312	
	0.7322	
	0.7321	
	0.7321	
	0.7329	
	0.7334	
	0.7332	
	0.7331	
	0.7340	
	0.7341	
	0.7339	
	0.7338	
	0.7340	
5-60	0.6337	0.6338
	0.6337	
	0.6340	
	0.6338	
	0.6335	
	0.6338	
	0.6341	
	0.6341	
	0.6340	
	0.6340	
	0.6333	
	0.6339	

DESIGNATION	DATA TAKEN	AVERAGE
5-60 (cont)	0.6335	
	0.6331	
	0.6325	
5-75		
5-90	0.3918	0.3920
	0.3920	
	0.3914	
	0.3917	
	0.3920	
	0.3919	
	0.3915	
	0.3922	
	0.3923	
	0.3923	
	0.3923	
	0.3923	
	0.3923	
	0.3922	
	0.3915	
5-105	0.2553	0.2570
	0.2559	
	0.2563	
	0.2560	
	0.2566	
	0.2567	
	0.2564	
	0.2571	
	0.2571	
	0.2574	
	0.2571	
	0.2575	
	0.2578	
	0.2572	
	0.2574	
5-120	0.1690	0.1679
	0.1699	
	0.1681	

DESIGNATION	DATA TAKEN	AVERAGE
5-120 (cont)	0.1624	
	0.1673	
	0.1654	
	0.1699	
	0.1657	
	0.1695	
	0.1701	
	0.1691	
	0.1677	
	0.1651	
	0.1697	
	0.1701	
5-135	0.0900	0.0904
	0.0898	
	0.0899	
	0.0904	
	0.0906	
	0.0904	
	0.0905	
	0.0904	
	0.0903	
	0.0903	
	0.0904	
	0.0901	
	0.0904	
	0.0905	
	0.0903	
5-150	0.0355	0.0357
	0.0356	
	0.0356	
	0.0357	
	0.0357	
	0.0357	
	0.0357	
	0.0357	
	0.0356	
	0.0357	
	0.0357	
	0.0357	
	0.0357	
	0.0357	
	0.0357	

APPENDIX III

DATA FROM STEM TO DISKS

DESIGNATION[+]	DATA TAKEN (Large)	AVERAGE	DATA TAKEN (Small)	AVERAGE
*51-51	0.086	0.0854	0.048	0.0504
	0.085		0.051	
	0.085		0.051	
	0.085		0.051	
	0.086		0.051	
51-52	0.078	0.0781	0.054	0.0536
	0.078		0.054	
	0.079		0.054	
	0.078		0.053	
	0.078		0.053	
51-53	0.096	0.096	0.043	0.0438
	0.096		0.044	
	0.096		0.044	
	0.096		0.044	
	0.096		0.044	
51-54	0.129	0.1308	0.0364	0.03674
	0.132		0.0370	
	0.131		0.0367	
	0.131		0.0368	
	0.131		0.0368	
51-55	0.174	0.1746	0.0315	0.03174
	0.175		0.0326	
	0.176		0.0318	
	0.174		0.0317	
	0.174		0.0317	

[+]See Fig. 2

*51 series 1" diameter stem

DESIGNATION	DATA TAKEN (Large)	AVERAGE	DATA TAKEN (Small)	AVERAGE
51-56	0.191	0.1914	0.0293	0.0296
	0.191		0.0295	
	0.191		0.0297	
	0.192		0.0297	
	0.192		0.0299	
51-57	0.269	0.2699	0.0244	0.0249
	0.269		0.0248	
	0.270		0.0250	
	0.270		0.0252	
	0.270		0.0253	
51-58	0.360	0.3606	0.0408	0.0416
	0.360		0.0418	
	0.361		0.0423	
	0.361		0.0416	
	0.361		0.0415	
51-59	0.414	0.4168	0.0195	0.02036
	0.418		0.0201	
	0.418		0.0205	
	0.417		0.0206	
	0.417		0.0206	

DESIGNATION	DATA TAKEN (Large)	AVERAGE	DATA TAKEN (Small)	AVERAGE
*52-51	0.0821	0.08246	0.0647	0.06544
	0.0825		0.0653	
	0.0825		0.0654	
	0.0828		0.0660	
	0.0824		0.0658	
52-52	0.0777	0.07792	0.0696	0.06986
	0.0770		0.0698	
	0.0785		0.0699	
	0.0786		0.0701	
	0.0785		0.0700	
52-53	0.117	0.1178	0.0612	0.06218
	0.118		0.0624	
	0.118		0.0623	
	0.118		0.0625	
	0.118		0.0625	
52-55	0.154	0.154	0.0406	0.04096
	0.154		0.0409	
	0.154		0.0412	
	0.154		0.0411	
	0.154		0.0410	
52-56	0.201	0.2016	0.0324	0.03258
	0.201		0.0326	
	0.202		0.0326	
	0.202		0.0326	
	0.202		0.0327	
52-57	0.267	0.2676	0.0749	0.07544
	0.267		0.0756	
	0.267		0.0754	
	0.269		0.0756	
	0.268		0.0757	

*52 series, 2.380" diameter stem

DESIGNATION	DATA TAKEN (Large)	AVERAGE	DATA TAKEN (Small)	AVERAGE
52-58	0.305	0.309	0.0260	0.02608
	0.310		0.0261	
	0.311		0.0261	
	0.310		0.0261	
	0.309		0.0261	
52-59	0.376	0.3772	0.0238	0.02414
	0.377		0.0240	
	0.378		0.0243	
	0.378		0.0245	
	0.377		0.0242	

Thermal Design Studies

Final Report
Contract NAS8-5270

PART IV

A FEASIBILITY STUDY OF A DIRECT ACQUISITION DEVICE FOR DETERMINATION OF THE RADIATION CONFIGURATION FACTOR

February 1967

Prepared for: George C. Marshall Space Flight Center
NASA
Huntsville, Alabama

Prepared by: Bureau of Engineering Research
University of Alabama
University, Alabama

PART IV

A FEASIBILITY STUDY OF A DIRECT ACQUISITION DEVICE FOR DETERMINATION OF THE RADIATION CONFIGURATION FACTOR

A. INTRODUCTION. In the report dated September 1965 several means of direct acquisition of the radiation configuration factor were discussed. It was decided to construct one of these after review and a conference with the technical monitor at NASA.

After some search of the available literature the IN2175 photodiode was selected as the sensor. These were arranged in a circuit as shown in Figure 1. Physically the photodiodes were located in the walls of a small hollow sphere. If one visualized three orthogonal axes located at the center of the sphere, the axes penetrate the surface of the sphere at six points. One of these points was made a small opening, while photodiodes were located at the other five. The sphere was painted black and mounted on small feet so that its opening was parallel to its base. The interior of the sphere was left white (the sphere is a ping pong ball).

A test chamber was constructed with dark walls, a bed of light below a diffusing glass screen, and an auxiliary system for measuring the output of the diodes. Figure 2 shows the voltmeter and two ammeter ranges.

In Figure 3 the light source, glass diffuser, photodiode sensor, a model, and details of the edge seals may be seen. The details of the

tight seal around the edge of the door and around the edge of the glass diffuser (slot in door) may be seen in Figure 4.

The roof of the chamber was lined on the inside with an iron sheet before the interior was painted.

Light weight positioning rods which fastened to a gimbal on one end and which have a magnet attached to the other end were used to position models over the detector as shown in Figure 5.

B. Description of Tests. Several series of tests were run in the chamber. In the first series of tests a bias voltage was set across the photodiodes and the current read. These readings were taken with the chamber illuminated but only black surfaces exposed to illumination. This gave a 'background reading.' The chamber was then lined with the material from which the model was made (both heavy gauge cardboard stock and, later, aluminum foil), and a reading taken with the chamber illuminated. This output with the background subtracted out should represent configuration factor one, while the reading for background, with the background subtracted out should represent the output for configuration factor zero.

To test the operation a series of circular models were mounted at various distances from the sensing head. The radii of the circles was 3 inches, 4 inches, 5 inches and 6 inches. Positioning shafts of 1 inch, 2 inches, 3 inches, 6 inches and 9 inches were used.

For the simple circular disk with parallel, centrally located area dA (the opening to the sensor) the radiation configuration factor

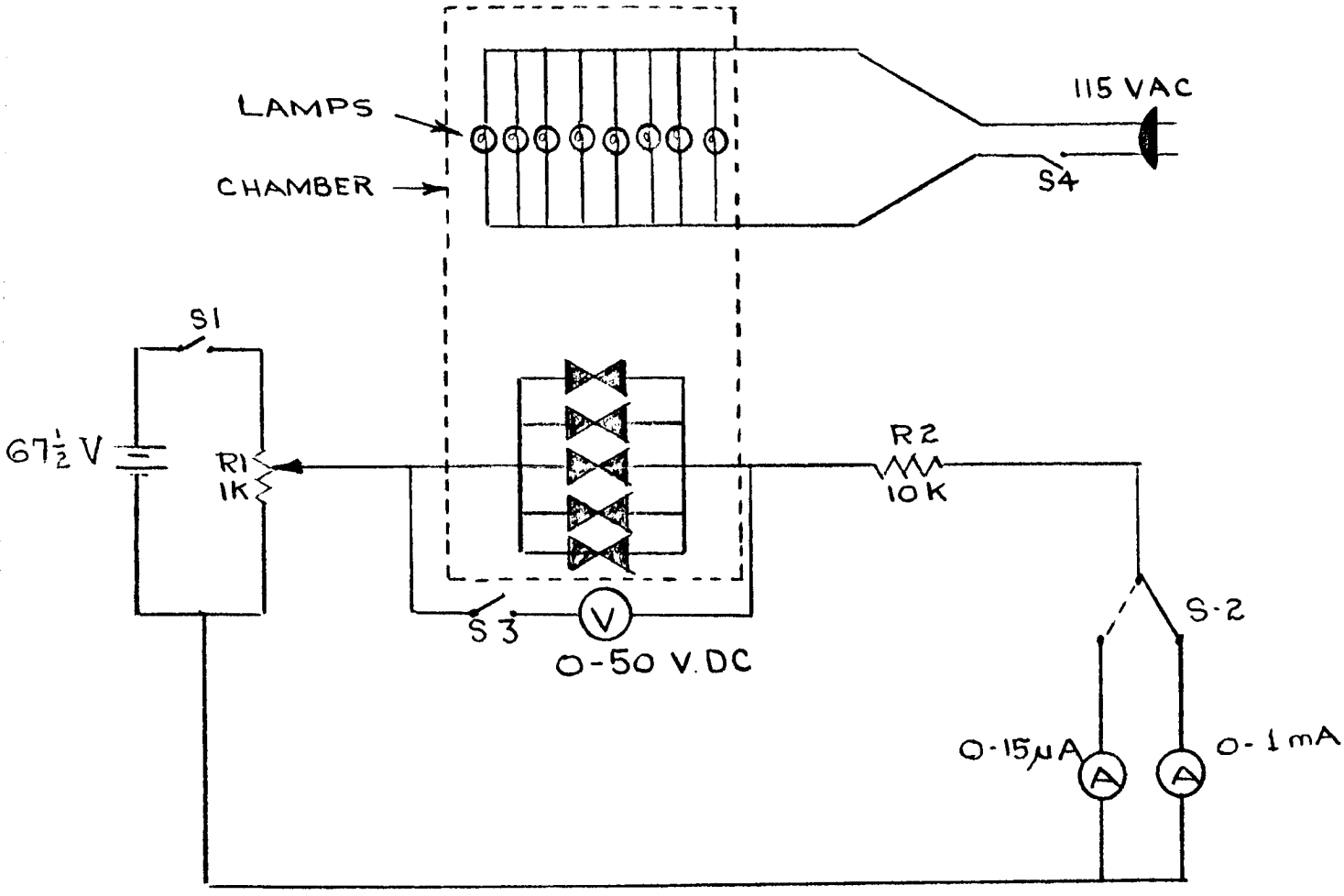

Figure 1. Circuit Diagram For Photodiode Detector.

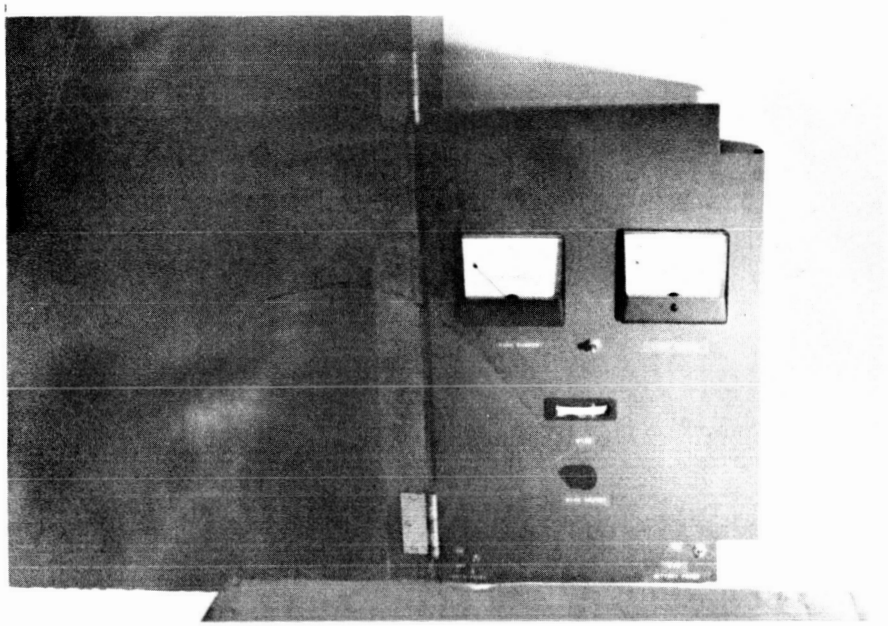

Figure 2. Control Panel for the Device to Allow Direct Acquisition of Configuration Factor

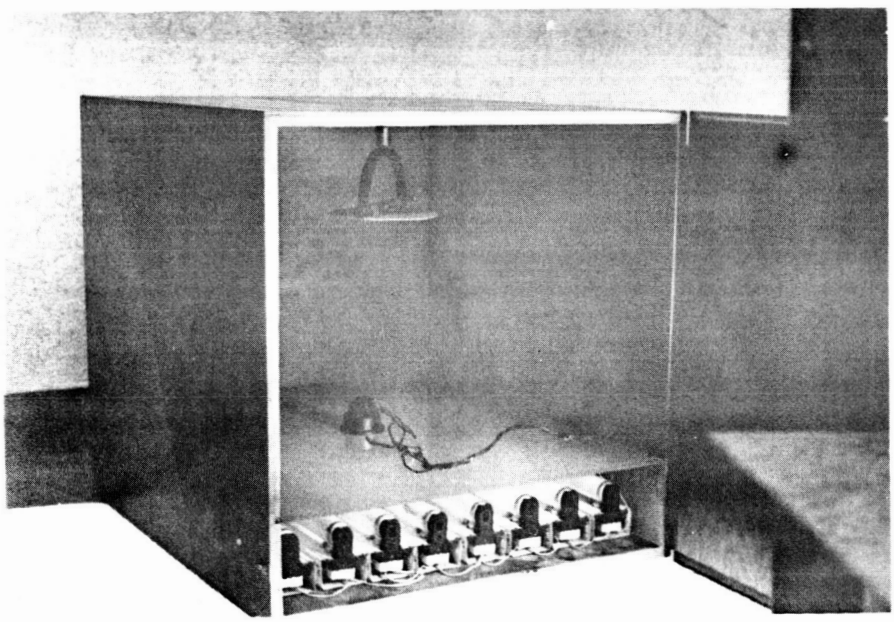

Figure 3. Interior View of Test Apparatus

Figure 4. Details of the Edge of the Test Chamber Door.

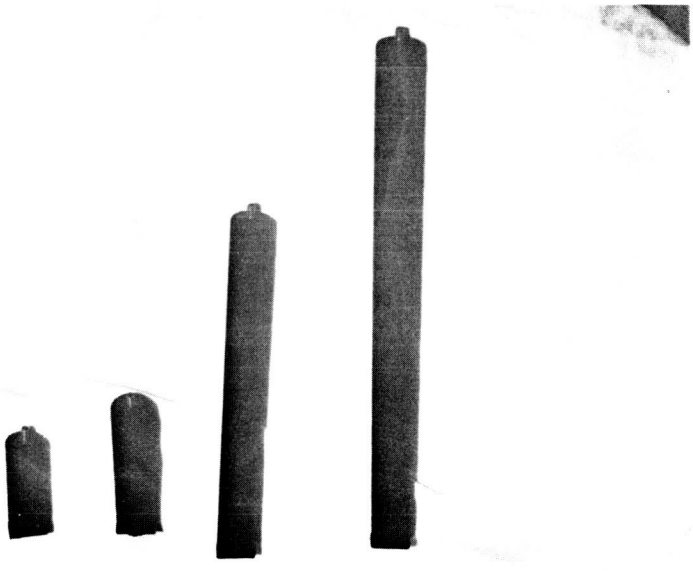

Figure 5. Magnetic Positioning Bars for Use in Test Chamber.

Figure 6. Current versus configuration factor for 20 volt diode bias

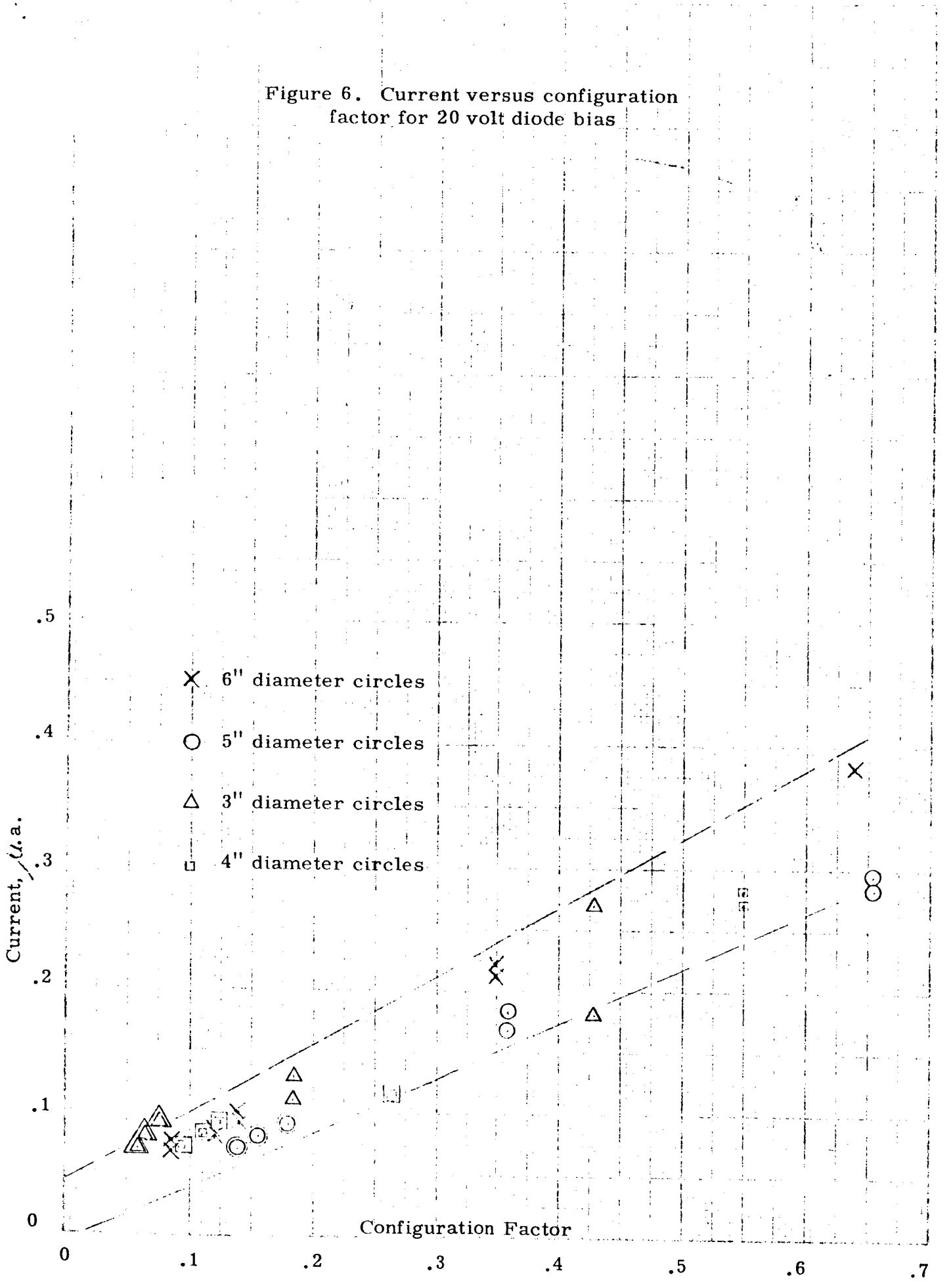

Figure 7. Current versus configuration factor for 40 volt diode bias

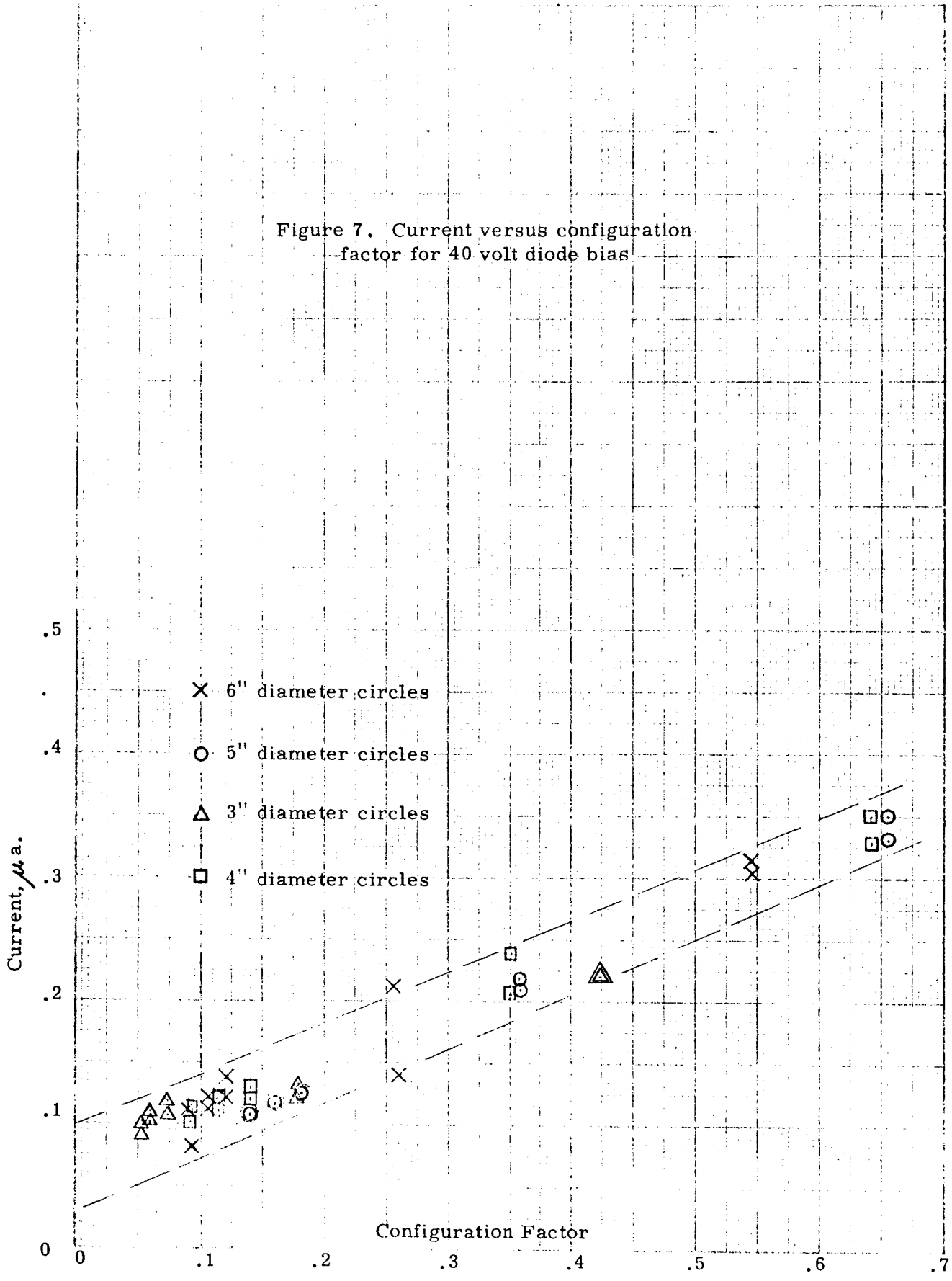

is easily calculated. This was done and net diode output was plotted versus configuration factor for all the combinations of height and diameter with bias voltage a parameter. These results are shown in Figures 6 and 7.

C. Criticism. These tests were conducted to see if this method could be refined to yield useful results directly, and the answer is yes. The results obtained were such that one could not divide (the current with the white liner less background) into (the current with any model less background) and get the configuration factor directly. Refinement of the apparatus would allow this to be done. Some of these refinements would be:

1. Vapor depositing aluminum inside the black body sphere before mounting the photodiodes.
2. Use of a regulated power supply.
3. Use of a very high impedance voltmeter.
4. Refinements of the light source to achieve more uniform illumination.
5. Use of two or more diffusing plates.
6. Construction of a chamber whose dimensions were several times as long or wide as high. This would tend to eliminate edge effects and multiple reflections.
7. Use of optical quality black paint. The paint used developed a sheen.

The actual apparatus as used cost approximately $200.00 with the principal costs being the diodes and the chamber. These refinements would yield a chamber capable of producing engineering accuracy for the configuration factor.

Thermal Design Studies

Final Report
Contract NAS8-5270

PART V

A STUDY OF THE THERMAL SIMILARITY OF A SELECTED SET OF MODELS WITH SIGNIFICANT RADIATION AND CONDUCTION

February 1967

Prepared for: George C. Marshall Space Flight Center
NASA
Huntsville, Alabama

Prepared by: Bureau of Engineering Research
University of Alabama
University, Alabama

PART V

A STUDY OF THE THERMAL SIMILARITY OF A SELECTED SET OF MODELS WITH SIGNIFICANT RADIATION AND CONDUCTION

A. Introduction. In the earlier part of the work performed under this contract a series of tests was performed to demonstrate the applicability of different types of scaling of thermal models. These results were very good. During the period of the extension it was determined that a series of tests should be run which would demand more of the thermal scaling in that speed-up of five times and twenty times in the test time were specified. Later, it was agreed that a speed-up in time of five and ten would be more realistic.

In addition it was agreed that the prototype whose behavior was being predicted would not be tested. These prototypes were to be similar to those previously tested in that the heat transferred by conduction and by radiation were both to be significant.

A secondary objective of the test was to attempt to show that decoupled radiation and conduction calculations may be in error if the interchange of heat with the external area of the conducting medium is neglected.

B. Description of Tests. A set of prototypes was designed which had large, moderate and small radiation configuration factor between the heated (active or driven) node and the unheated (passive or modeled) node. Also it was decided that the exchanging area of the conduction path should

be small, medium, and large. Consideration of these two sets of three requirements yields a nine element, three by three matrix.

The first set of prototypes were modeled using thermal and geometric scaling. The reduction of scaling parameters proposed by Mr. B. P. Jones were reduced (see Tables 1 and 2) for geometric and temperature scaling. The resulting models required use of materials which were not engineering materials and which would be difficult to form. Conversely, if normally available engineering materials were used, the dimensions required became critical for tolerance and for stability during machining. These models are summarized in Tables 4, 5 and 6.

A second set of models was designed replacing geometric scaling by scaling of the thermal capacitance term, (MC_p). The resulting models are shown in Tables 7, 8 and 9.

The results of several of these tests are shown in Figures 1, 2 and 3. The first set of models shown in Table 5 were constructed and tested. The results are shown in Figure 1. Figure 2 shows the results of the test of the second set of models in Table 7. Figure 3 shows the results of the tests of the first set of models of Table 9.

It should be noticed that the modeled node did not respond in the last tests. This was because the area of the conduction path became so large that the conduction path became, in effect, a radiation fin.

C. Discussion. The results of these tests reflect the difficulty in speeding-up the test by too large a factor. In an attempt to scale a metal conducting

Table 1. Reduction of Pi Groups
Proposed by Jones for Geometric Scaling

π GROUPS (JONES)	Specify $\epsilon = \epsilon^*$ $\frac{t^*}{t} = K_1; \frac{1}{5}, \frac{1}{20}$	Geometric Scaling $\frac{C_j^*}{C_j} = \frac{D^{*3}}{D^3}$ $(\epsilon_j = \epsilon_j^*)$ $E_{kj} = E_{kj}^*$; $F_{kj} = F_{kj}^*$ $C_j^*/C_j = \rho C_p (D^*)^3 / \rho C_p (D)^3 = (D^*/D)^3$	Geometric Scaling with Temperature Ratios Equal $T_j = T_j^*$ $A_k^* = D^{*2}$ $T_k = T_k^*$ $A_j = D^2$ $A_k = D^{*2}$ $A_j^* = D^{*2}$
$\frac{T_i}{T_k} = \frac{T_i^*}{T_k^*}$	$\frac{T_i}{T_k} = \frac{T_i^*}{T_k^*}$	$\frac{T_i}{T_k} = \frac{T_i^*}{T_k^*}$	IDENTITY
$\frac{E_{kj} F_{kj} A_k}{\epsilon_j A_j} = \frac{E_{kj}^* F_{kj}^* A_k^*}{\epsilon_j^* A_j^*}$	$\frac{E_{kj} F_{kj} A_k}{A_j} = \frac{E_{kj}^* F_{kj}^* A_k^*}{A_j^*}$	$\frac{A_k}{A_j} = \frac{A_k^*}{A_j^*}$	IDENTITY
$\frac{\epsilon_i \sigma A_i T^3 t}{C_j} = \frac{\epsilon_i^* \sigma A_i^* T^{*3} t^*}{C_j^*}$	$\frac{\epsilon_i \sigma A_i T_i^3}{C_j} = \frac{\epsilon_j^* \sigma A_j^* T_j^{*3} K_1}{C_j^*}$	$\frac{A_i T_i^3}{D^3} = \frac{A_j^* T_j^{*3} K_1}{D^{*3}}$	$\frac{D^*}{D} = K_1$
$\frac{C_{kj} t}{C_j} = \frac{C_{kj}^* t^*}{C_j^*}$	$\frac{C_{kj}}{C_j} = \frac{C_{kj}^* K_1}{C_j^*}$	$C_{kj} = C_{kj}^* K_1 (\frac{D}{D^*})$	$C_{kj}^* = C_{kj} K_1^2$ (Not Linear Scaling)
$\frac{q_j t}{C_j T_j} = \frac{q_j^* t^*}{C_j^* T_j^*}$	$\frac{q_j}{C_j T_j} = \frac{q_j^* K_1}{C_j^* T_j^*}$	$\frac{q_j}{T_j} = \frac{q_j^* K_1}{T_j^*} (\frac{D}{D^*})^3$	$q_j^* = q_j K_1^2$
$\frac{\alpha_j^s A S t}{C_j T_j} = \frac{\alpha_j^{*s} A^* S^* t^*}{C_j^* T_j^*}$	DROPPED	———	———

Table 2. Reduction of Pi Groups Proposed by Jones for Temperature Scaling together with Geometric Scaling

π GROUPS (JONES)	Specify $\epsilon = \epsilon^*$ $\frac{t^*}{t} = K_1; \frac{1}{5}, \frac{1}{20}$	Geometric Scaling $\frac{C_j^*}{C_j} = \frac{D^{*3}}{D^3}$ $(\epsilon_j = \epsilon_j^*)$ $E_{kj} = E_{kj}^*$; $F_{kj} = F_{kj}^*$ $C_j^*/C_j = \rho C_p (D^*)^3 / \rho C_p (D)^3 = (D^*/D)^3$	IV. Temperature Scaling $\frac{T_j^*}{T_j} = K_2$
$\frac{T_j}{T_k} = \frac{T_j^*}{T_k^*}$	$\frac{T_j}{T_k} = \frac{T_j^*}{T_k^*}$	$\frac{T_j}{T_k} = \frac{T_j^*}{T_k^*}$	$\frac{T_k^*}{T_k} = K_2$ sets initial condition on passive model
$\frac{E_{kj}F_{kj}A_k}{\epsilon_j A_j} = \frac{E_{kj}^* F_{kj}^* A_k^*}{\epsilon_j^* A_j^*}$	$\frac{E_{kj}F_{kj}A_k}{A_j} = \frac{E_{kj}^* F_{kj}^* A_k^*}{A_j^*}$	$\frac{A_k}{A_j} = \frac{A_k^*}{A_j^*}$	IDENTITY
$\frac{\epsilon_j \sigma A_j T^3 t}{C_j} = \frac{\epsilon_j^* \sigma A_j^* T^{*3} t^*}{C_j^*}$	$\frac{\epsilon_j \sigma A_j T_j^3}{C_j} = \frac{\epsilon_j^* \sigma A_j^* T_j^{*3} K_1}{C_j^*}$	$\frac{A_j T_j^3}{D^3} = \frac{A_j^* T_j^{*3} K_1}{D^{*3}}$	$\frac{D^*}{D} = K_2^3 K_1$
$\frac{C_{kj} t}{C_j} = \frac{C_{kj}^* t^*}{C_j^*}$	$\frac{C_{kj}}{C_j} = \frac{C_{kj}^* K_1}{C_j^*}$	$C_{kj} = C_{kj}^* K_1 (\frac{D}{D^*})^3$	$C_{kj}^* = C_{kj} K_2^9 K_1$
$\frac{q_j t}{C_j T_j} = \frac{q_j^* t^*}{C_j^* T_j^*}$	$\frac{q_j}{C_j T_j} = \frac{q_j^* K_1}{C_j^* T_j^*}$	$\frac{q_j}{T_j} = \frac{q_j^* K_1}{T_j^*} (\frac{D}{D^*})^3$	$q_j^* = K_2^{10} K_1^2 q_j$
$\frac{\alpha_j^s A S t}{C_j T_j} = \frac{\alpha_j^{*s} A^* S^* t^*}{C_j^* T_j^*}$	DROPPED	———	———

Table 3. Reduction of Pi Groups Proposed by Jones for Warped Model

π GROUPS (JONES)	Warped Model $\epsilon = \epsilon^*$ $\epsilon \approx 1$ $\epsilon^* \approx 1$ $E_{kj} = E_{kj}^*$	SPECIFY $\frac{A_k^*}{A_k} = K_3$ $\frac{T_j^*}{T_j} = K_2$	SPECIFY $\frac{A_j^*}{A_j} = K_4$ $K_4 \neq K_3$
$\frac{T_j}{T_k} = \frac{T_j^*}{T_k^*}$	$\frac{T_j}{T_k} = \frac{T_j^*}{T_k^*}$	set initial condition on passive model.	NO CHANGE
$\frac{E_{kj}F_{kj}A_k}{\epsilon_j A_j} = \frac{E_{kj}^* F_{kj}^* A_k^*}{\epsilon_j^* A_j^*}$	$\frac{F_{kj}A_k}{A_j} = \frac{F_{kj}^* A_k^*}{A_j^*}$	$\frac{F_{kj}}{A_j} = \frac{F_{kj}^*}{A_j^*} K_3$	$F_{kj}^* = F_{kj}(\frac{K_4}{K_3})$
$\frac{\epsilon_j A_j T^3 t}{C_j} = \frac{\epsilon_j^* A_j^* T^{*3} t^*}{C_j^*}$	$\frac{A_j T_j^3}{C_j} = \frac{A_j^* T_j^{*3} K_1}{C_j^*}$	$\frac{A_j}{C_j} = \frac{A_j^* K_2^3 K_1}{C_j^*}$	$C_j^* = C_j K_4 K_2^2 K_1$
$\frac{C_{kj} t}{C_j} = \frac{C_{kj}^* t^*}{C_j^*}$	$\frac{C_{kj}}{C_j} = \frac{C_{kj}^* K_1}{C_j^*}$	$\frac{C_{kj}}{C_j} = \frac{C_{kj}^* K_1}{C_j^*}$	$C_{kj}^* = C_{kj} K_4 K_3^3$
$\frac{q_j t}{C_j T_j} = \frac{q_j^* t^*}{C_j^* T_j^*}$	$\frac{q_j}{C_j T_j} = \frac{q_j^* K_1}{C_j^* T_j^*}$	$\frac{q_j}{C_j} = \frac{q_j^* K_1}{C_j^* K_2}$	$q_j^* = q_j K_2^4 K_4$
$\frac{\alpha_j^s A S t}{C_j T_j} = \frac{\alpha_j^{*s} A^* S^* t^*}{C_j^* T_j^*}$	———	———	———

Table 4. Three Sets of Three Thermally Similar Models Having Small Interacting Area of Conduction Path

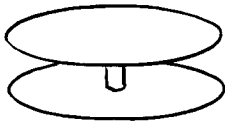

PROTOTYPE P-1

D=9.5 in L=2 in
d=3 in d_i=2.94 in
T_k=64° F T_j=-250° F
St. Mat'l = St. Steel

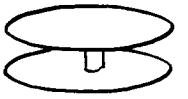

MODEL 1-a

D^*=5.8 in L^*=1.22 in
d^*=1.83 in d_i^*=
T_k^*=300° F T_j^*=-155° F
K_1=0.2 K_2=1.45
St. Mat'l =

MODEL 1-b

D^*=2.9 in L^*=0.61 in
d^*=0.915 in d_i^*=0.49 in
T_k^*=300° F T_j^*=-155° F
K_1=0.1 K_2=1.45
St. Mat'l = Plaster

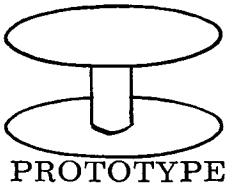

PROTOTYPE P-4

D=9.5 in L=9 in
d=3 in d_i=2.92 in
T_k=64° F T_j=-250° F
St. Mat'l = St. Steel

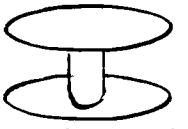

MODEL 4-a

D^*=5.8 in L^*=5.49 in
d^*=1.83 in d_i^*=1.67 in
T_k^*=300° F T_j^*=-155° F
K_1=0.2 K_2=1.45
St. Mat'l = Hastelloy B

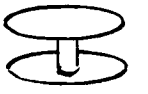

MODEL 4-b

D^*=2.9 in L^*=2.75 in
d^*=0.915 in d_i^*=
T_k^*=300° F T_j^*=-155° F
K_1=0.1 K_2=1.45
St. Mat'l =

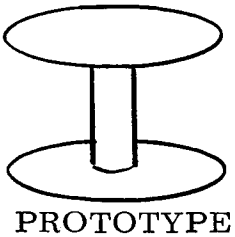

PROTOTYPE P-7

D=9.5 in L=18 in
d=3 in d_i=2.95 in
T_k=64° F T_k^*=-250° F
St. Mat'l = St. Steel

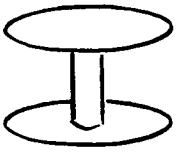

MODEL 7-a

D^*=5.8 in L^*=11 in
d^*=1.83 in d_i^*=
T_k^*=300° F T_j^*=-155° F
K_1=0.2 K_2=1.45
St. Mat'l =

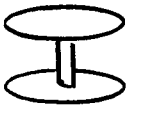

MODEL 7-b

D^*=2.9 in L^*=5.5 in
d^*=0.915 in d_i^*=0.535 in
T_k^*=300° F T_j^*=-155° F
K_1=0.1 K_2=1.45
St. Mat'l = Plaster

Table 5. Three Sets of Three Thermally Similar Models Having Moderate Interacting Area of Conducting Path

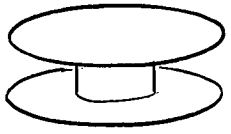

PROTOTYPE P-2

D=9.5 in L=2 in
d=6 in d_i=5.98 in
T_k=64° F T_j=-250° F
St. Mat'l = St. Steel

MODEL 2-a

D^*=5.8 in L^*=1.22 in
d^*=3.66 in d_i^*=1.97 in
T_k^*=300° F T_j^*=-155° F
K_1=0.2 K_2=1.45
St. Mat'l = Teflon

MODEL 2-b

D^*=2.9 in L^*=0.61 in
d^*=1.83 in d_i^*=1.51 in
T_k^*=300° F T_j^*=-155° F
K_1=0.1 K_2=1.45
St. Mat'l = Teflon

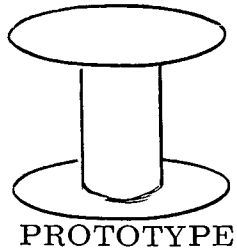

PROTOTYPE P-5

D=9.5 in L=9 in
d=6 in d_i=5.98 in
T_k=64° F T_j=-250° F
St. Mat'l = St. Steel

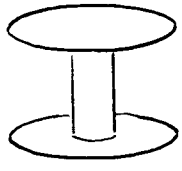

MODEL 5-a

D^*=5.8 in L^*=5.49 in
d^*=3.5 in d_i^*=3.33 in
T_k^*=300° F T_j^*=-155° F
K_1=0.2 K_2=1.45
St. Mat'l = Hastelloy B

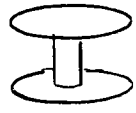

MODEL 5-b

D^*=2.9 in L^*=2.75 in
d^*=1.83 in d_i^*=1.162 in
T_k^*=300° F T_j^*=-155° F
K_1=0.1 K_2=1.45
St. Mat'l = Plaster

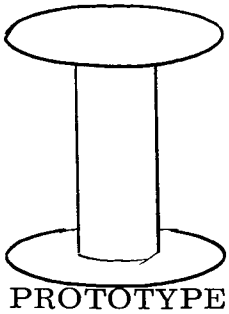

PROTOTYPE P-8

D=9.5 in L=18 in
d=6 in d_i=5.98 in
T_k=64° F T_j=-250° F
St. Mat'l = St. Steel

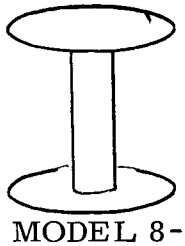

MODEL 8-a

D^*=5.8 in L^*=10.98 in
d^*=3.66 in d_i^*=3.12 in
T_k^*=300° F T_j^*=-155° F
K_1=0.2 K_2=1.45
St. Mat'l = Plaster

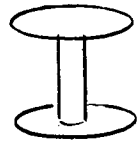

D^*=2.9 in L^*=5.49 in
d^*=1.83 in d_i^*=1.29 in
T_k^*=300° F T_j^*=-155° F
K_1=0.1 K_2=1.45
St. Mat'l = Teflon

Table 6. Three Sets of Three Thermally Similar Models Having Large Interacting Area of Conducting Path

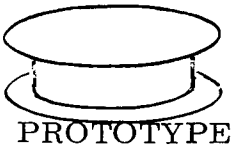

PROTOTYPE P-3

D=9.5 in L=2 in
d=2 in d_i=7.93 in
T_k=64° F T_j=-250° F
St. Mat'l = St. Steel

MODEL 3-a

D^*=5.8 in L^*=1.22 in
d^*=4.85 in d_i^*=4.0 in
T_k^*=300° F T_j^*=-155° F
K_1=0.2 K_2=1.45
St. Mat'l = Plaster

MODEL 3-b

D^*=2.9 in L^*=0.61 in
d^*=2.43 in d_i^*=2.245
T_k^*=300° F T_j^*=-155° F
K_1=0.1 K_2=1.45
St. Mat'l = Hastelloy B

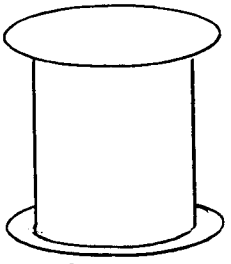

PROTOTYPE P-6

D=9.5 in L=9 in
d=7.95 in d_i=7.93 in
T_k=64° F T_j=-250° F
St. Mat'l = St. Steel

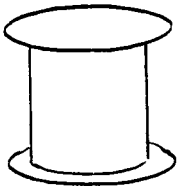

MODEL 6-a

D^*=5.8 in L^*=5.49 in
d^*=4.85 in d_i^*=4.17 in
T_k^*=300° F T_j^*=-155° F
K_1=0.2 K_2=1.45
St. Mat'l = Plaster

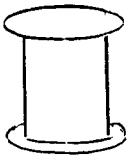

MODEL 6-b

D^*=2.9 in L^*=2.745 in
d^*=2.43 d_i^*=1.82
T_k^*=300° F T_j^*=-155° F
K_1=0.1 K_2=1.45
St. Mat'l = Plaster

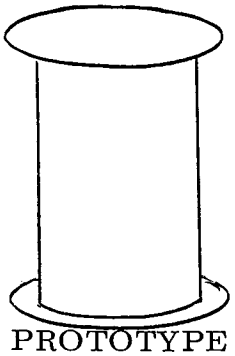

PROTOTYPE P-9

D=9.5 in L=18 in
d=7.95 in d_i=7.94 in
T_k=64° F T_j=-250° F
St. Mat'l = St. Steel

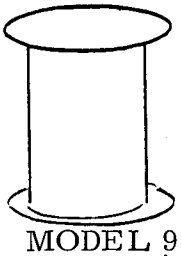

MODEL 9-a

D^*=5.8 in L^*=10.98 in
d^*=4.85 in d_i^*=4.47 in
T_k^*=300° F T_j^*=-155° F
K_1=0.2 K_2=1.45
St. Mat'l = Teflon

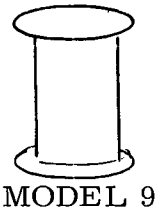

MODEL 9-b

D^*=2.9 in L^*=5.49 in
d^*=2.43 in d_i^*=
T_k^*=300° F T_j^*=-155° F
K_1=0.1 K_2=1.45
St. Mat'l =

Table 7. Alternate Set of Models for Table 4
Using Thermal Capacitance Scaling

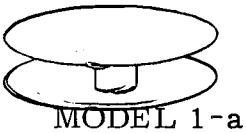

PROTOTYPE P-1	MODEL 1-a	MODEL 1-b
D=9.5 in L=2 in	D^*=9.5 in L^*=2 in	D^*=9.5 in L^*=2 in
d=3 in d_i=2.91 in	d^*=3 in $d_i{}^*$=2.91 in	d^*=3 in $d_i{}^*$=2.8 in
T_k=143° F T_j=-218° F	$T_k{}^*$=143° F $T_j{}^*$=-218° F	$T_k{}^*$=300° F $T_j{}^*$=-155° F
K_5=5	K_1=0.2 K_2=1.0	K_1=0.1 K_2=1.26
St. Mat'l = St. Steel	St. Mat'l = St. Steel	St. Mat'l = St. Steel

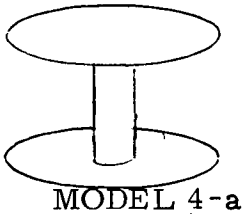

PROTOTYPE P-4	MODEL 4-a	MODEL 4-b
D=9.5 in L=9 in	D^*=9.5 in L^*=9 in	D^*=9.5 in L^*=9 in
d=3 in d_i=2.92 in	d^*=3 in $d_i{}^*$=2.92 in	d^*=3 in $d_i{}^*$=2.84 in
T_k=143° F T_j=-218° F	$T_k{}^*$=143° F $T_j{}^*$=-218° F	$T_k{}^*$=300° F $T_j{}^*$=-155° F
K_5=5	K_1=0.2 K_2=1	K_1=0.1 K_2=1.26
St. Mat'l = St. Steel	St. Mat'l = St. Steel	St. Mat'l = St. Steel

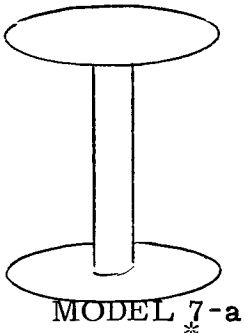

PROTOTYPE P-7	MODEL 7-a	MODEL 7-b
D=9.5 in L=18 in	D^*=9.5 in L^*=18 in	D^*=9.5 in L^*=18 in
d=3 in d_i=2.92 in	d^*=3 in $d_i{}^*$=2.92 in	d^*=3 in $d_i{}^*$=2.84 in
T_k=143°F T_j=-218° F	$T_k{}^*$=143° F $T_j{}^*$=-218° F	$T_k{}^*$=300° F $T_j{}^*$=-155° F
K_5=5	K_1=0.2 K_2=1	K_1=0.1 K_2=1.26
St. Mat'l = St. Steel	St. Mat'l = St. Steel	St. Mat'l = St. Steel

Table 8. Alternate Set of Models for Table 5
Using Thermal Capacitance

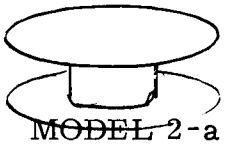

PROTOTYPE P-2
D=9.5 in L=2 in
d=6.0 in d_i=5.97 in
T_k=143°F T_j=-218° F
K_5=5
St. Mat'l = St. Steel

MODEL 2-a
D^*=9.5 in L^*=2 in
d^*=6.0 in d_i^*=5.97 in
T_k^*=143° F T_j^*=-218° F
K_1=0.2 K_2=1.0
St. Mat'l = St. Steel

MODEL 2-b
D^*=9.5 in L^*=2 in
d^*=6.0 in d_i^*=5.94 in
T_k^*=300° F T_j^*=-155° F
K_1=0.1 K_2=1.26
St. Mat'l = St. Steel

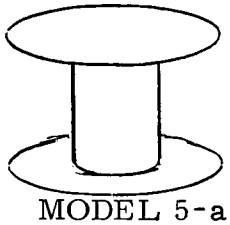

PROTOTYPE P-5
D=9.5 in L=9 in
d=6.0 in d_i=5.94 in
T_k=143°F T_j=-218° F
K_5=5
St. Mat'l = St. Steel

MODEL 5-a
D^*=9.5 in L^*=9 in
d^*=6.0 in d_i^*=5.94 in
T_k^*=143° F T_j^*=-218° F
K_1=0.2 K_2=1
St. Mat'l = St. Steel

MODEL 5-b
D^*=9.5 in L^*=9 in
d^*=6.0 in d_i^*=5.88 in
T_k^*=300° F T_j^*=-155° F
K_1=0.1 K_2=1.26
St. Mat'l = St. Steel

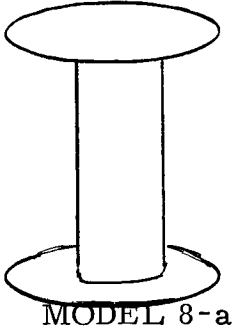

PROTOTYPE P-8
D=9.5 in L=18 in
d=6.0 in d_i=5.96
T_k=143°F T_j=-218°F
K_5=5
St. Mat'l = St. Steel

MODEL 8-a
D^*=9.5 in L^*=18 in
d^*=6.0 in d_i^*=5.96
T_k^*=143° F T_j^*=-218° F
K_1=0.2 K_2=1
St. Mat'l = St. Steel

MODEL 8-b
D^*=9.5 in L^*=18 in
d^*=6.0 in d_i^*=5.92 in
T_k^*=300° F T_j^*=-155° F
K_1=0.1 K_2=1.26
St. Mat'l = St. Steel

Table 9. Alternate Set of Models for Table 6
Using Thermal Capacitance

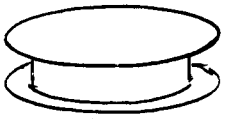

PROTOTYPE P-3	MODEL 3-a	MODEL 3-b
D=9.5 in L=2 in	D^*=9.5 in L^*=2 in	D^*=9.5 in L^*=2 in
d=7.95 in d_i=7.92 in	d^*=7.95 in d_i^*=7.92 in	d^*=7.95 in d_i^*=7.92 in
T_k=143°F T_j=-218° F	T_k^*=143° F T_j^*=-218° F	T_k^*=300° F T_j^*=-155° F
K_5=5	K_1=0.2 K_2=1.0	K_1=0.1 K_2=1.26
St. Mat'l = St. Steel	St. Mat'l = St. Steel	St. Mat'l = St. Steel

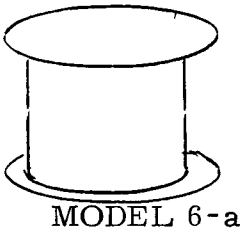

PROTOTYPE P-6	MODEL 6-a	MODEL 6-b
D=9.5 in L=9 in	D^*=9.5 in L^*=9 in	D^*=9.5 in L^*=9 in
d=7.95 in d_i=7.92 in	d^*=7.95 in d_i^*=7.92 in	d^*=7.95 in d_i^*=7.89 in
T_k=143°F T_j=-218° F	T_k^*=143° F T_j^*=-218° F	T_k^*=300° F T_j^*=-155° F
K_5=5	K_1=0.2 K_2=1	K_1=0.1 K_2=1.26
St. Mat'l = St. Steel	St. Mat'l = St. Steel	St. Mat'l = St. Steel

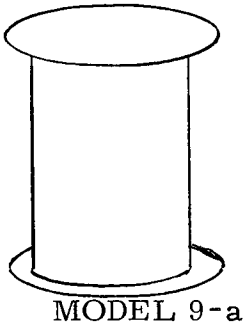

PROTOTYPE P-9	MODEL 9-a	MODEL 9-b
D=9.5 in L=18 in	D^*=9.5 in L^*=18 in	D^*=9.5 in L^*=18 in
d=7.95 in d_i=7.92 in	d^*=7.95 in d_i^*=7.92 in	d^*=7.95 in d_i^*=7.89 in
T_k=143°F T_j=-218° F	T_k^*=143° F T_j^*=-218° F	T_k^*=200° F T_j^*=-155° F
K_5=5	K_1=0.2 K_2=1	K_1=0.1 K_2=1.26
St. Mat'l = St. Steel	St. Mat'l = St. Steel	St. Mat'l = St. Steel

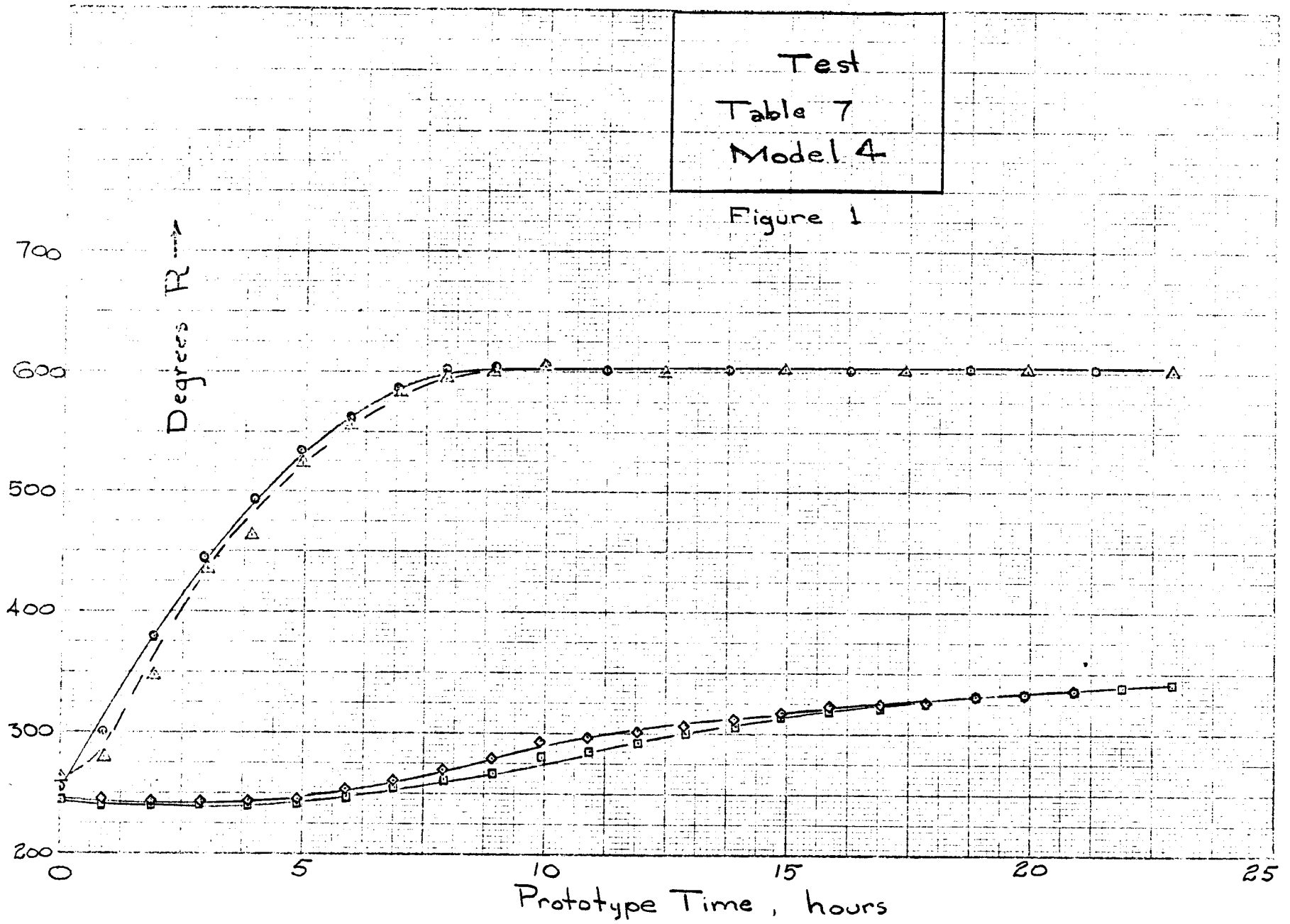
Test
Table 7
Model 4
Figure 1
Degrees R
700
600
500
400
300
200
0
5
10
15
20
25
Prototype Time, hours

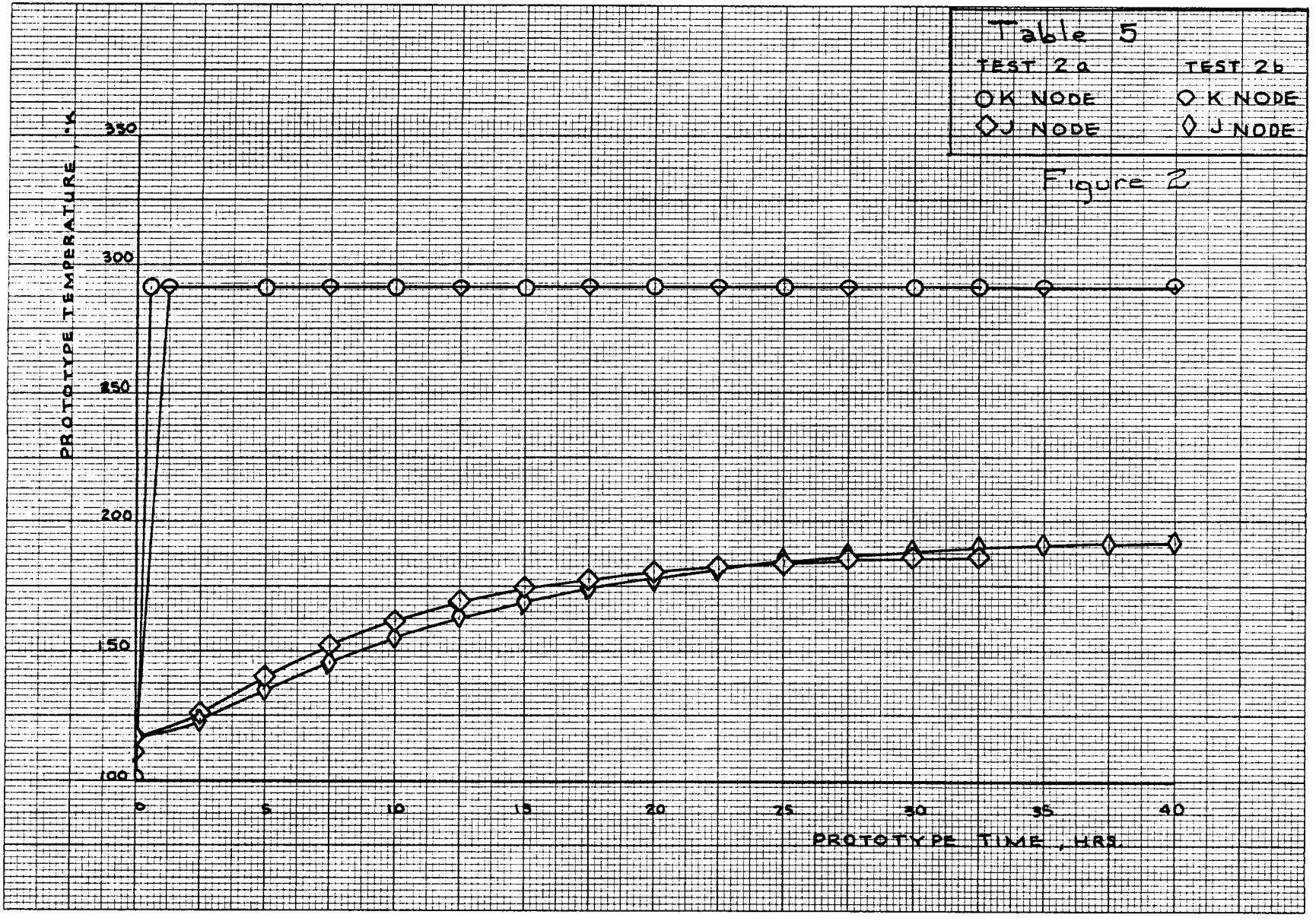
Table 5
TEST 2a
K NODE
J NODE
TEST 2b
K NODE
J NODE
Figure 2
PROTOTYPE TEMPERATURE, °K
350
300
250
200
150
100
0
5
10
15
20
25
30
35
40
PROTOTYPE TIME, HRS.

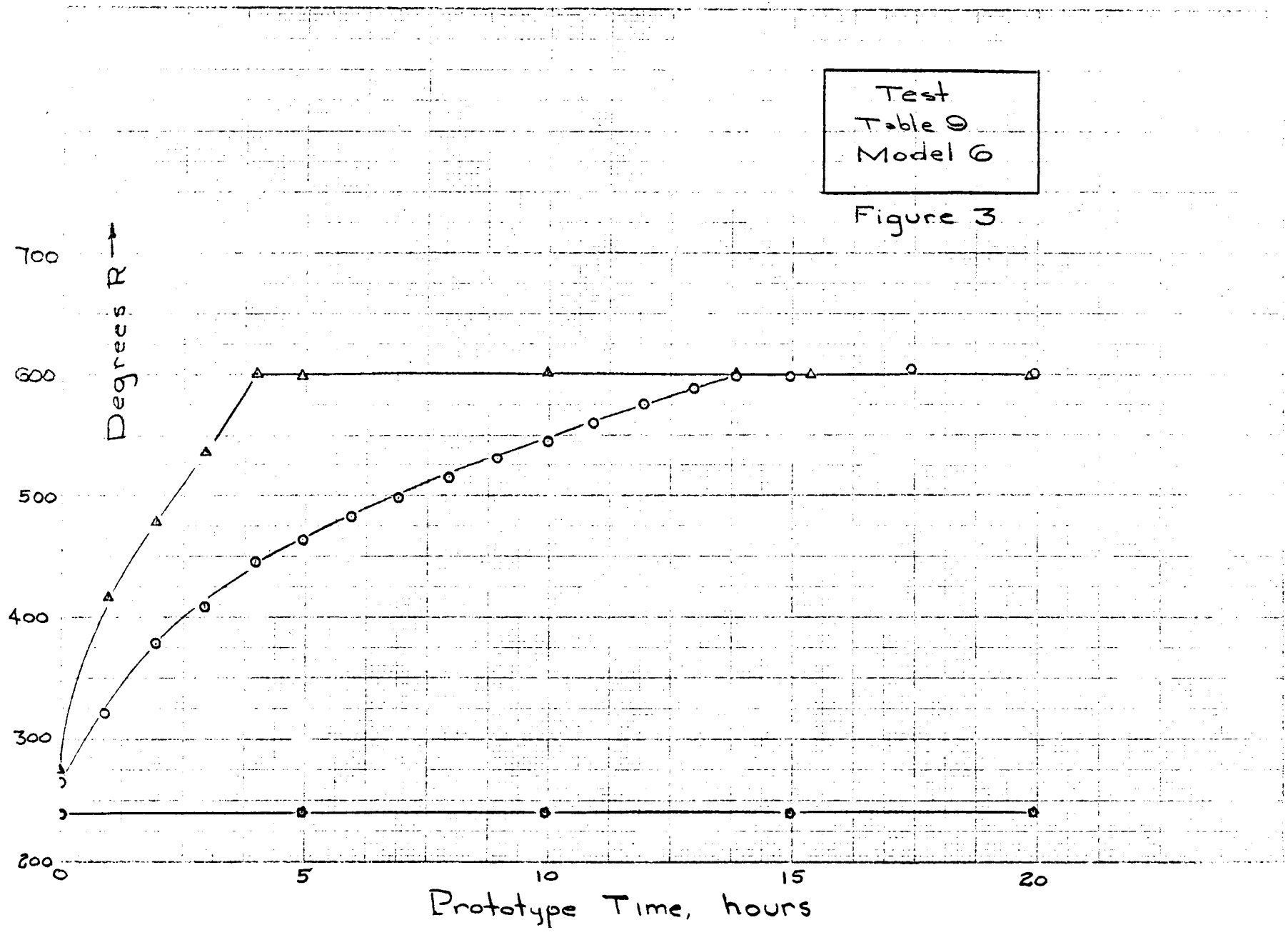
Test
Table 9
Model 6
Figure 3
Degrees R
700
600
500
400
300
200
0
5
10
15
20
Prototype Time, hours

member it is sometimes necessary to change material from the conducting metal to an essentially insulating nonmetal. To achieve the required conductivity in the nonmetal thicker walls are required. The end result is that one of the assumptions in the derivation of the modeling parameters used begins to become invalid. That is that the thermal capacitance is located in the nodes and is negligible in the conduction path. In the last models tested the nodes which were assumed isothermal and also assumed to contain the thermal capacitance were probably smaller thermal reservoirs than the conduction member.

The experimental program was plagued most by difficulties with the heating elements. It is desirable for close control of temperature to have the heating elements mechanically attached to the heated node. From the point of view of reliability and ease of use of a 'back-up' system radiant type heaters should be used. The spare heater could be in place and used in the event of a failure.

Several problems which were peripheral to the test program and which tend to limit the application of thermal similitude have been encountered. These have been communicated to the technical monitor through other channels.

The Appendix shows a typical set of data collected from a test. The ratio R is the steady-state decoupled ratio of heat transferred by radiation and conduction between bodies at the initial temperatures. For a correctly modeled test R remains constant. The value of R was set to unity to attempt to assure significant radiation and conduction exchange in the coupled experiment.

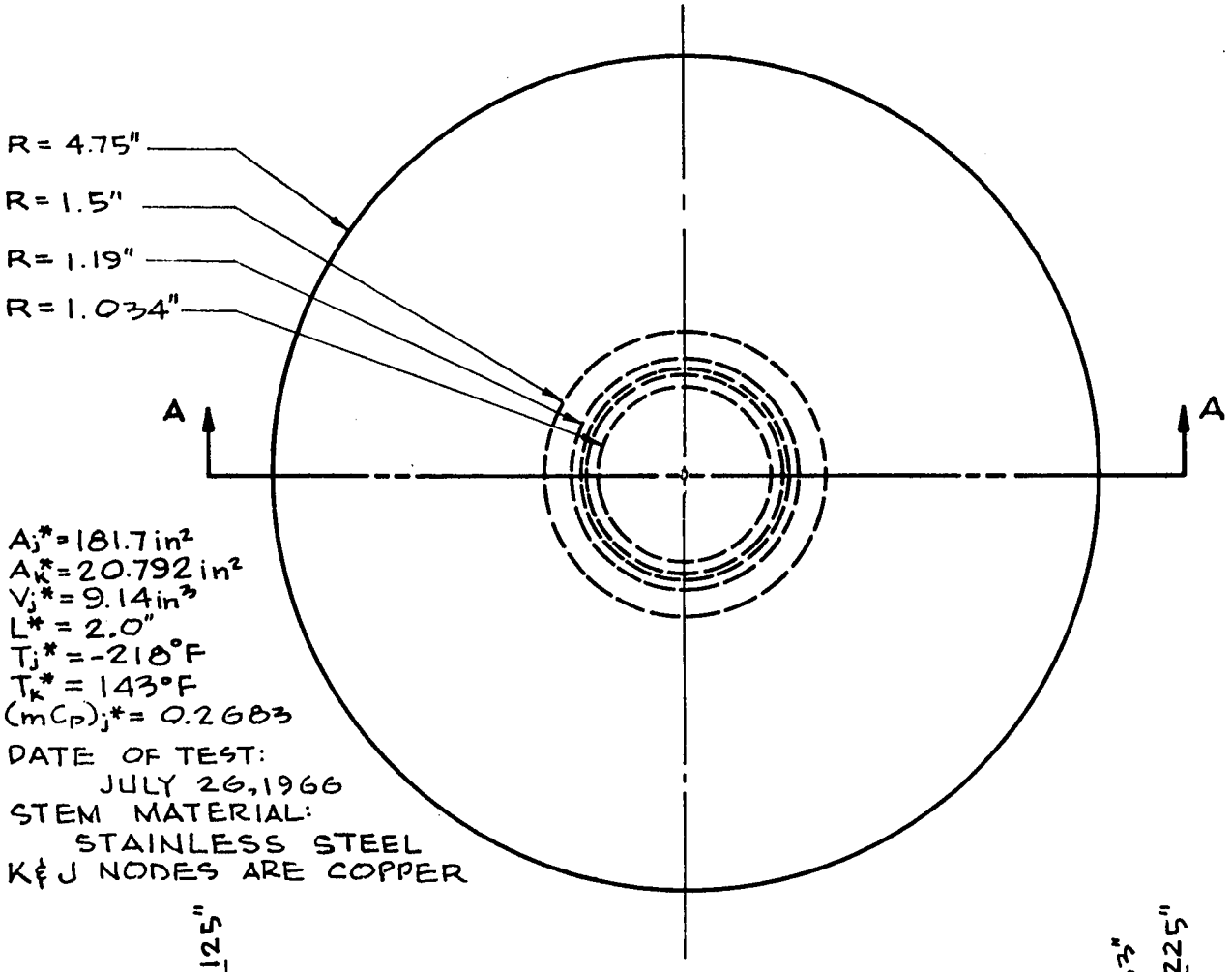

$A_j^* = 181.7\ in^2$
$A_k^* = 20.792\ in^2$
$V_j^* = 9.14\ in^3$
$L^* = 2.0"$
$T_j^* = -218°F$
$T_k^* = 143°F$
$(mC_p)_j^* = 0.2683$

DATE OF TEST:
JULY 26, 1966
STEM MATERIAL:
STAINLESS STEEL
K & J NODES ARE COPPER

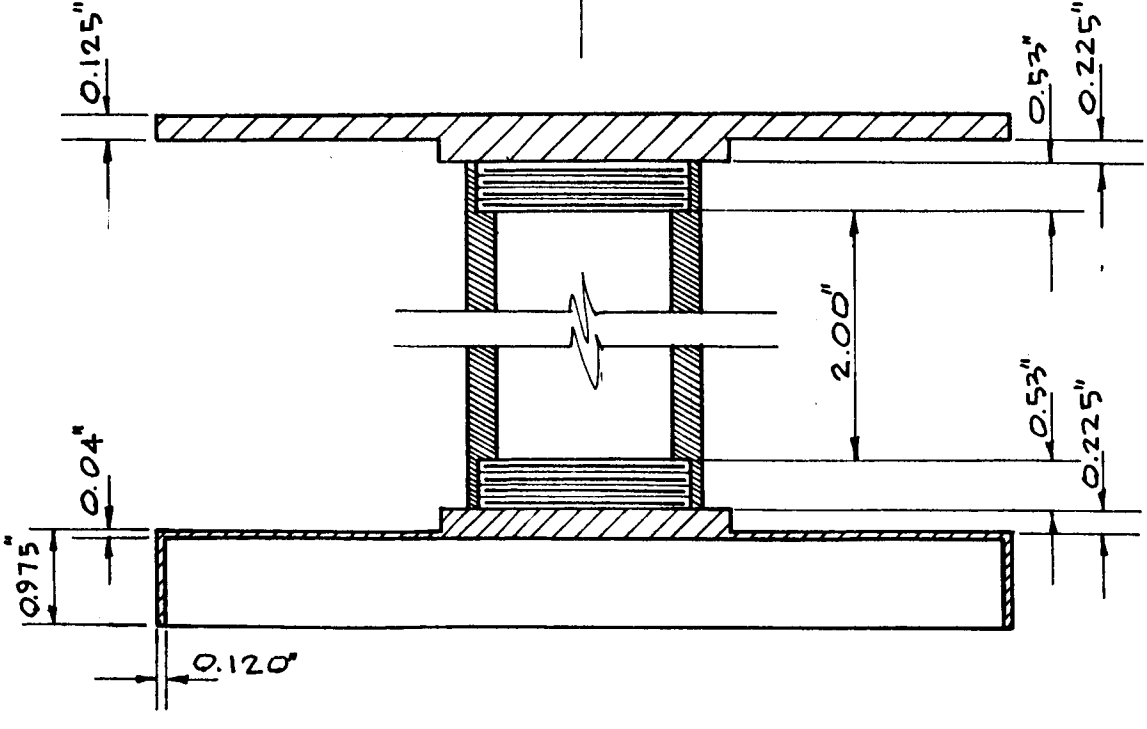

SCALE: 1" = 2"

DRAWN BY HORN	DATE 8/9/66	PROJECT NAS 8-5270	TEST 1-a	
APPROVED BY	DATE			

BUREAU OF ENGINEERING RESEARCH UNIVERSITY OF ALABAMA

TEST 1-a

1. LN_2 USED: $1\frac{3}{4}$ TANKS
2. COOLDOWN TIME: 10 HRS.
3. TEST TIME: 2.5 HRS.
4. INITIAL TEMPERATURES:

   $T_K^* = 143°F$ $T_j^* = -218°F$

   $T_K = 143°F$ $T_j = -218°F$
5. CHAMBER PRESSURE:

   $P = 2.6 \times 10^{-6}$ mm Hg
6. POWER INPUT:

   $E = 104$ V.

   $I = 1.04$ A.
7. HEAT TRANSFER RATIO:

   $R = q_{RAD.}/q_{COND.} = 1.0$
8. EMISSIVITY:

   $\epsilon = 1.0$
9. DATE OF TEST: JULY 26, 1966

$K_1 = 0.2$
$K_2 = 1.0$
$K_5 = 5.0$

$\frac{D^*}{D} = K_1 K_2^3 K_5 = 1$

$D = 9.5''$
$D^* = 9.5''$

$\frac{d^*}{d} = \frac{D^*}{D} = 1$

$d = 2.38''$
$d^* = 2.38''$
$C^*_{KJ} = C_{KJ}\left(\frac{D^*}{D}\right)^3 \frac{1}{K_1 K_5}$

STAINLESS STEEL STEM

$k = 9.4 \ \frac{BTU}{HR\text{-}FT\text{-}^\circ F}$

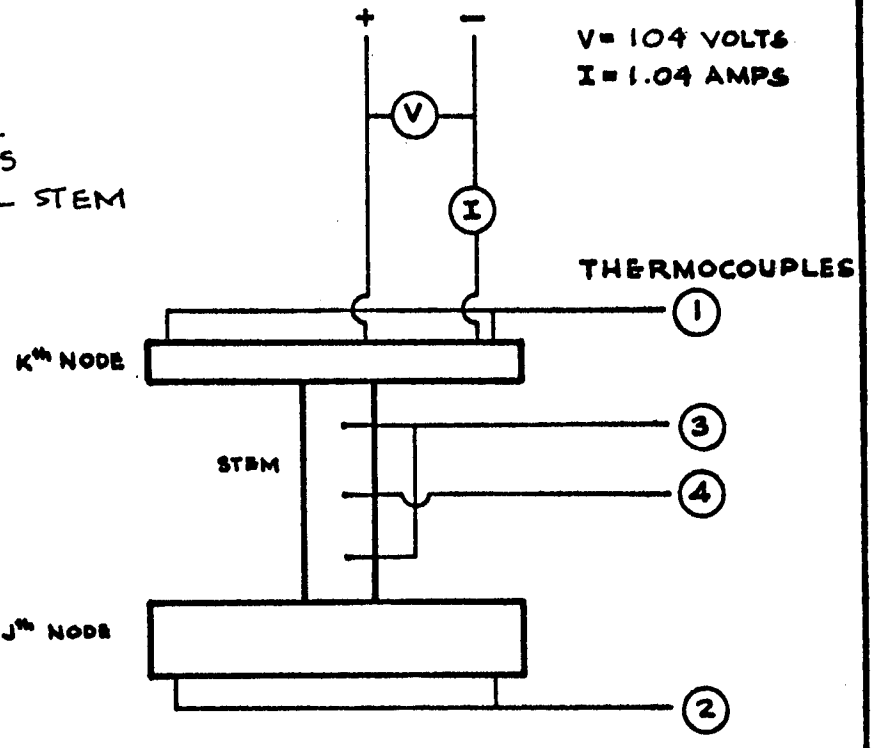

MODEL TEMPERATURE

$T_K^* = 143^\circ F$

TEST STARTED

$T_j^* = -218^\circ F$

TEST STOPPED

$T_j^* = +26^\circ F$

TIME TO RUN

$t^* = 2.5$ HRS

PRESSURE = 2.6×10^{-6} mm Hg.

DRAWN BY RMH	DATE 27 JUNE 64	PROJECT NAS8-5270	TEST 1-a
APPROVED BY	DATE		

BUREAU OF ENGINEERING RESEARCH UNIVERSITY OF ALABAMA

MODEL DATA

t^*, MIN.	T_K^*, °K	T_S^*, °K	T_J^*, °K		t^*, MIN.	T_K^*, °K	T_S^*, °K	T_J^*, °K
0.0	134.5	134.5	134.5		49.5	335	298.5	233
1.5	140.5	134.5	134.5		51.0	335	299.5	235
3.0	163	134.5	134.5		52.5	335	300	237.5
4.5	191.5	146	134.5		54.0	335	300.5	239
6.0	224	161.5	135.5		55.5	335	301	240.5
7.5	257	180.5	136.5		57.0	335	301.5	242.5
9.0	294	201	139.5		58.5	335	302	244
10.5	327	222	143.5		60.0	335	302.5	245
12.0	335	242	147		61.5	335	303.5	246
13.5	335	256	152		63.0	335	304	248
15.0	335	262	156		64.5	335	304	249
16.5	335	267.5	161		66.0	335	305	250
18.0	335	271	166		67.5	335	306	251
19.5	335	275	170		69.0	335	307	252
21.0	335	276.5	174.5		70.5	335	307	253
22.0	335	278.5	178.5		72.0	335	308	254.5
24.0	335	279.5	183		73.5	335	308	256
25.5	335	282	186		75.0	335	308	256.5
27.0	335	283	190		76.5	335	308	257
28.5	335	284	194.5		78.0	335	308	258
30.0	335	285	197		79.5	335	309.5	259
31.5	335	286	200.5		81.0	335	310	260
33.0	335	287.5	204		82.5	335	310.5	260.5
34.5	335	289	207		84.0	335	311	261
36.0	335	290	210.5		85.5	335	312	261.5
37.5	335	291	213		87.0	335	312	262
39.0	335	292	216.5		88.5	335	312	262.5
40.5	335	292.5	219		90.0	335	312	263
42.0	335	293.5	222		91.5	335	312	263
43.5	335	294.5	224		93.0	335	312	264
45.0	335	296	227		94.5	335	312	264.5
46.5	335	297	229		96.0	335	312	265
48.0	335	297.5	230.5		97.5	335	312	265

DRAWN BY	DATE	PROJECT	
RMH	27 JULY 66	NAS8-5270	MODEL DATA - TEST 1-a.
APPROVED BY	DATE		

BUREAU OF ENGINEERING RESEARCH UNIVERSITY OF ALABAMA

MODEL DATA

t^*, MIN.	T_K^*, °K	T_S^*, °K	T_J^*, °K		t^*, MIN.	T_K^*, °K	T_S^*, °K	T_J^*, °K
99.0	335	312	266		129.0	335	315	269.5
100.5	335	312	266		130.5	335	315	269.5
102.0	335	312	266		132.0	335	315.5	269.5
103.5	335	312	266		133.5	335	315.5	269.5
105.0	335	312	266		135.0	335	315.5	269.5
106.5	335	312.5	266.5		136.5	335	315.5	269.5
108.0	335	313	266.5		138.0	335	315.5	269.5
109.5	335	313	267		139.5	335	315.5	269.5
111.0	335	314	267		141.0	335	315.5	270
112.5	335	314	267		142.5	335	315.5	270
114.0	335	314.5	268		144.0	335	315.5	270
115.5	335	314.5	268.5		145.5	335	315.5	270
117.0	335	314.5	268.5		147.0	335	315.5	270
118.5	335	314.5	268.5		148.5	335	315.5	270
120.0	335	314.5	269		150.0	335	315.5	270
121.5	335	314.5	269		151.5	335	315.5	270
123.0	335	314.5	269		153.0	335	315.5	270
124.5	335	314.5	269		154.5	335	315.5	270
126.0	335	314.5	269		156.0	335	315.5	270
127.5	335	315	269.5					

DRAWN BY RMH	DATE 28 JULY 66	PROJECT NAS8-5270	MODEL DATA - TEST 1-a.	
APPROVED BY	DATE			

BUREAU OF ENGINEERING RESEARCH UNIVERSITY OF ALABAMA

PROTOTYPE DATA

t HOURS	T_K °K	T_S °K	T_j °K	t HOURS	T_K °K	T_S °K	T_j °K
0.000	134.5	134.5	134.5	4.125	335	298.5	233
0.125	140.5	134.5	134.5	4.250	335	299.5	235
0.250	163	134.5	134.5	4.375	335	300	237.5
0.375	191.5	146	134.5	4.500	335	300.5	239
0.500	224	161.5	135.5	4.625	335	301	240.5
0.625	257	180.5	136.5	4.750	335	301.5	242.5
0.750	294	201	139.5	4.875	335	302	244
0.875	327	222	143.5	5.000	335	302.5	245
1.000	335	242	147	5.125	335	303.5	246
1.125	335	256	152	5.250	335	304	248
1.250	335	262	156	5.375	335	304	249
1.375	335	267.5	161	5.500	335	305	250
1.500	335	271	166	5.625	335	306	251
1.625	335	275	170	5.750	335	307	252
1.750	335	276.5	174.5	5.875	335	307	253
1.875	335	278.5	178.5	6.000	335	308	254.5
2.000	335	279.5	183	6.125	335	308	256
2.125	335	282	186	6.250	335	308	256.5
2.250	335	283	190	6.375	335	308	257
2.375	335	284	194.5	6.500	335	308	258
2.500	335	285	197	6.625	335	309.5	259
2.625	335	286	200.5	6.750	335	310	260
2.750	335	287.5	204	6.875	335	310.5	260.5
2.875	335	289	207	7.000	335	311	261
3.000	335	290	210.5	7.125	335	312	261.5
3.125	335	291	213	7.250	335	312	262
3.250	335	292	216.5	7.375	335	312	262.5
3.375	335	292.5	219	7.500	335	312	263
3.500	335	293.5	222	7.625	335	312	263
3.625	335	294.5	224	7.750	335	312	264
3.750	335	296	227	7.875	335	312	264.5
3.875	335	297	229	8.000	335	312	265
4.000	335	297.6	230.5	8.125	335	312	265

DRAWN BY	DATE	PROJECT	
HORN	7/28/66	NAS8-5270	TEST 1-a
APPROVED BY	DATE		

BUREAU OF ENGINEERING RESEARCH UNIVERSITY OF ALABAMA

PROTOTYPE DATA

t HOURS	T_K °K	T_S °K	T_j °K	t HOURS	T_K °K	T_S °K	T_j °K
8.250	335	312	266	10.750	335	315	269.5
8.375	335	312	266	10.875	335	315	269.5
8.500	335	312	266	11.000	335	315.5	269.5
8.625	335	312	266	11.125	335	315.5	269.5
8.750	335	312	266	11.250	335	315.5	269.5
8.875	335	312.5	266.5	11.375	335	315.5	269.5
9.000	335	313	266.5	11.500	335	315.5	269.5
9.125	335	313	267	11.625	335	315.5	269.5
9.250	335	314	267	11.750	335	315.5	270
9.375	335	314	267	11.875	335	315.5	270
9.500	335	314.5	268	12.000	335	315.5	270
9.625	335	314.5	268.5	12.125	335	315.5	270
9.750	335	314.5	268.5	12.250	335	315.5	270
9.875	335	314.5	268.5	12.375	335	315.5	270
10.000	335	314.5	269	12.500	335	315.5	270
10.125	335	314.5	269	12.625	335	315.5	270
10.250	335	314.5	269	12.750	335	315.5	270
10.375	335	314.5	269	12.875	335	315.5	270
10.500	335	314.5	269	13.000	335	315.5	270
10.625	335	315	269.5				

DRAWN BY	DATE	PROJECT	
HORN	7/28/66	NAS 8-5270	TEST 1-a
APPROVED BY	DATE		

BUREAU OF ENGINEERING RESEARCH UNIVERSITY OF ALABAMA

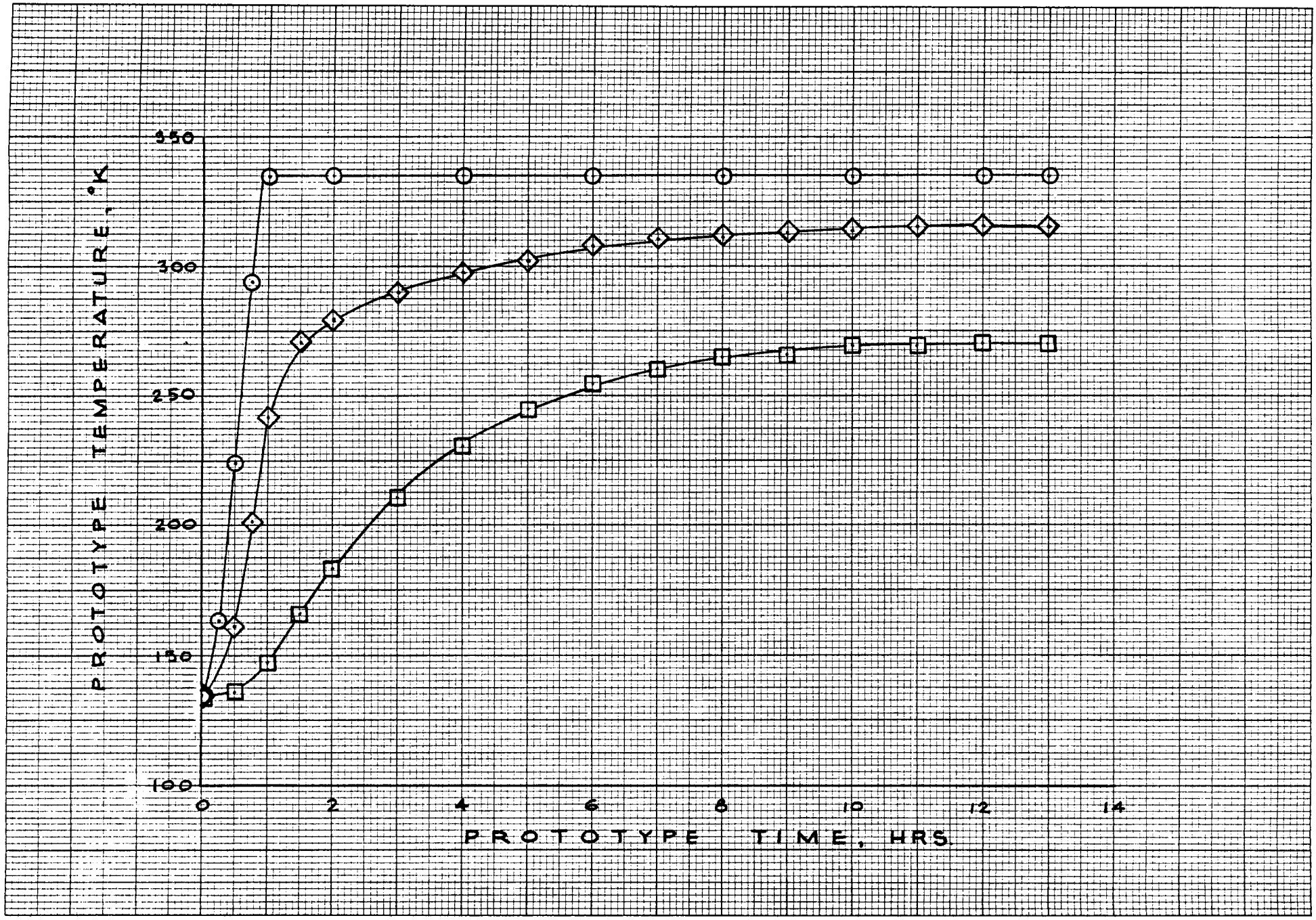
PROTOTYPE TEMPERATURE, °K
350
300
250
200
150
100
0
2
4
6
8
10
12
14
PROTOTYPE TIME, HRS.

DEGREES FAHR.
-50 -100 -150 -200 -250 -300
0
50
100
150
200
250
300